

GEOPHYSICAL STUDIES IN LAMU EMBAYMENT TO DETERMINE ITS
STRUCTURE AND STRATIGRAPHY.

BY

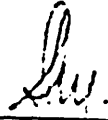
Silas Masinde Simiyu

THIS THESIS HAS BEEN ACCEPTED FOR
THE DEGREE OF MASTER OF SCIENCE
AND A CANDIDATE FOR THE DEGREE OF
UNIVERSITY LIBRARY. MSc 1989

A thesis submitted in partial fulfillment
for the degree of Master of Science
(Geology) in the University of Nairobi.

Nairobi, 1989.

This thesis is my original work and has not been presented for a degree in any other university

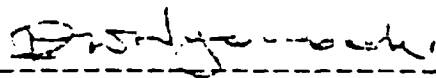


Silas Masinde Simiyu

This thesis has been submitted for examination with our knowledge as University supervisors.



P.S. Enegal



I.O. Nyembok

023097514

CONTENTS

Page

I	LIST OF FIGURES	(vi)
II	ABSTRACT	(vii)
III	ACKNOWLEDGEMENTS	(x)

CHAPTER 1INTRODUCTION

1.1	LOCATION, PHYSIOGRAPHY AND COMMUNICATION	1
1.2	PURPOSE OF THE STUDY	3
1.3	GEOLOGICAL SETTING	6
1.4	EXPLORATION HISTORY	6

CHAPTER 2GRAVITY SURVEYS AND DATA INTERPRETATION

2.1	INTRODUCTION	16
2.2	SURVEY PROCEDURE	17
2.2.1	GRAVITY MEASUREMENTS	17
2.2.2	ELEVATION MEASUREMENTS	18
2.2.3	MONITORING OF INSTRUMENT DRIFT	18
2.2.4	DENSITY DETERMINATION	22
2.3	DATA REDUCTION	24
2.3.1	ELEVATION ESTIMATION AND ACCURACY	25
2.3.2.1	DRIFT CORRECTION	26
2.3.2.2	TIDAL CORRECTION	29
2.3.2.3	LATITUDE CORRECTION	29
2.3.2.4	TERRAIN CORRECTION	30
2.3.2.5	FREE AIR CORRECTION	30
2.3.2.6	BOUGUER CORRECTION	32

2.4	ACCURACY OF THE SURVEY	32
2.5	INTERPRETATION OF THE DATA	33
2.5.1	QUALITATIVE INTERPRETATION	35
2.5.1.1	THE BOUGUER ANOMALY MAP	35
2.5.1.2	REGIONAL FIELD SEPARATION	38
2.3.1.3	INTERPRETATION OF STRUCTURES	41
2.5.2	QUANTITATIVE INTERPRETATION OF STRUCTURES	54
2.6	DISCUSSION OF GRAVITY RESULTS	70

CHAPTER 3

SEISMIC SURVEYS AND DATA INTERPRETATION

3.1	INTRODUCTION	74
3.2	DATA ACQUISITION AND QUALITY	75
3.3	REFLECTION IDENTIFICATION	80
3.4	MIS-TIES AND THEIR CORRECTION	81
3.5	DIGITISATION OF SEISMIC SECTIONS	83
3.6	TWO WAY TIME MAP CONSTRUCTION	83
3.7	VELOCITY DETERMINATION	85
3.8	DEPTH CONVERSION	87
3.9	CROSS SECTIONS FROM SEISMIC SECTIONS	88
3.10	INTERPRETATION OF DATA	90
3.10.1	GENERAL STRUCTURE	90
3.10.2	SEISMIC STRATIGRAPHY	93
3.10.3	MAJOR SEISMIC STRUCTURES	94
3.10.4	UNCONFORMITIES	96
3.11	DISCUSSION OF SEISMIC RESULTS	97

CHAPTER 4

WELL LOG DATA INTERPRETATION

4.1	INTRODUCTION	100
4.2	STRATIGRAPHY	102
4.3	DISCUSSION OF WELL LOG DATA	120

CHAPTER 5

GEOLOGICAL SYNTHESIS OF GEOPHYSICAL AND WELL LOG DATA

5.1	STRUCTURE	126
5.2	BASIN GEOLOGICAL HISTORY	130

CHAPTER 6

PETROLEUM POTENTIAL OF THE BASIN

6.1	STRATIGRAPHIC EVIDENCE	136
6.2	STRUCTURAL EVIDENCE	139

CHAPTER 7

CONCLUSIONS AND RECOMMENDATION	141
--------------------------------	-----

CHAPTER 8

REFERENCES	144
APPENDICES-GRAVITY DATA	154

LIST OF FIGURES

FIG	Page
1.1 Location and communication map of the study area.	2
1.2 The extent of Lamu embayment	6
1.3 Communication, Seismic lines, gravity stations and well location map.	11
1.4 General stratigraphy of Lamu embayment	13
2.1 'Single base' method illustration	19
2.2 Drift correction curves	21
2.3 Density determination Profiles	23
2.4 Bouguer anomaly map	36
2.5 Regional anomaly Profile	39
2.6 Gravity profile GP 1	43
2.7 Gravity profile GP 2	45
2.8 Gravity profile GP 3	46
2.9 Gravity profile GP 4	48
2.10 Gravity profile GP 5	49
2.11 Gravity profile GP 6	52
2.12 Gravity profile GP 7	53
2.13 The fit of a cylinder model to gravity profiles	56
2.14 The fit of a cylinder model to gravity profile GP 1	59
2.15 The fit of a cylinder model to gravity profile GP 2	60
2.16 The fit of a cylinder model to gravity profile GP 3	61
2.17 The fit of a cylinder model to gravity profile GP 4	62
2.18 Proposed model for the formation of Walu-Pandanguo anticline	64
2.19 Validity of depth estimation assumption	68
2.20 The fit of a cylinder model on profile GP 6	69

LIST OF FIGURES

FIG		Page
2.21	The extent of oceanic crust in Lamu embayment	73
3.1	Two way time (TWT) maps. (In pocket)	
3.2	Cross sections of the study area	89
3.3	Rose diagram of fault orientation in the area	91
4.1	Well correlation diagram of Walu, Pundanguo and Kipini wells.	103
4.2	Well correlation diagram of Kipini, Pate, Dodori and Mararani wells.	104
4.3	Fence diagram of Walu, Pandanguo, Kipini, Pate, Dodori and Mararani wells.	121
5.1	Structural map of Lamu area	127

LIST OF TABLES

TABLE		
3.1	Velocity values in Pate well.	86
3.2	Depth conversion table from time and velocity.	87

ABSTRACT

The area of study comprises part of one of the hydrocarbon-potential basins in Kenya; the Lamu basin. Major transgression and regression cycles dominated the area during different Mesozoic times. These depositional cycles together with tectonics associated with rifting and separation of Gondwanaland and also of Madagascar from Africa and the occasional doming of central Kenya resulted in a highly deformed basement with thick sedimentary cover due to subsidence and tilting.

The study of the Geophysical anomalies in the area, indicated by gravity and seismic data as well as the study of 6 deep wells drilled within the area revealed that the major tectonic disturbances of the area were caused by basement complex block faulting.

Bouguer anomalies indicate major basement variation in the northwest of the study area. Towards the coast, it becomes featureless with a two fold gravity gradient. This is attributed to the thinning of the continental crust and the presence of oceanic crust below the coastal sediments.

The analysis of seismic data has shown that structures in the area are fault controlled. The major fracturing is mainly along a NNW-SSE direction. A minor trend in a NE-SW direction has been confirmed.

It has also confirmed the presence of rounded closed highs that represent potential drilling locations. Well logs have shown

(ix)

that the area has good source reservoir and caprocks that could combine very well with the closed highs to accumulate oil and gas pools.

ACKNOWLEDGEMENTS

Thanks are due to Dr. P.S. Bhogal Department of Physics University of Nairobi for his supervision of the thesis, encouragement, discussions and suggestions that have led to the completion of this project.

Prof. I. O. Nyambok, Chairman, Department of Geology University of Nairobi who encouraged me to take up Petroleum Geology as a course, organized with the Ministry of Energy and Regional Development for me to receive data (on Lamu) from the National Oil Company of Kenya and supervised the project to its completion receives my deepest appreciation.

I wish to thank Mr. E.W Dindi of the Department of Geology, University of Nairobi for his constructive criticism, especially on gravity and seismic interpretation.

I am grateful to the German Academic Exchange Service (DAAD) for giving me a scholarship that has enabled me to do my postgraduate studies at the University of Nairobi. The National Council for Science and Technology (N.C.S.T.) for sponsoring the research and the Department of Surveying and Photogrammetry of the University of Nairobi for allowing me to use their field equipment.

Special thanks go to the administration police of Witu (Lamu district) who gave me the necessary security while doing my fieldwork, Miss Florence Kayere of the Department of Geology, University of Nairobi who typed my work, and to my wife Jane for her patience and continuous encouragement throughout the M.Sc. course.

1. INTRODUCTION

1.1 Location, Physiography and Communication

Lamu area is located in the northern part of Kenya coast, about 350 km north of Mombasa (Fig. 1.1.). The area for the purpose of this study is bounded by latitudes 1.500°S and 2.500°S and longitudes 40.00°E and 41.75°E . It covers an area of about 24000 km² and constitutes part of Block 5; one of the blocks earmarked by the Government of Kenya for leasing as part of the current oil exploration intensification programme.

The area may be divided into two physiographic units, namely the coastlands and the Tana river regions. Geomorphologically, the coastal plains consist of alluvial lowlands of the Tana river delta with accumulations of terrigenous material brought in by the Tana river. The material is moved along the coast by long-shore and coastal currents, forming wide beaches with arrays of dune ridges behind them. The Tana river strip forms a belt of dense bushes and swamps. Elevation changes are gradual and generally show a decrease towards the sea, or more locally towards the Tana river. The highest elevation being slightly more than 70 m above sea level around Walu.

The area is served by two major roads and one dry weather road. The main Garissa-Garsen road traverses the western part of the area with motorable tracks branching off to Masalani and Mai.

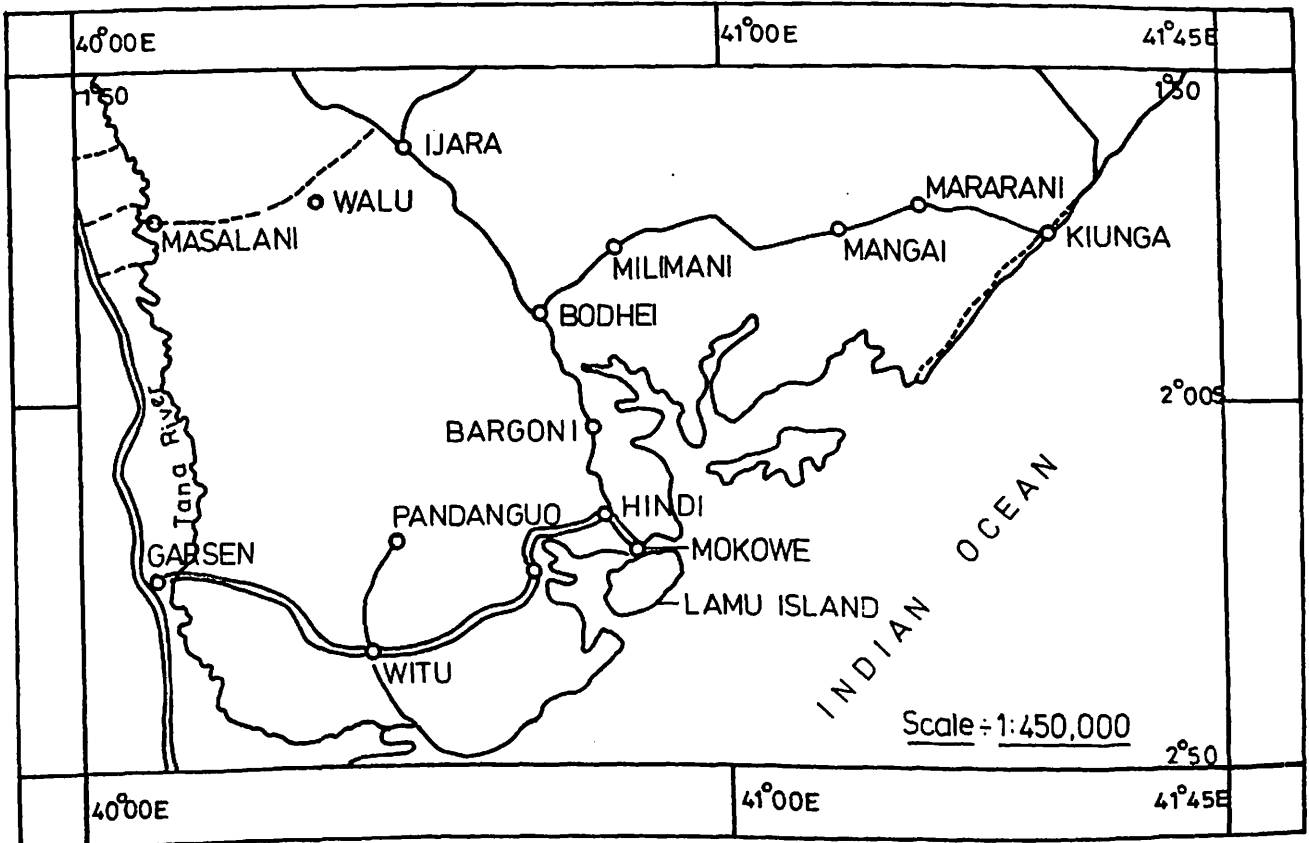
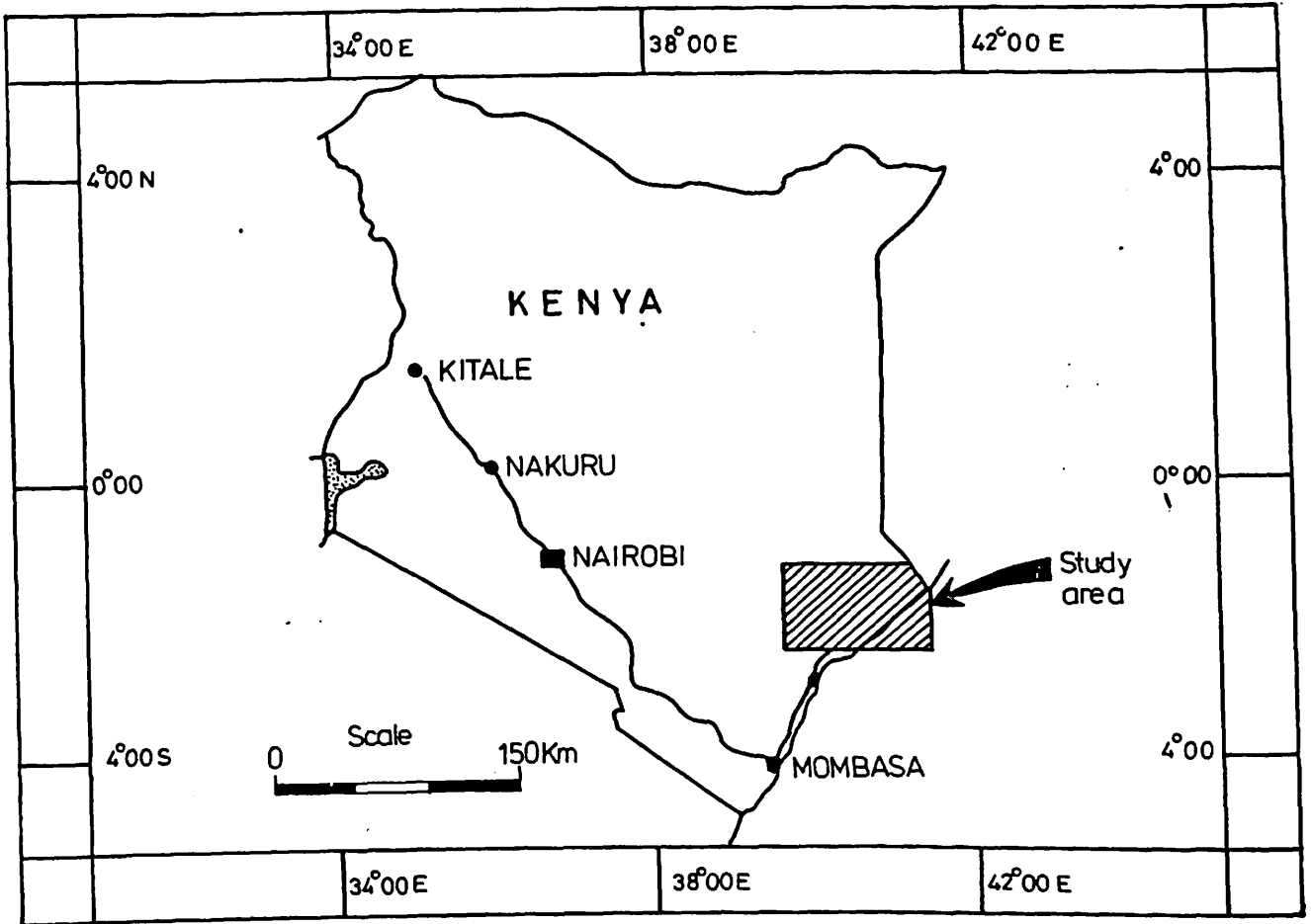


Fig.1.1 LOCATION AND COMMUNICATION MAP OF THE STUDY AREA

The second major road traverses the southern part from Garsen through Witu to Lamu with motorable tracks branching off to Kipini and Pandanguo. A dry weather road crosses the middle of this area southwards through Ijara, Bodhei, Majengo and Hindi with a branch to Mararani and Kiunga. The presence of thorny bushes and poorly drained marshy grassland make communication difficult, especially along the Tana river strip which forms a belt of 1 - 3 km wide of heavy dense bushes. Towards the coast, are shallow lakes and on the main coastland are tidal flats covered by beach sands, muds, silts and alluvials with mangrove forests in some parts. All these contribute to the communication problems in the area.

1.2 PURPOSE OF THE STUDY

Geophysical survey of Lamu area by oil companies using gravity and seismic methods revealed that Lamu area comprises a sedimentary basin of great thickness and of a complex structural nature. (O'Hollarain, 1971).

Selley (1985), Chapman (1973) and North (1984) noted that prior to the late seventies oil exploration companies' confidentiality of results and economic consideration outweighed the need to systematically analyse and explain the formation, the relationship between structural element fabrics, the tectonic factors concerned and the geologic history of a potential field. The companies generally looked for direct indicators for the presence of oil and gas.

A potential trap was delineated and a test-well drilled with the recovered cores being analysed for presence or absence of hydrocarbons. The results were classified as confidential for a long time. This method was more economical and faster for the oil companies but not favourable for understanding the area's subsurface geology and hence petroleum potential.

The writer was charged with the task of carrying out the analysis of the structural, stratigraphic and tectonics of the area using the old gravity, seismic and well log data that were acquired by oil companies (O'Hollorain 1971) (which are no longer confidential) and kept with National Oil Company of Kenya (NOCK). These data were first to be tested for quality and completeness and where possible acquire new data before interpretation was done.

By using the oil companies and his own data, the writer aimed at:

- (i) Delineating the basement characteristics using gravity data.
- (ii) Delineating sedimentary structures and lithologic thicknesses from seismic reflection data.
- (iii) Determining the palaeoenvironments of deposition and lithologic variations from well data.
- (iv) Determining (from i, ii, and iii) the structural fabrics (faults and folds) of the study area, their trends and the distribution of major and minor structural elements.
- (v) Evaluating the sedimentational and structural history of the area.

The above procedures were used to determine the presence of potential oil traps, their type, controls on their condition, extent, pattern and trend. It was also determined whether the palaeo-environmental conditions were favourable for abundant occurrence of petroleum generating organisms.

1.3 GEOLOGIC SETTING

The study area is geologically part of the Lamu embayment (Fig. 1.2). It does not have many rocks outcropping and is covered by superficial sands of fluvial origin associated with the Tana river drainage basin. Along the coastline are sands associated with longshore currents. The only rock outcrops are Pleistocene limestones encountered at Mokowe, Witu, Pate island and Lamu island and Upper Miocene limestones at Walu.

In the present study, the only reliable information on the near surface geology was obtained from shallow wells drilled in the study area by BP-Shell (1959) and from water boreholes. The well data shows that superficial deposits overlie Pleistocene raised reef and back reef limestones which are shallow water, sandy and detrital. Underlying the Pleistocene reef limestones is a succession of Pliocene sands, mainly calcareous with marine fossil foraminifera. These beds appear nearly horizontal and have light brown rounded quartz grains, garnet and sandy clays. These in turn are underlain by Miocene limestones with interbedded shales and minor calcareous sandstones showing cyclic sedimentation.

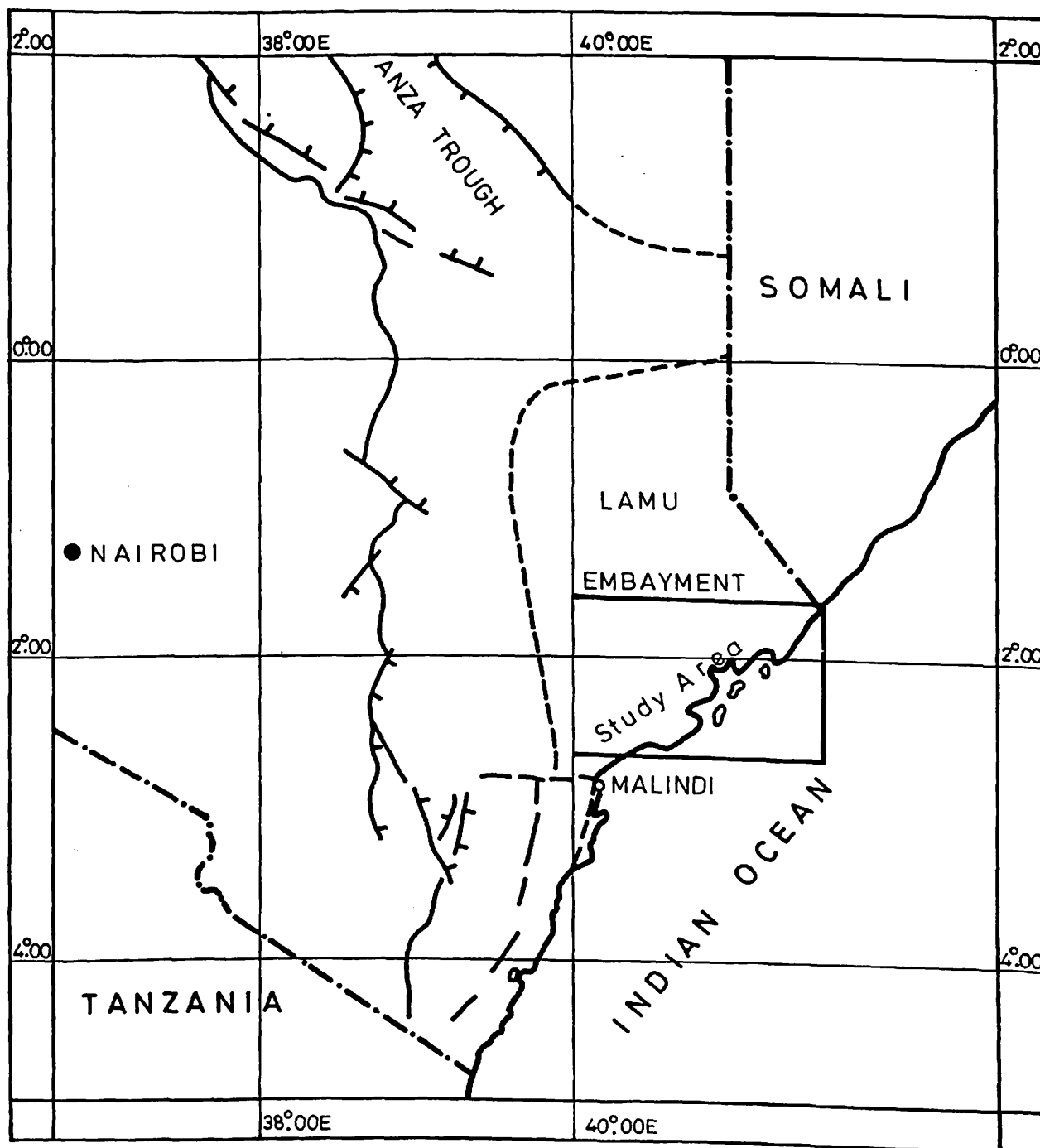


Fig. 1.2 THE EXTEND OF THE LAMU EMBAYMENT AND LOCATION OF THE STUDY AREA WITHIN THE EMBAYMENT

1.4 EXPLORATION HISTORY

Very little geologic work has been done in the study area and therefore information on the geology is scarce. Most of the geological work has been done in the southern and the western part adjacent to this area. Gedge (1892) mapped the western part of the area, mainly centered on the Tana river region. He suggested that the Tana river was an outlet in an alluvial delta. Hobley (1894) worked in the western part of the Tana river and noted that the area was covered by alluvial sediments which extend up to 39th meridian where rocks of the basement system are exposed.

Matherson (1963) did some reconnaissance work at Galole and Lamu. In Matherson's discussion of the geology, he noted that the area was covered by superficial soils of Pleistocene to Recent age and that the underlying geology can only be inferred from the change of the type of soil cover.

Williams (1962) mapped the Fundi Isa area which is to the south of the present area. He reported a thick series of sandstones, siltstones and shales deposited under sub-aerial and lacustrine conditions which he correlated with the middle and upper members of the Permo-Triassic Duruma formation that occurs further south. He further reported a sequence of fossiliferous upper Jurassic marine sediments with conglomerates and overlying

fossiliferous limestones occupying a narrow belt across the area and a wide variety of Quaternary deposits occurring in the area which include Pleistocene lagoonal clayey sands and marls, reddish dune sands, poorly exposed raised coral reefs and associated conquinoid limestones. A thin series of fluviatile sediments which he thought to have been deposited in the lower Pleistocene times was also reported. In his report, he discussed vast areas mantled by reddish brown wind blown sands which are probably of late Pleistocene age. Recent deposits include marine sands and muds flanked by high coastal dunes with a prominent development of alluvial silt. Seawards, he reported a thin series of marine sands and clays with bright red clayey sands of Oligocene age. He also reported a gentle fold in the area with NNW-SSE axis and inferred faults with trends NNW-SSE and NNE-SSW. He suggested that faulting and folding took place after the Upper Jurassic times with a possibility of further faulting during the lower Miocene.

Stockley (1928) noted that the NNE-SSW faulting along the Kenyan coast was related to late Miocene rift faulting, noting that the structure parallels one of the common East African rift valley trends.

The exploration for oil along the Kenyan coast started in 1933 when H.G. Busk and J.P. de Vertuil from the Darcy Exploration Company and the Anglosaxony Petroleum Company Limited mapped the Kenyan coast with a view to determine the petroleum potential of

the region (Busk H.G., and de Veruil J.P.1933). They noted that there was no folding in the general sense throughout the area, but only gentle warping connected with fault movement after deposition. Dips were mostly very low 20 - 30 which increased towards the coast. They concluded that commercial oil could not be found on the Kenyan coast because the thickness of impervious sedimentary rocks is too small. They argued that if oil occurred then there was abundant opportunity for seepages as the area is highly faulted which in fact had not been recorded.

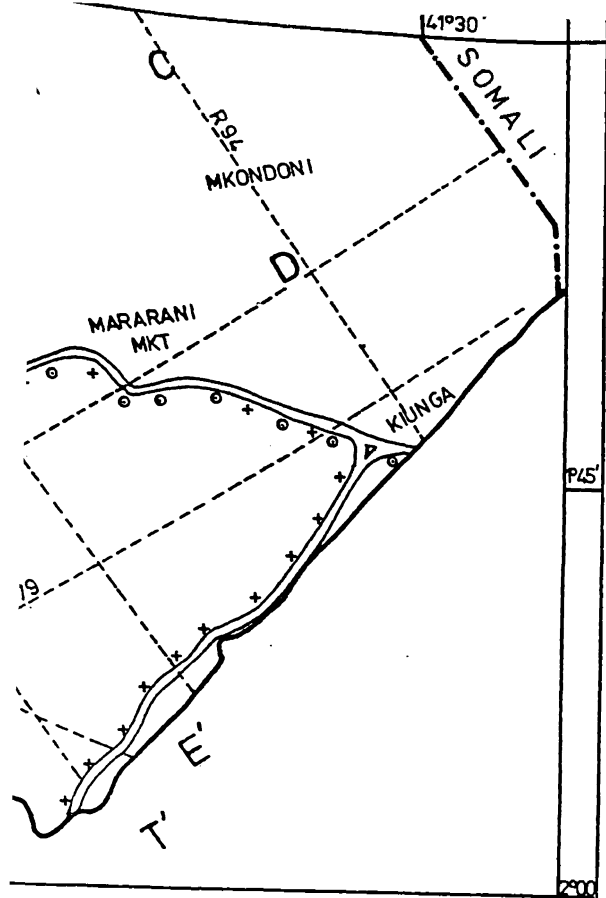
In 1959 four shallow wells (Lamu 1, Lamu 2, Lamu 3, and Lamu 4) were drilled by BP-Shell within the area. The aim was to obtain stratigraphic information in view of lack of exposures and to investigate the presence of structural features that could form potential traps. From the four wells, the stratigraphy was correlated resulting in the succession below:

1. Superficial sands of fluvial origin associated with the Tana river drainage.
2. Pleistocene raised reef limestones and back reef deposits.
3. Pliocene succession of calcareous sands with marine fossils.
4. Miocene limestones with interbedded shales and minor calcareous sand showing cyclic sedimentation.

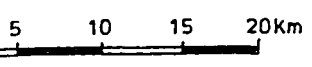
The correlation and horizontal dips indicated that overlying beds had not been disturbed much. This implied that structures

indicated by gravity anomalies do not affect beds of younger age and are therefore deep seated. During drilling, several shows of dry and wet gas were encountered.

Most of the geophysical work was done between 1954 and 1971. The gravity data in Lamu Embayment was collected by Geopprosco and BP-Shell between 1954 and 1971. Geopprosco's gravity survey consisted of 1600 km of widely spaced traverses along available roads(Fig.1.3). A Worden gravimeter NO. 212 was used throughout and an accuracy of 1.g.u was estimated from the gravity observations. The survey was related to the gravity base at the Mombasa Airport (I.G.B. No. 357495) Elevations were determined using theodolites and standard levelling practice. An accuracy of 0.3 m was estimated although an error of 5.5 m was noted. Positioning was by airphotos and mosaics, magnetic compasses and 1:500,000 maps, an accuracy of 30 m North-South being claimed between stations. No terrain corrections were applied. The BP-Shell data was obtained in the same way as Geopprosco's where 1:500,000 tie line copied scale maps were used. From this gravity data, the outline of the Lamu basin was delineated. Seismic data was acquired by BP-Shell (1954-1971). The seismic surveys were used to delineate a number of seismic highs on which deep wells were drilled(Fig 1.3). The analysis of the gravity, seismic and well log data by BP Shell (1971) delineated complex structural features within Witu-Kipini area. The structural elements were divided as follows (O'Hollarain, 1971)



- MAJOR ROADS
- MORTORABLE TRACKS
- SEISMIC LINE INTERPRETED
- SEISMIC LINE ALONG ROAD
- GRAVITY STATIONS BY OIL COMPANIES
- GRAVITY STATIONS BY THE AUTHOR
- DRILLED WELL — DRY
- DRILLED WELL — GAS SHOW



1. The Tana syncline with a NNW-SSE axis flanking the Kipini anticlinal structure on the western side and having a number of NNW-SSE faults.
2. The Kipini-Pandanguo anticlinal structure which extends from Walu southwards through Pandanguo-Witu to Kipini.

Walters and Linton (1973) correlated the stratigraphy from deep wells drilled by BP-Shell within and outside the present study area (Fig. 1.4). and noted that the Lamu embayment contains sediments of up to 10,000m thick, varying in age from Carboniferous - Permian (Karoo) to Quaternary. The earliest marine beds being middle Jurassic in age and most of the subsequent Mesozoic and Tertiary stages being represented in the overlying sedimentary succession. Basement highs were initiated during the end of Cretaceous and early Tertiary by large scale normal faulting. Regional epeirogenic movements occurred at the beginning of the Middle Eocene, near the close of the Oligocene and also in mid-Pliocene times in each case affecting profoundly the depositional regime within the embayment.

In discussing the stratigraphy of the Kenya Coast, Karanja (1982) reported that the Tertiary sediments of Lamu overlie older sediments with an unconformity and represent a distinct cycle of deposition. He suggested that Karoo age deposits of the order of 4000-6000 m thick underlie the Jurassic and younger sediments. He further reported that the Mombasa-Lamu basin was initiated as

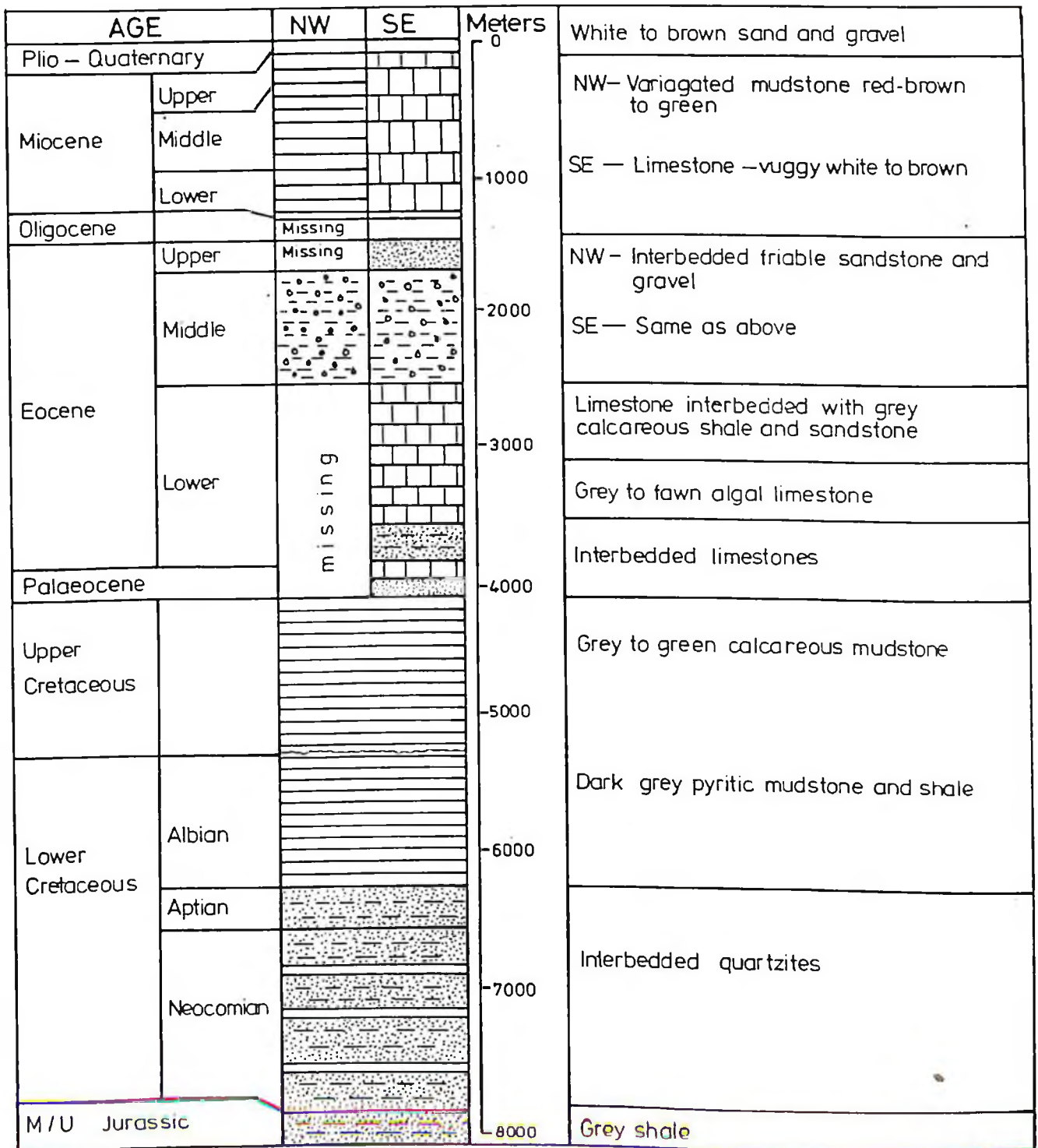


Fig. 1.4 GENERALISED STRATIGRAPHY OF LAMU EMBAYMENT

(After Waters and Linton; 1973)

a continental rift which developed from late Carboniferous to Jurassic. The development of this rift was tectonically controlled by the main deformational trend of the Precambrian rocks. Starting from the middle Jurassic, the basin developed into a passive margin of sedimentary beds with post rift sediments composed of mainly prograding marine sequences deposited in cycles separated by periods of marine and continental environments.

The pre-drift occurrence of Madagascar on the East African coast is supported by Rabinowitz et,al., (1982). They noted that the occurrence of diapirs of salt origin on the continental margin of north eastern-Kenya and south-eastern Somali coast point to the fact that this was a restricted basin environment favourable for evaporite deposition. This implies that the evaporites formed during the rift and early drift stages. They suggested that the continental margin bordering Kenya and Tanzania was created by transform motion of Madagascar along Africa, the direction of motion being shown by the alignment of the diapirs.

Coffin et, al., (1986) carried out deep seismic studies of the crustal structure in the western Somali basin situated on the eastern offshore part of the Lamu embayment. The aim of the project was to study the evolution of the western Somali basin and the East African continental margin. They noted the following:

1. Madagascar island fits very well on the Tanzania-Kenya-Somali coast and especially at Lamu.
2. Crustal structures on the Lamu coast are similar to those found on many passive margins around the world.
3. The mantle dips landward and disappears beneath a thick wedge of continental rise sediments.
4. The Jurassic sediments overlie the oceanic crust.
5. The Karroo sediments do not extend seaward from the mainland onto the Somali basin.

An attempt has been made to establish the existence of a palaeo-triple junction of Jurassic age in Eastern Kenya (Reeves et. al. 1986). They postulate that two arms represented by the Mombasa coast and Somali coast respectively developed into part of the Indian Ocean. The third arm (Anza graben) which is concealed by a cover of Quaternary sediments and volcanic rocks remains as a rifted, sediment filled trough extending at least as far northwest towards the Lake Turkana. A geometrical fault pattern correlation with the well established mid-Cretaceous Niger delta is attempted whereby, the Anza trough is correlated with the Benue trough. They however note that for this triple-junction to exist the pre-drift Madagascar has to be re-assembled in close proximity to the Tanzania-Kenya-Somali coast.

2. GRAVITY SURVEY AND DATA INTERPRETATION

2.1 INTRODUCTION

Gravity data on Lamu was collected by BP-Shell (1954-1971) and Geoprosco (1955). The BP-Shell data used in the present study was noted by Swain and Khan (1977) to contain a series of suspected errors arising from the use of incorrect density values. Besides this, the quoted coordinates could be inaccurate due to 1:500,000 scale maps used which had been tie-line copied. Geoprosco's (1955) survey consisted of 1600 km of widely spaced traverses, mainly along available roads and motorable tracks that existed by then with a station interval of 5 km being used.

The data acquired by both BP-Shell and Geoprosco was found inadequate by the writer due to wide traverses and station spacing used. The large scale maps and density values used were suspected to have affected the Bouguer and latitude corrections. In some areas where there was no proper communication, data was not collected at all. It was therefore necessary to do more work in the area to cover some of the sections that had not been mapped and to reduce the traverse and station spacing in order to improve on the data coverage. Density value for the area were to be determined and used as a check on the oil companies' results.

2.2 SURVEY PROCEDURE

2.2.1 GRAVITY MEASUREMENTS

Gravity survey and altimeter heighting were done simultaneously. Density determinations were carried out using the density profile method proposed by Nettleton (1962) to be discussed in section 2.2.4. Gravity observations were made at 205 stations using a Worden gravity meter (Gisco Model C.G.2 No. 232 G). The location of gravity base station was planned in advance based on the density of the BP-Shell data in the area. The survey was related to and tied to an international base station No. IGSN71, value 9780346.1 g.u. at Mombasa airport. Gravity stations were established along roads and motorable tracks. A few stations were established at trigonometrical points. An approximate station spacing of 3 km was used and vehicle odometer was used to obtain this spacing. Position control was obtained by use of a prismatic compass, visual observation of road orientations, junctions and drifts on topographic maps of scale 1:50,000. Six base stations were located at road junctions for future relocation.

The precision of gravity readings was about 0.01 mgals and a maximum loop closure error estimate of 0.5 mgals. This was done using the Geodetic survey method proposed by Clack(1944).

Most of the literature published concerning gravity field practice stresses the importance of returning to a base station every two to three hours to monitor and make corrections for the

instrument drift. This practice was only used in a few cases due to the difficulty of communications in the area. However, it will be shown in section 2.2.3 that gravimeter drifts could be adequately monitored and corrected for without such frequent base station readings.

2.2.2 ELEVATION MEASUREMENTS

The single base method, Swain and Khan (1977) was used. In this method two Pauline altimeters were used. At the start, both altimeters A1 and A2 were read simultaneously at the base station, then one altimeter was read continuously at the base station and A2 used for the roving measurements, (Fig. 2.1). As the work continued, the altimeter A1 at the base station was read at suitable intervals (10 minutes) so that a graph of the diurnal variation was drawn and used to correct for the values of A2. At the end of the field traversing the two altimeters were read at the base to check for vibration induced drifts in the field altimeter A2 and to complete the drift curve.

2.2.3 MONITORING OF INSTRUMENT DRIFT

Accuracy standards of gravity surveys are set so as to ensure signal/noise ratio large enough to adequately 'see' the target. The field data are therefore monitored right from the acquisition stage in order to arrive at a realistic estimate of the final plotted Bouguer anomaly. One of the parameters that requires very careful monitoring is the drift of the gravity meter used.

GRAVITY STATION NUMBER

TIME

	BASE	1	2	3	4	5	6	7	8	9	10	11	12
T ₁	A ₁ A ₂												
T ₂	A ₁	A ₂											
T ₃	A ₁		A ₂										
T ₄	A ₁			A ₂									
T ₅	A ₁				A ₂								
T ₆	A ₁					A ₂							
T ₇	A ₁						A ₂						
T ₈	A ₁							A ₂					
T ₉	A ₁								A ₂				
T ₁₀	A ₁						A ₂						
T ₁₁	A ₁				A ₂								
T ₁₂	A ₁		A ₂										
T ₁₃	A ₁ A ₂												
T ₁₄	A ₁								A ₂				
T ₁₅	A ₁									A ₂			
T ₁₆	A ₁										A ₂		
T ₁₇	A ₁											A ₂	
T ₁₈	A ₁												A ₂
T ₁₉	A ₁										A ₂		
T ₂₀	A ₁								A ₂				
T ₂₁	A ₁						A ₂						
T ₂₂	A ₁				A ₂								
T ₂₃	A ₁		A ₂										
T ₂₄	A ₁ A ₂												

FIG. 21 FIELD PROCEDURE IN THE SINGLE BASE METHOD

In this survey daily drift curves were studied to isolate suspect stations that could be repeated or discarded altogether. The practice in most cases was to take a morning start-of-loop base reading and a mid-day end-of-loop base reading, then a mid-day start-of-loop base reading and an evening end-of-loop base reading. Thus there were at least four base readings in a day. During the survey, more than 30% gravity station repeatability was ensured.

Repeat differences were calculated as repeat observed gravity minus original observed gravity. The repeat differences were used to plot daily drift curves as follows:

- (i) The drift value was plotted along the vertical axis, the morning base (MB) reading was defined as having been read at zero time.
- (ii) The days's drift was given by evening base reading (EB) minus morning base reading (MB) i.e. $g_{EB} - g_{MB}$
- (iii) The EB reading was represented by a point at $(t_{EB}, g_{EB} - g_{MB})$
- (iv) A straight line joining the origin (MB) with NB (Noon Base reading) and EB then represented the assumed drift over the day. The introduction of NB into the curve acted as a check on the accuracy of the curve.

The assumed linear curve was then tested by plotting one point for each repeat reading. If they lied close to the drift line and were randomly distributed above and below the line (Fig. 2.2)

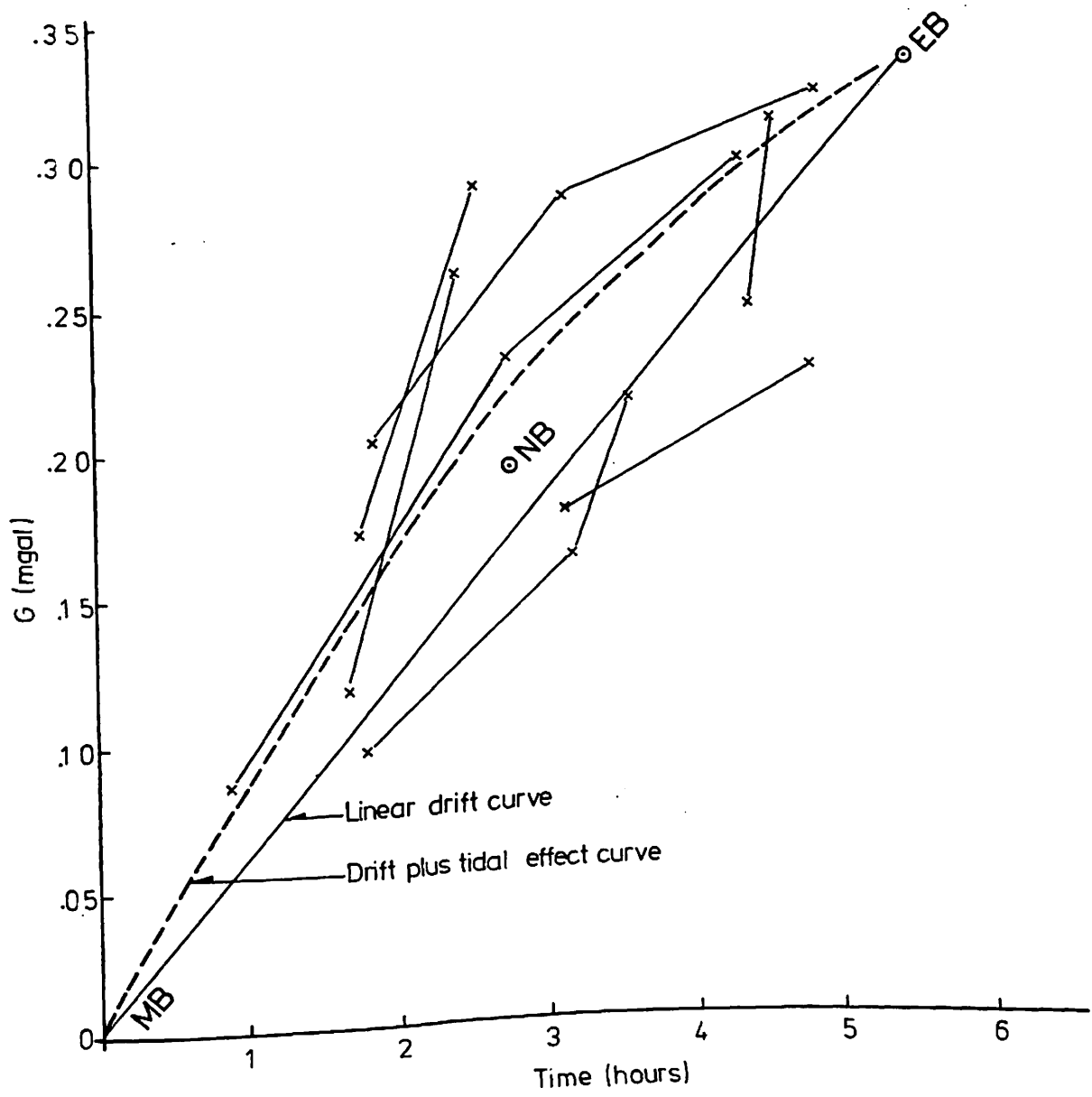


Fig.2.2 DRIFT AND TIDAL EFFECTS CORRECTION CURVE

then the drift curve was accepted. For the gravity meter, a maximum daily drift of 0.35 mgals was noted.

2.2.4 DENSITY DETERMINATION

The Bouguer corrections depend on the density of the surface material within the range of the elevation differences of the survey. Therefore some sort of estimate of surface densities must be made. In view of the lack of outcrops in the study area, the density profile method (Nettleton 1962) was resorted to. A series of closely spaced gravity traverses and stations were taken across small hills and valleys of known dimension in different locations within the area. The gravity values taken across these structures were reduced, the calculation being repeated a number of times, different densities being assumed for each computation and gravity profiles drawn. The density value which gave the smoothest reduced gravity profile across the topographic irregularity (hill or valley) was taken to be the average density value of the study area. The shape of the profile depends on the shape and dimension of the topographic feature (Fig. 2.3)

This method has more advantages than using rock samples because:

- (i) The gravity survey extended over areas of nearly the same geology so it was not necessary to use variable densities for gravity data reduction for different parts of the survey.

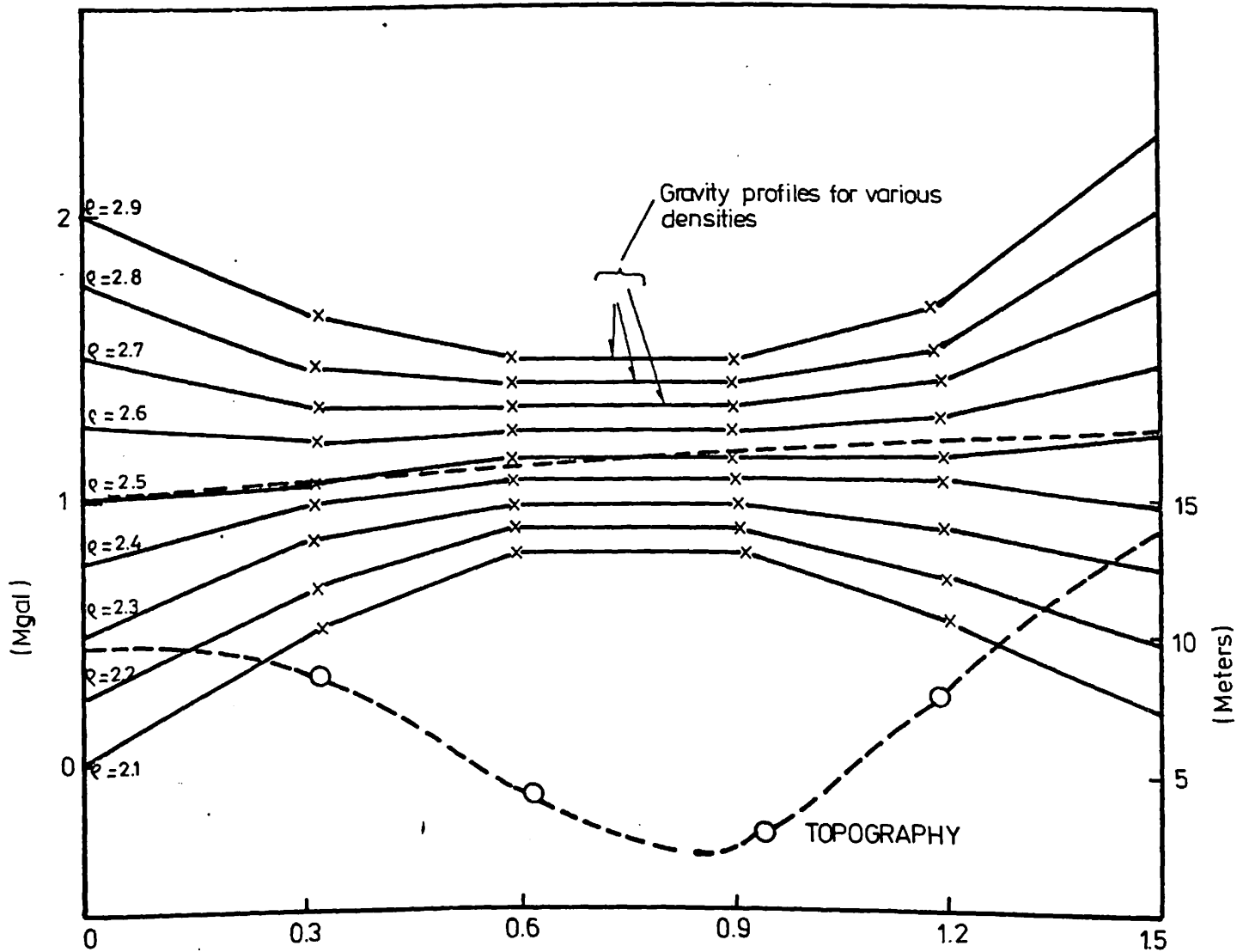


Fig. 2.3 GRAVITY PROFILES FOR DETERMINATION OF SUB-SURFACE DENSITY

(ii) It averages the actual densities in a way that would be impossible in working from surface samples.

(iii) It samples comparatively large mass of material.

This method has also some disadvantages as noted by Dobrin (1976). It is known that topographic features owe their existence to contrasts in lithology, thus they may not be necessarily representative of the areas' density value. Errors due to this effect were corrected for by using small hills and small valleys of nearly the same dimension and then finding an average. The effect of erosion resistant materials on the hills is partly cancelled by the effect of the less resistant material forming valleys.

2.3 DATA REDUCTION

To investigate subsurface variation from the gravity data obtained during a survey, the data cannot be used in the form in which it is obtained. Observed gravity values depend on latitude, elevation, topography around the station and on the distribution of mass within the earth. When contribution due to the above first three factors except the fourth have been corrected for, what remains is the contribution due to density contrasts from ground level downwards. The anomalous gravity field that result is the Bouguer anomaly. Isolation of the contribution due to the density variation in the crust is achieved by using methods of removing the longest wavelength

components, assuming that these are due to density variations in the upper mantle. The outcome of the regional separation is a residual anomaly map which can be interpreted in terms of density contrast in the earth. The various corrections performed and data reduction procedures applied to the data are outlined in this section.

2.3.1 ELEVATION ESTIMATION AND ACCURACY

To test for the accuracy of altimeters, some trigonometric points of known elevations were included. The greatest problem with altimeter surveying is that air pressure at any point on earth changes constantly due to changing weather patterns. The calculation of elevation from fixed (single) base altimeter data is based on the assumption that the changes in air pressure between the two points, the base station and the field station will coincide exactly in time and space of change. Thus the difference in air pressure between the two points is assumed constant and wholly attributable to elevation differences. This assumption is unrealistic as the changes are normally not the same within a certain distance between the two points.

For this assumption to hold, a distance of radius less than 25 km between the field altimeter A2 and base altimeter A1 was ensured. Temperatures were monitored using a pair of whirling hygrometer (wet and dry bulb). Temperature effects on the altimeter were corrected using a chart provided by the manufacturer. Some

altimeter readings were taken at known trigonometric points. This gave a maximum error of 4.0 metres. After the survey, stations were joined up into a network of loops and a check on the survey accuracy made. This gave a closure error of 3.2 metres which was distributed by using the least square method (Clendinning and Oliver, 1969). This reading error was reduced by taking three readings at a station and averaging them to get the optimum value. This could possibly give an error of about 0.01 of a metre. The calibration error is noted to be very small (0.01 of a metre).

When repeat readings were taken at the old BP-Shell station, a maximum difference of approximately 3 metres was noted. This difference seem to be due to altimeter inaccuracies, limitations of a single base method and uncertainties in relocation of the exact spot where these readings were taken.

2.3.2 REDUCTION OF GRAVITY DATA

2.3.2.1 DRIFT CORRECTION

The observed gravity value is a reading corrected for meter constant, tidal drift and instrument drift. This is a value which under normal survey conditions in the absence of other factors causing mass withdrawal should be repeatable at any future time providing that both the station and base station used are recoverable.

Initially, all the readings (originals and repeats) are reduced to observed gravity values according to the linear equation

$$g = g_{ST} - \frac{g_{EBS} - g_{MBS}}{t_{EBS} - t_{MBS}} t_{ST} + (-g_{MBS}) + g_B$$

- where
- g_B = observed gravity at the base station (mgals)
 - g_{ST} = the gravity reading at a station (mgals)
 - g_{EBS} = the evening (end of loop) base station reading (mgals)
 - g_{MBS} = the morning (start of loop) base station reading (mgals).
 - g = the observed gravity at a station
 - t_{EBS} = the time when evening base station reading was taken
 - t_{MBS} = the time when the morning base station reading was taken
 - t_{ST} = the time when the station reading g_{ST} was taken

Proper reduction of the resulting data is very important because any errors in the final Bouguer gravity value will be a combination of the errors involved in the observed gravity value and in each of the reductions applied. The Bouguer gravity B_g is the result of the expression.

$$B_g = g_0 - g_\rho + \frac{(dg)}{(dh)}h - 2\pi\rho G_h + g_T$$

where

- g_0 = the observed gravity value corrected for instrument drift and tidal effects (mgals)

g_0 = the theoretical gravity or the latitude effect (mgals)

h = station elevation (metres)

$\frac{dg}{dh}$ = the free air effect (0.30861 mgals⁻¹ above sea level)

ρ = the Bouguer density used (2.5 gm/cm³)

$2\pi\rho Gh$ = Bouguer correction (0.1048 x h)

G = the universal gravitational constant
(6.67 x 10⁻⁸ cms³ g⁻¹ cm³)

g_T = the terrain correction.

Hence

$$B_g = g_0 - g_0 + 0.3086h - 0.1048 \times h + g_T$$

It follows that the total probable error in Bouguer gravity e_{Bg} results from errors in all the above parameters and may be expressed as

$$e_{Bg}^2 = e_{g_0}^2 + e_{g_0}^2 + (c.e_h)^2 + e_T^2$$

where

C = the combined free air and Bouguer effect

$$\frac{(dg)h}{(dh)} - (2\pi\rho G)h = 0.2038h$$

e_{g_0} = error in the observed gravity value

e_{g_0} = error in the theoretical gravity value

e_h = error in the elevation value

e_T = error in the terrain correction used (as for the study area, no terrain corrections were made due to the area

being flat).

Thus, the error expression becomes

$$e_{8g^2} = e_{g_0^2} + e_{g_{\phi}^2} + (C.e_h)^2$$

2.3.2.2 TIDAL CORRECTION

The gravitational effects of the sun and moon on the earth which produces ocean tides are sufficient to have appreciable effects on a gravimeter.

Since in the present operation, the gravimeter was returned to a base station at intervals of less than six hours, any tidal effect on the drift curve is expected to be only slight and therefore does not greatly affect the gravity difference determination (Nettleton 1962). Consequently, it is assumed that the error due to tidal correction is negligible and was partly taken care of during the drift correction. Work done in the southern coast (Dindi 1982) has shown the range of tidal corrections to be generally low (0.01 to 0.02mgals).

2.3.2.3 LATITUDE CORRECTION

Latitude corrections must be applied to gravity data to correct for the effect of the oblate shape of the earth and the centrifugal force created by the earth's spin.

As a function of latitude, the theoretical gravity attraction decreases from the poles to the equator according to the

International gravity formular (Telford et. al. 1983).

$$g_{\phi} = 978031.85 (1 + 0.0053024 \sin^2 \phi + 0.0000059 \sin^2 2\phi) \text{mgal}$$

ϕ = The latitude of the gravity station in degrees.

This equation gives the gravity value that would result if the earth was a perfect oblate spheroid. By subtracting the theoretical gravity value from the observed gravity value, the Bouguer anomaly gravity remains.

2.3.2.4 TERRAIN CORRECTION

In areas where topography differs significantly from the assumed topography of a flat surface, terrain corrections must be made to account for the negative effect (i.e upward attraction) of a hill where a station is located near a hill. However, in the study area, terrain effects cannot be significant since the topography is reasonably flat and local topographic irregularities are rare.

2.3.2.5 FREE AIR CORRECTION

Despite the fact that the actual value of gravity is obtained on the physical surface of the earth, the standard value is given on an ellipsoid. The variation of the observed gravity value in the region between the earth's surface and the ellipsoid is not known as it is dependent on the variation of the mass within the earth which is not known, On the other hand, the variation of the theoretical gravity with elevation is known. It is therefore proper to reduce the standard gravity value from the standard

surface to the point on the physical earth. In this survey, theoretical values were continued upwards from the ellipsoid to the station. These corrections to gravity values take care of the free-air effects and Bouguer effect. The free-air correction takes care of the vertical decrease of gravity with increase of elevation, The rate of change this vertical gradient of gravity can be calculated quite accurately from the gravity formula and the radius of the earth. The value so calculated is:

$$g_h = g - 0.3086h \text{ mgal}$$

where

g_h = value of gravity in mgals at a height h in metres.

g = Gravity value at a reference level, commonly sea level.

The variations of the vertical gradient with latitude (only 2% from equator to the pole) and with elevation (only 0.3% from sea level to 10 km) are too small to require attention in the reduction of any gravity measurements for geophysical prospecting (Nettleton 1962). Therefore, we may consider the normal vertical gradient $\frac{dg}{dh}$ as a constant and with value of $-0.3086 \text{ mgal m}^{-1}$ which gives a simple correction called the free-air correction.

2.3.2.6 BOUGUER CORRECTION

The Bouguer correction is a correction which takes into account the effect of the material between datum level and the gravity station. The correction depends on the thickness and density of this material. A 2.5 g/cm density value was used for the correction. The Bouguer effect tends to increase the gravity and therefore is always opposite to free air effect. Thus the free-air and Bouguer effects are always opposite in sign.

In calculating corrections to gravity stations, the free-air and the Bouguer corrections were combined into a single factor which depends on the density (ρ) of the surface rocks within the range of topograph differences. This factor is:

$$C = \left(\frac{dg}{dh} - 2\pi \rho G \right) \text{ mgal}$$

where

$$\frac{dg}{dh} = 0.3086 \text{ mgal}$$

$$G = 6.67 \times 10^{-8} \text{ cm g s}^{-2}$$

$$\rho = 2.5 \text{ g/cm}^3$$

$$\begin{aligned} \text{therefore } C &= (0.3086 - 0.04193 \rho) \text{ mgal m} \\ &= 0.2038 \text{ mgal m}^{-1} \end{aligned}$$

2.4 ACCURACY OF THE SURVEY

In section 2.3, it was shown that error due to terrain effect is negligible because of the uniform topography. It was also shown that the error due to theoretical gravity used is small since the

area is within 2.5 degrees of the equator and topographic maps of scale 1:50,000 had been used.

This implies that the remaining errors that could constitute the Bouguer anomaly error are due to:

- (i) Observed gravity
- (ii) The elevation correction

i.e.
$$e_{Bg}^2 = e_{g0}^2 + (c \cdot e_h)^2$$
$$c = \frac{(dg - 2\pi\rho G)}{dh} \text{ mgalm}^{-1}$$
$$= 0.2038 \text{ mgalm}^{-1}$$

$$e_{g0}(\text{max}) = 0.5$$

$$e_h(\text{max}) = 4.0$$

$$e_{Bg}^2 = (0.5)^2 + (4.0 \times 0.2038)^2$$
$$= 0.25 + 0.6645$$
$$e_{Bg} = \sqrt{0.9145}$$
$$= 1.0 \text{ mgal}$$

It is noted that part of this error is due to height estimates used.

This is likely to be the major contributing factor in the 1.1 mgals maximum Bouguer anomaly difference between the data obtained during the present survey and that of BP-Shell (1954 - 1971) and Geoprosco (1955).

2.5 INTERPRETATION OF GRAVITY DATA

Gravity fieldwork and data reduction is usually completed by the

preparation of a map showing station locations with reduced or corrected values (with latitude, elevation, Bouguer and terrain corrections having been made).

The distribution of reduced gravity values shown by any Bouguer anomaly map is caused by departures from the uniform mass distribution within the earth crust that has been assumed in reducing the station. This means that the gravity pattern of the map is caused by the sum of departures from the uniform ideal spheroid shape of the earth beginning at the surface and extending into the interior.

The earth may be considered as made up of a series of shells which may be of different densities. Gravity measurements are therefore not sensitive to vertical variations in density so long as the density is constant in horizontal layers. However, any horizontal variation in density will cause lateral variation in gravity (Dobrin 1976)

Interpretation of gravity data in the present study was done by determining the lateral variation in density which was taken to be related to lateral variations in geology. It was assumed that geologic condition that results in lateral variation in density and therefore geology will cause a gravity anomaly. The magnitude of this anomaly will depend on the density contrasts involved, the magnitude and the form of geologic deformation.

The cause of gravity variations was taken to be due to four possible causes:

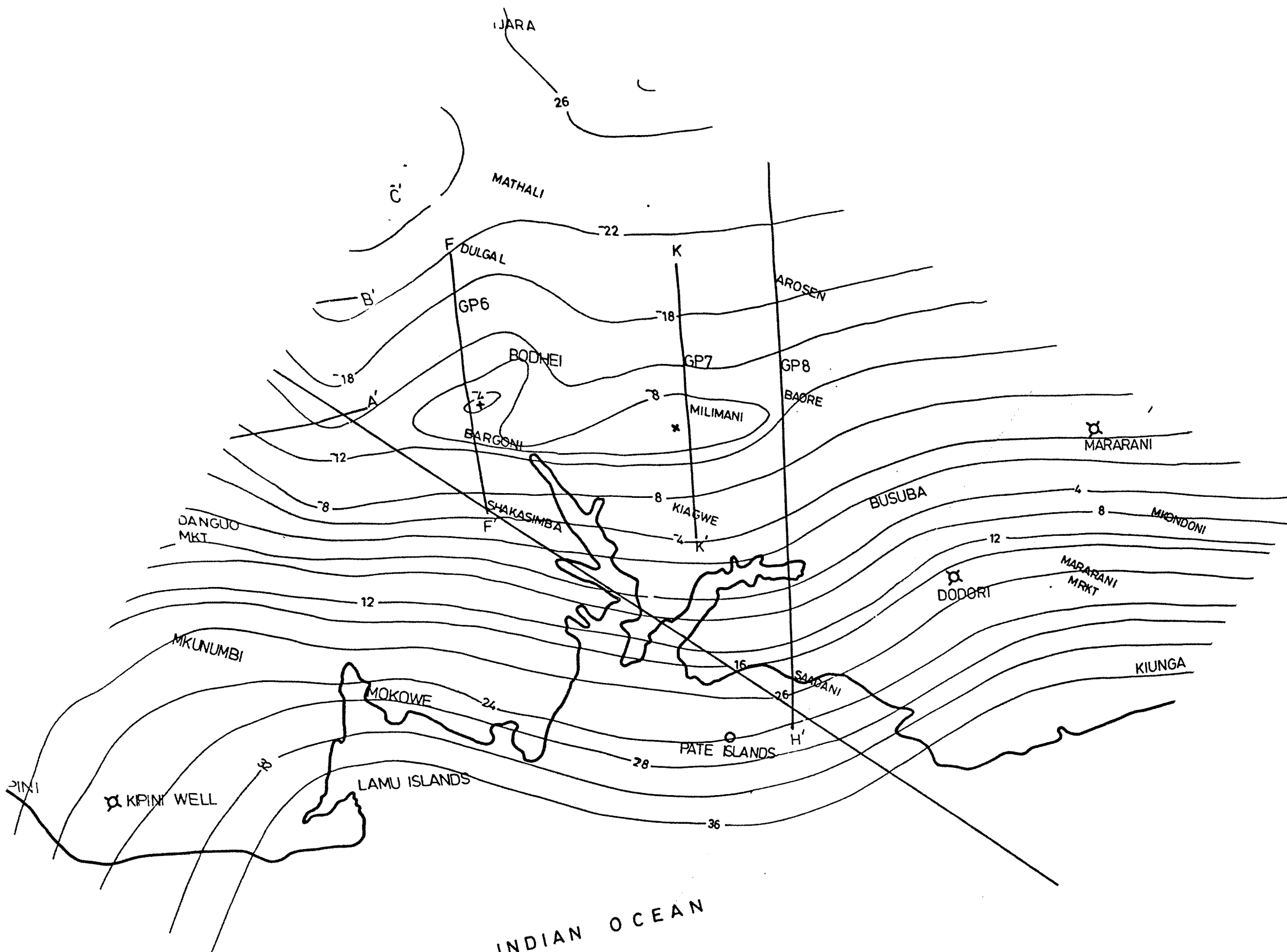
- (i) Variations in basement topography resulting in basement highs and lows.
- (ii) Igneous intrusions
- iii) Variations in the type (density) of basement rocks on which sedimentary rocks are overlain.
- (iv) Lateral variations in the density of overlying sediments.

To determine the dimensions of causative bodies, simple models were used. Complex models were not attempted as the author had no access to appropriate computer softwares. Results of interpretation using simple models were later found to be geologically reasonable and in good agreement with findings from seismic reflection and borehole logging. Initially the data were interpreted qualitatively to identify any interesting structures and trends. A few of these structures were then selected for quantitative interpretation through 2D modelling. This was done using a pocket calculator.

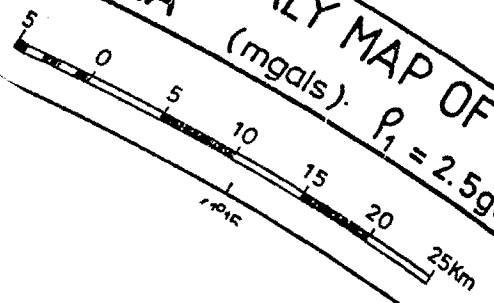
2.5.1 QUALITATIVE INTERPRETATION

2.5.1.1 THE BOUGUER ANOMALY MAP

A Bouguer anomaly map was drawn at a scale of 1:250,000 with a contour interval of 4 mgals (Fig. 2.4). To obtain this map, Bouguer anomaly values were posted onto a gravity station map. Contouring was done by hand using the values at the stations for



BOUGUER ANOMALY MAP OF THE STUDY AREA (mgals). $\rho_1 = 2.5 \text{ g cm}^{-3}$



interpolation. The Bouguer anomaly in the area varies from high positive offshore to low negative onshore. The decrease in the field is both in the westward and northward direction. The map shows that the western and north western parts were the most tectonically disturbed before they adjusted isostatically, Coffin et al (1986). The Bouguer anomalies in the western part are part of the regional anomaly. This implies that the causative bodies are deep seated basement structures that have led to gravity highs and lows. The eastern part of the study area appears to be less disturbed with a uniform decrease of Bouguer anomaly values northward. There is a small localised positive anomaly superimposed on the regional around Bodhei. The Bouguer anomaly map shows three structures of interest.

- (i) A major NNW-SSE trending anticlinal structure along the Walu- Pandanguo line, EE1(profile GP5)
- (ii) A NE-SW synclinal structure crossing the Walu-Pandanguo structure at approximately 750 along Kitole -Jarakuda line, CC1(profile GP2)
- (iii) A minor localised antiform around Bodhei and Milimani with a NE-SW trend.

On comparing the Bouguer anomaly map of Kenya (Swain and Khan 1977) with the Bouguer anomaly map of the study area, a general agreement is noted as regards the Bouguer anomaly trends (increase of anomaly values towards the sea) and on the

occurrence of the Walu-Pandanguo anticlinal structure. The Kenya map does not however show the Kitole-Jarakuda synclinal structure and the Bodhei antiform.

2.5.1.2 REGIONAL FIELD SEPARATION

Regional effects are large scale disturbances arising from density irregularities which may be at much greater depth than those of possible structures in which we are interested. The removal of this effects is normally desirable.

In the present study, the regional effect was determined by drawing a profile across the least disturbed region (GP 8). This profile was compared with those drawn across anomalous regions. It was ensured that these profiles start at a distance away from particular anomalies before crossing them.

The residual was found superimposed on the regional and by smoothing out the residual, the regional remained. The same procedure was followed for several other profiles, each time comparing with profile GP 8 from the non-disturbed region. From all these profiles, an average regional profile for the whole area was determined (Fig. 2.5)

The choice of the profile direction to be used for determination of the regional anomaly was dictated by the trend of the Bouguer anomaly contours. The contours show that the regional gradient

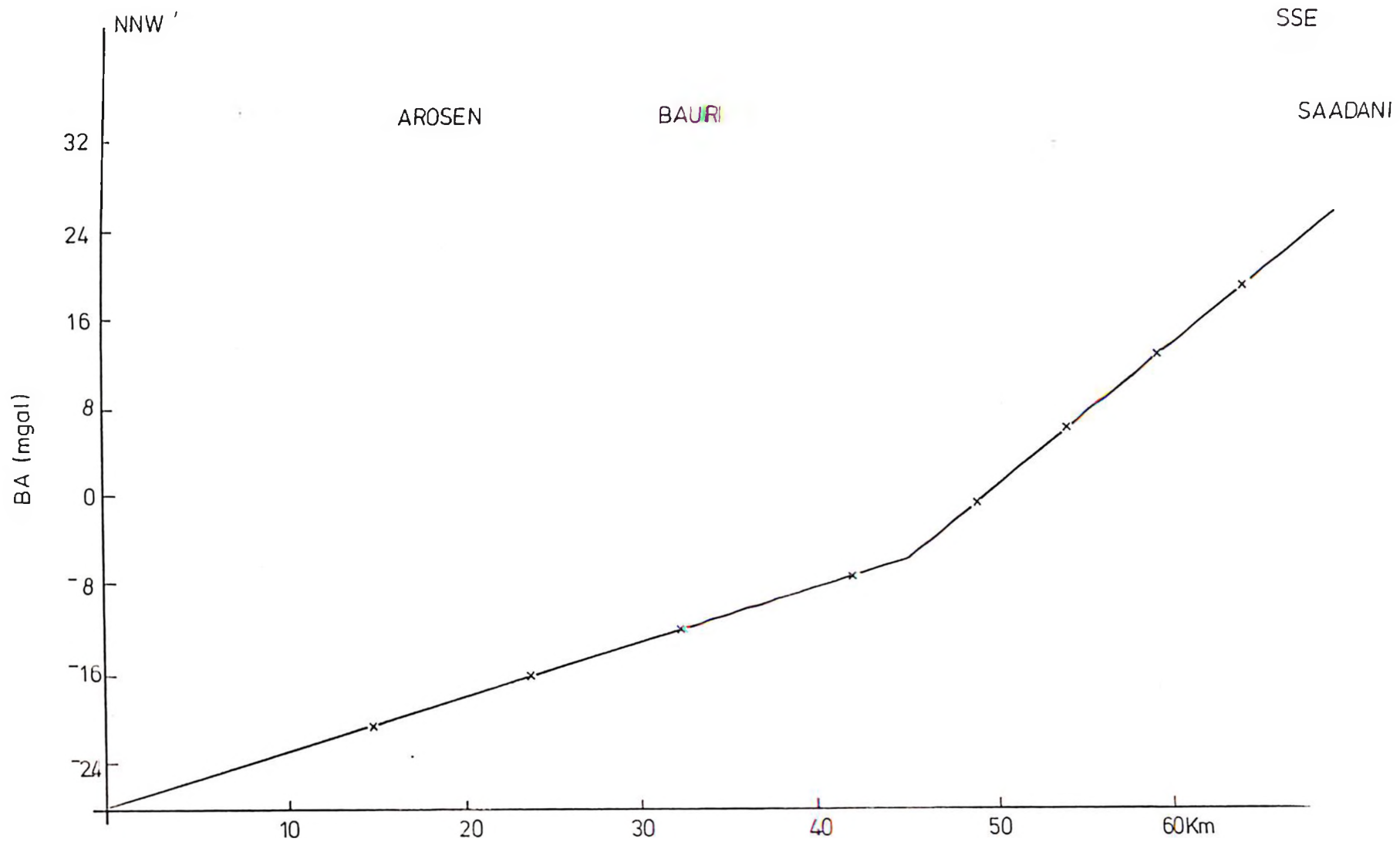


Fig.2.5 REGIONAL ANOMALY PROFILE

Scale - 1:250,000

strikes roughly NW-SE. All the profiles were drawn in that direction.

It should be noted here that the regional determination in the present study involved a considerable amount of arbitrary judgement without any very definite quantitative basis. The final regional profile determined show that the regional anomaly increases towards the sea (from NW to SE). The regional gradient occurs in two parts. The first part is mostly onshore and the second part is offshore.

Onshore, there is an average gradient of 0.4 mgal/km. Towards the offshore part, this gradient changes along Witu-Mkunumbi-Busuba line to a gradient of 1.3 mgal/km. The gradient change seem to correspond to the regional dip of sediments (as will be shown by seismic later). The major structures in the study area occur onshore within the region of gradient 0.4 mgal/km. This gradient is fairly small compared to the average size (magnitude) of the anomaly associated with the structures (10 mgals). The regional effect was therefore assumed to be negligible.

However, for the Bodhei structure, the small size of the anomaly necessitated regional-residual separation before interpretation could be done.

2.5.1.3 INTERPRETATION OF STRUCTURES

2.5.1.3.1 WALU-PANDANGUO ANTICLINE

This is a deep seated anticlinal structure which seem to be due to a basement high. It extends for about 60 km from Walu in the northwest of the area to Pandanguo in the south-east. A closed high along this structure occurs at the Walu well. The peak value is - 4 mgals. This appears to be the most raised section of the basement high. Southwards the anomaly becomes less pronounced and disappears before reaching Mkunumbi, south of Pandanguo. In the region of Alitubo, this anomaly is interrupted by a NE-SW trending synclinal structure. The syncline divides the Walu-Pandanguo anticline into two parts with the north-western half forming a pronounced oval outline. The nature of the Bouguer anomaly north of Walu suggests that the structure might be extending outside the present area at the north-western corner. The trend of the anomaly contours however suggest that this extension may only be for a short distance. At Walu, the anomaly is about 40 km East-West and decreases southwards to less than 30 km to the south east of Pandanguo well. The diminishing of the anomaly southwards suggest that the structure plunges in that direction.

Four profiles across this anomaly and one along the hinge-line have been used to analyse the structure. Since the Walu well is located right on the hingeline, profiles GP 1 and GP 5 were drawn through it (Fig. 2.4). At Pandanguo, profiles GP 4 and GP 5

were drawn as close as possible to the Pandanguo well. These wells served as controls on gravity results.

Gravity control within the area of this anomaly is good as gravity stations are closely spaced. Since the trend of this major anomaly is in the regional gradient and is part of the regional, no regional residual separation was done on the Bouguer anomaly profiles. Also profiles to be used for structural analysis were taken perpendicular to the anomaly and hence the regional trend. Because of these factors, the effect of the regional on the anomaly interpretation is thought to be negligible.

PROFILE GP 1

The profile was across Walu from Kivukoni through the Walu well to Calcal (Fig. 2.6) and is symmetrical about a point slightly west of Walu well. This profile was chosen specifically for studying the dimensions of the structure around Walu. The profile shows that the anomaly is well pronounced with an amplitude of 11 mgals. The anomaly has a smaller wavelength here than to the south. On the flanks of the peak, the fall off of the anomaly is sharp, this may imply that the causative body is shallow at this place.

PROFILE GP 2

This profile (Fig. 2.7) was taken in an approximately northeast-southwest direction from south of Kitole running through Alitubo

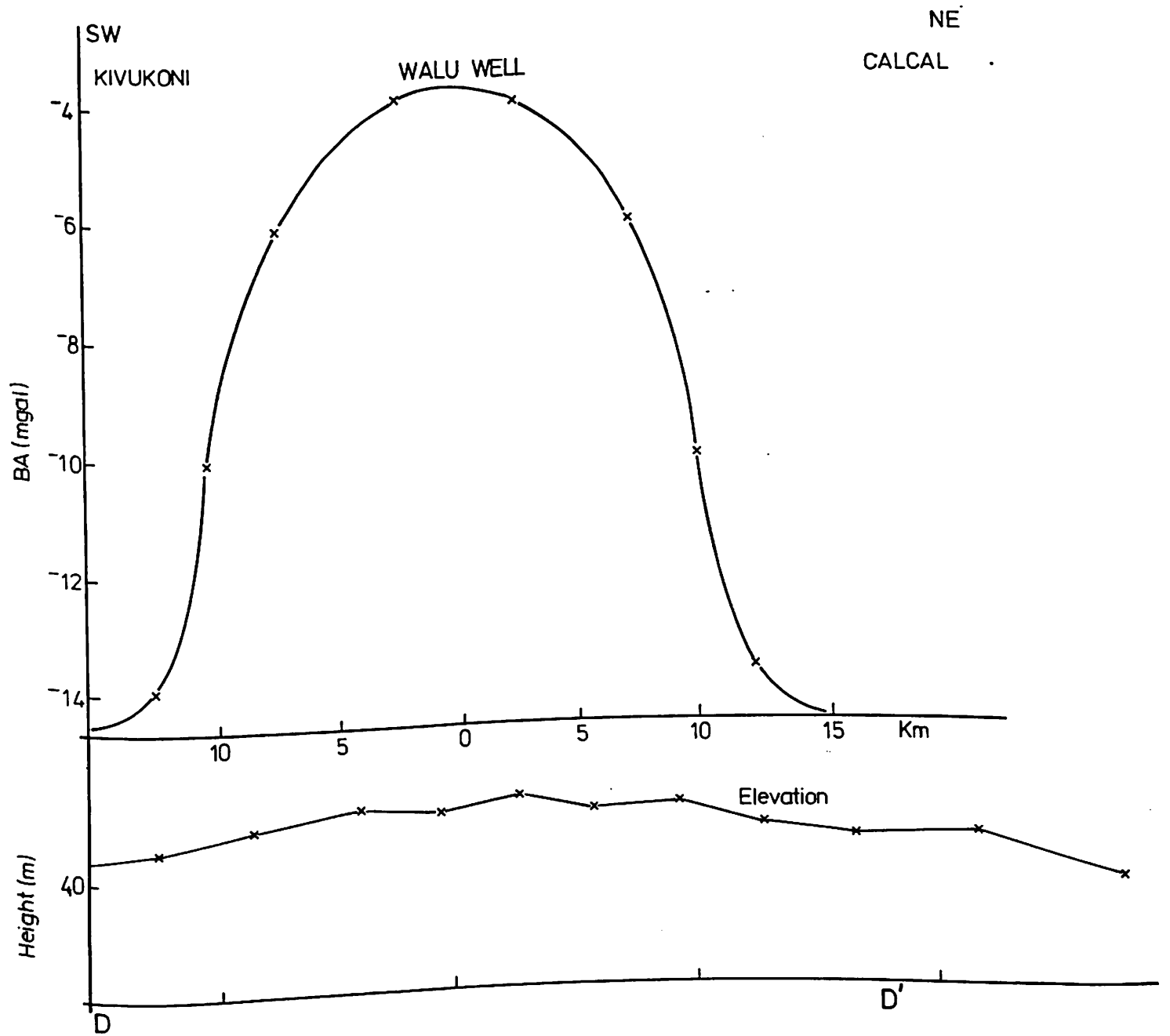


Fig. 2.6 BOUGUER ANOMALY PROFILE GP1
 ($\rho_2 = 2.67 \text{ gcm}^{-3}$)
 Scale = 1:250,000

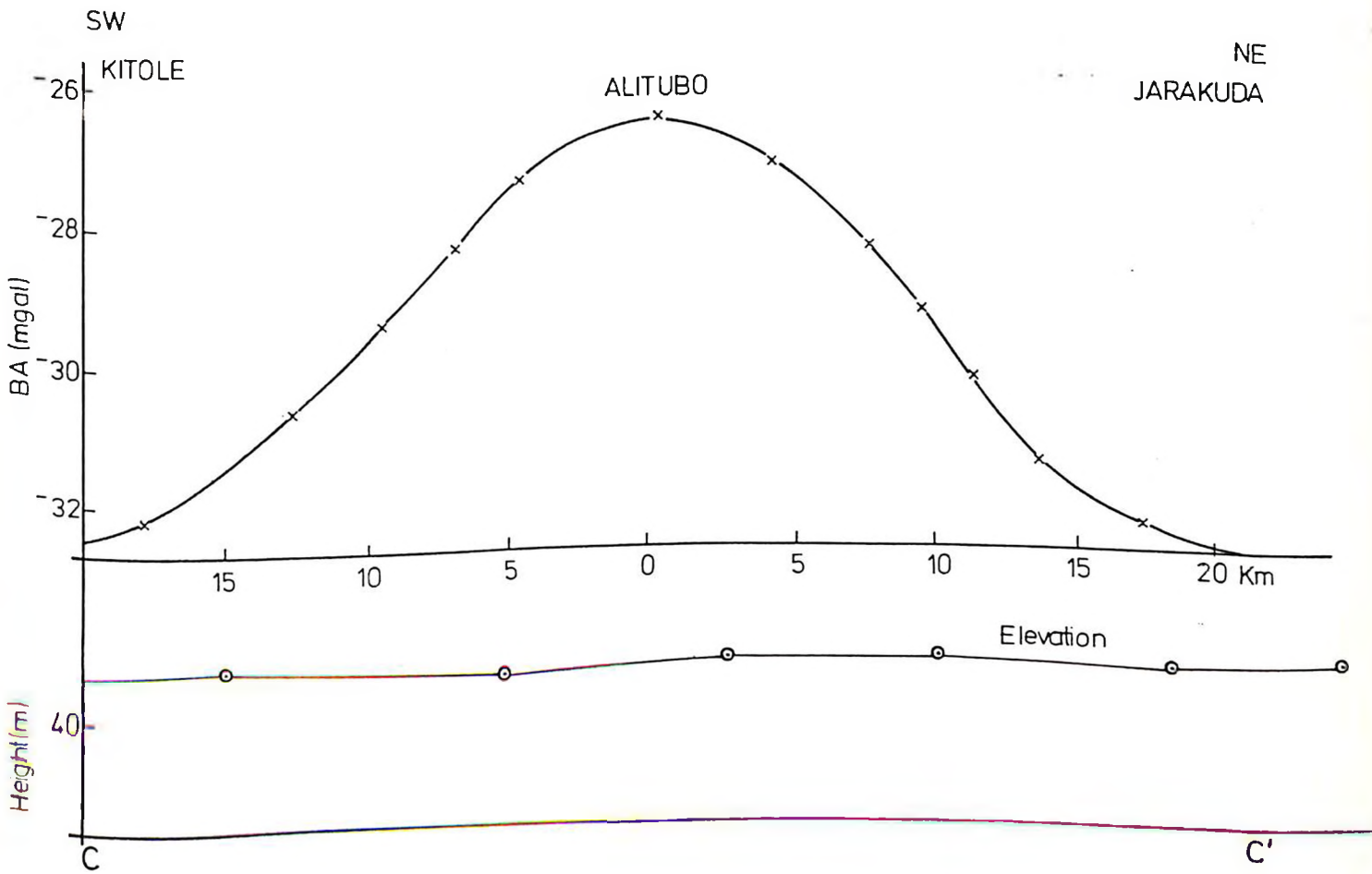


Fig.2.7 BOUGUER ANOMALY PROFILE GP2
($\rho_2 = 2.67 \text{ gcm}^{-3}$)
Scale = 1:250,000

to Jarakuda. The profile is symmetrical about Alitubo with an amplitude of 6 mgals. The fall off of the profile on the flanks of the peak is gentle suggesting that the body causing the anomaly is very deep. It is expected to be much more deeper than at Walu. This profile was chosen with the aim of studying the nature of disturbance on the Walu-Pandanguo trend by the NE-SW synclinal structure in the vicinity of Alitubo.

PROFILE GP 3

A Bouguer anomaly profile GP 3 (Fig. 2.8) was made in a NE-SW direction across the anomaly. This profile was taken some 12 km south of profile GP 2. It was used for comparison with profile GP2 to give a picture of the sort of change of depth to the structure to the immediate south of Kitole-Alitubo-Jarakuda line of disturbance. The Profile passes through Pangani with a peak amplitude of 10 mgals at Delisa. The flanks of the peak are sharper than GP 2 but less than GP 1. This implies that at this point (Delisa), the structure is deeper than at Walu (GP 1) and less deeper than at Alitubo (GP 2)

PROFILE GP 4

This profile is at the southern-most limit of the anomaly. It was taken from Tula running through Pandanguo to Rufu (Fig. 2.9). At Pandanguo, it passes about 2.5 km south of the Pandanguo well. The peak of the profile is at Pandanguo where it has an amplitude of about 9 mgals. The flanks of the peak of the profile are

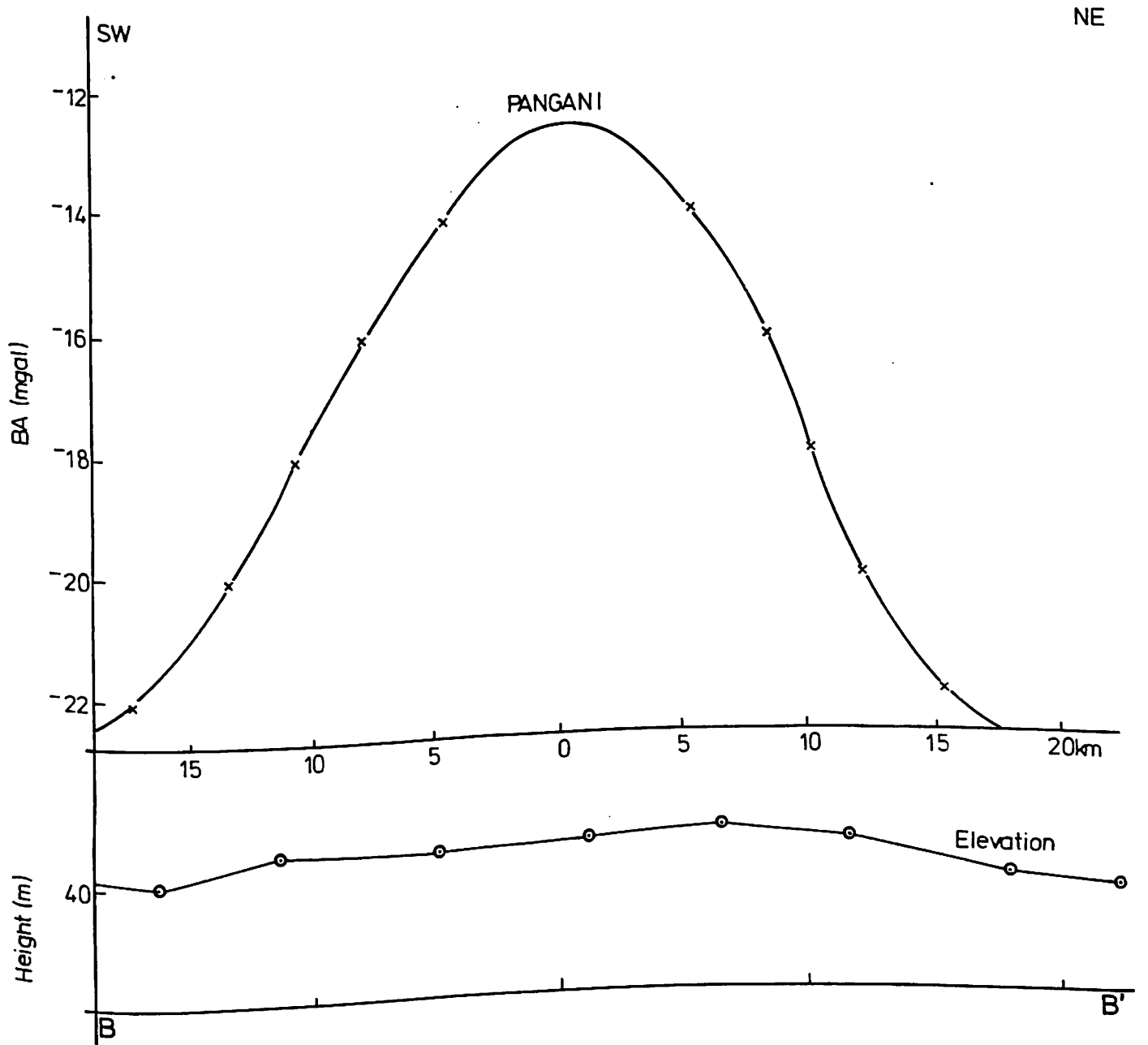


Fig. 2.8 BOUGUER ANOMALY PROFILE GP3
($\rho_2 = 2.67 \text{ gcm}^{-3}$)
Scale = 1:250,000

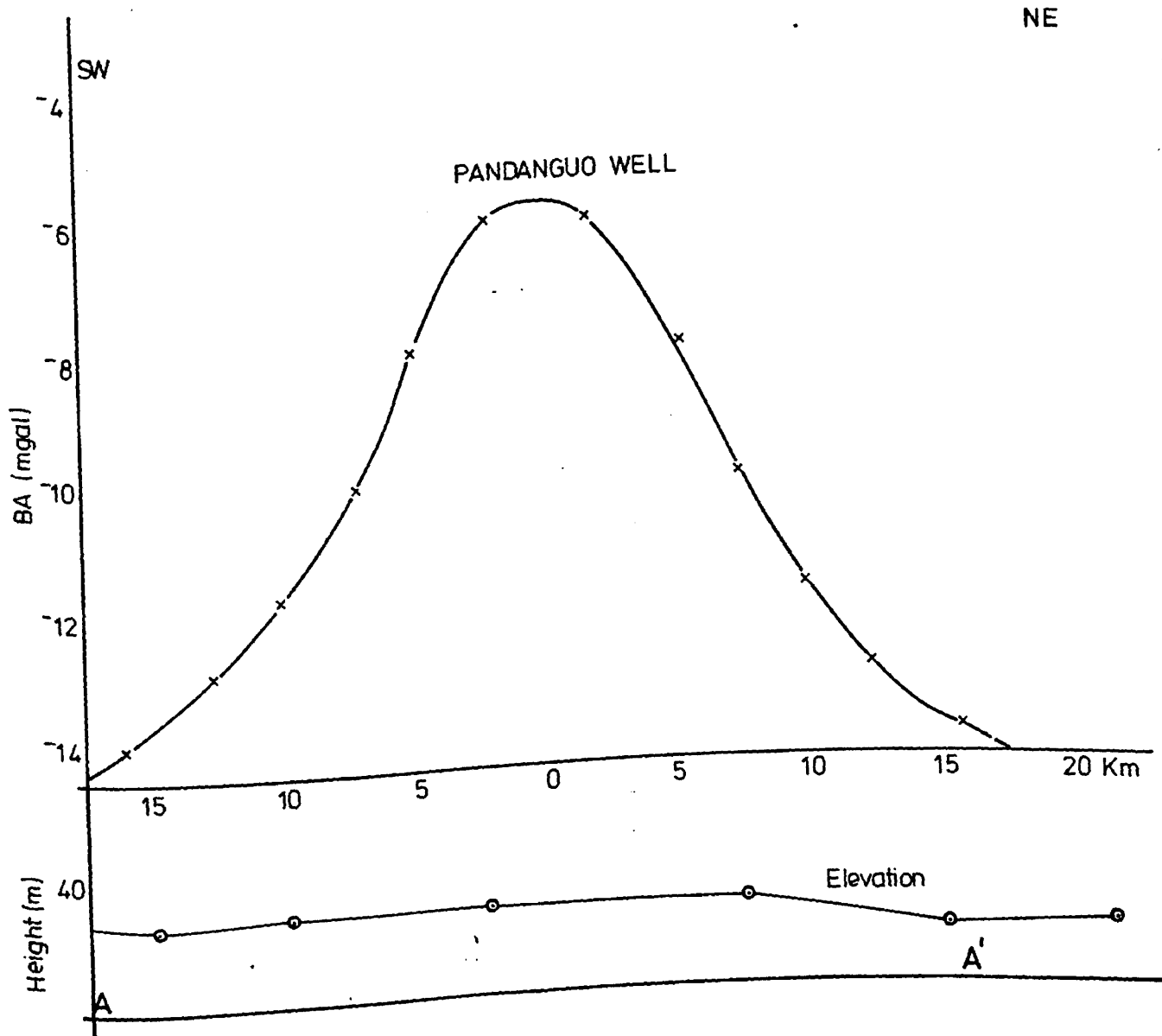


Fig. 2.9 BOUGUER ANOMALY PROFILE GP4
($\rho_2 = 2.67 \text{ gcm}^{-3}$)
Scale $\div 1:250,000$

sharper than in profiles GP 3 and GP 2.

The profiles discussed show that the depth to the structure increases from Pandanguo to Delisa and Alitubo. At Walu, the structure is shallowest.

PROFILE GP 5

This profile was taken perpendicular to other profiles (GP1, GP2, GP3 and GP4) along the hingeline of the structure running through Pandanguo, Delisa, Alitubo, Hara and the Walu well (Fig. 2.10). The aim of this profile was to give a complete picture of the structure's hingeline that had been shown to be far from simple by profiles GP1, GP2, and GP4. The profile shows two different gradients from Walu to Alitubo and from Alitubo to Pandanguo. The Walu-Alitubo gradient is very sharp and suggests that there was an abrupt discontinuation of the structure by some sort of subsidence at Alitubo (block form).

The profile has two gradients which join into an asymptotic curve around Delisa. This results in a step sort of appearance suggesting the presence of a step-fault. The profile at Alitubo shows a narrow trough (graben) implying great thickness of sedimentary cover.

2.5.1.3.2 KITOLE-JARAKUDA SYNCLINE

This synclinal structure has NE-SW trend with two near-elliptical

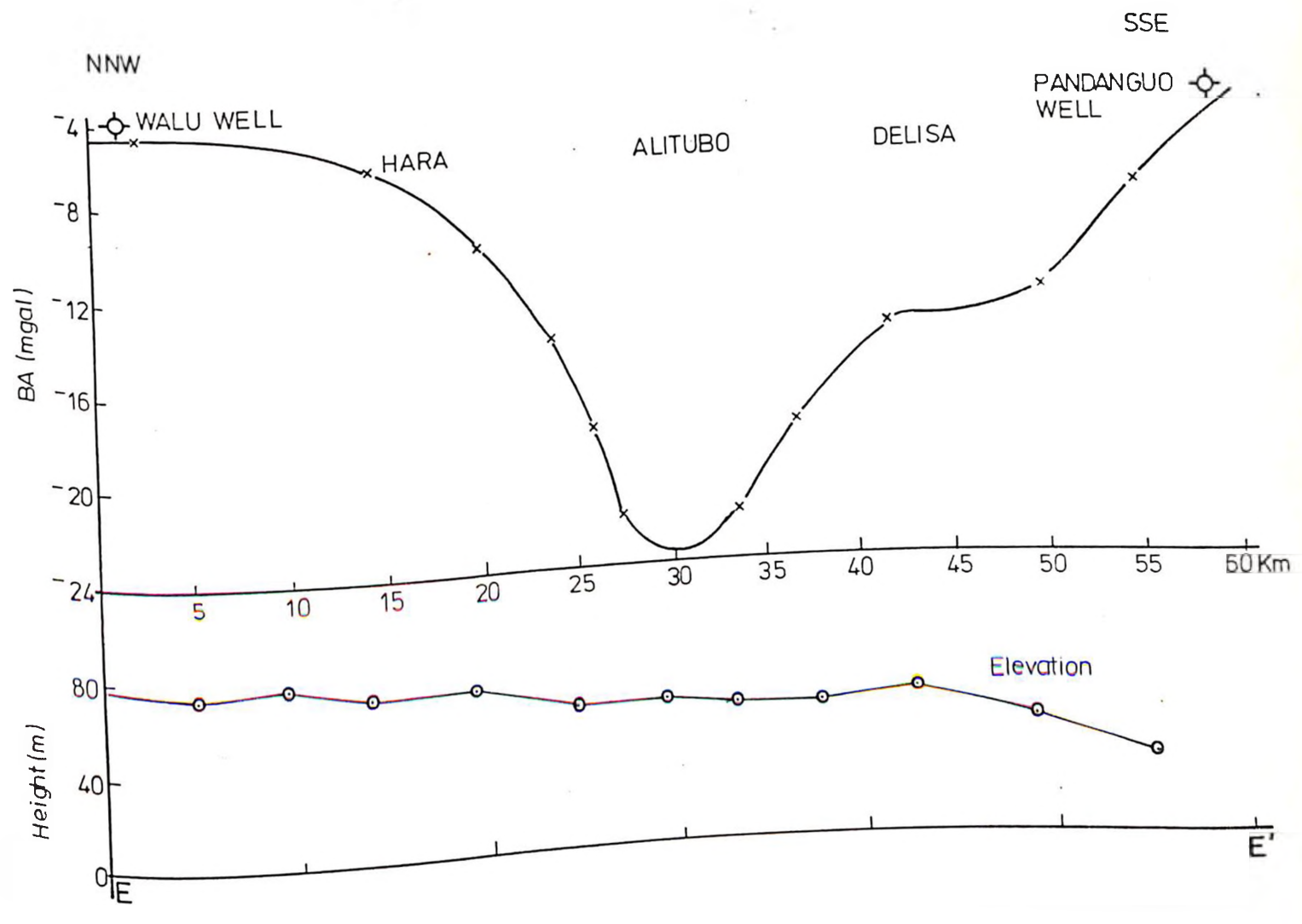


Fig. 2.10 BOUGUER ANOMALY PROFILE GP 5
($\rho_2 = 2.67 \text{ gcm}^{-3}$)
Scale $\div 1:250,000$

troughs at Kitole and Jarakuda. The two troughs have similar minimum Bouguer anomaly values of - 30 mgals. In the northeastern part, the structure broadens and becomes shallow especially north of Mathali. Further north to the NE of Ijara, another trough appears with a - 30 mgals minimum Bouguer anomaly values. This trough extends outside the study area. Since gravity stations are not well distributed within the Ijara area, the definition of this trough based on contours is not reliable.

The three troughs are similar in that they all have about the same anomaly amplitude and are almost circular in outline. It is concluded that the troughs are part of a single basin with a NE-SW trend. That is, the troughs form the deepest parts of the sedimentary basin. The separation of Kitole and Jarakuda into two troughs is likely to have been caused by the resistance of the Walu-Pandanguo structure to subsidence.

2.5.1.3.3 THE BODHEI GRAVITY HIGH

The anomaly is localised around Bodhei and occur as two joined anomalies forming a near elliptical sort of figure with a NE-SW trend. The maximum Bouguer anomaly value of -4 mgals is at the western part. The anomaly extends for a distance of 40 km from west of Bargoni to west of Milimani. It has an average width of 7 km. The profiles GP6, and GP7 were drawn across the anomaly in a NW-SE direction (perpendicular to the anomaly trend).

PROFILE GP 6

The profile GP6 (Fig. 2.11) is from Dulcal through Bargoni to Shaka Simba. This profile shows the anomaly as a residual superimposed on the regional. After separation of the regional by smoothing, a residual anomaly of amplitude 9 mgals remained. The peak of the anomaly was found to be at a point 3 km NE of Bargoni. The superimposition of the Bouguer anomaly onto the regional suggests that the causative body is not deep seated.

PROFILE GP 7

This profile (Fig. 2.12) was drawn with the aim of trying to relate the dimension of the structure at the two peaks (Bargoni and Milimani). The profile runs through Milimani and Kiangwe. After removing the regional anomaly by smoothing, a residual anomaly of amplitude about 7 mgals remained with the peak slightly south of Milimani. Comparing the residuals of profile GP6 and GP 7, it is noted that profile GP 7 has a more gentle fall-off of the profile on the flanks of the peak. The amplitude and nature of the profile flanks suggests that the structure is deeper on the northeastern side.

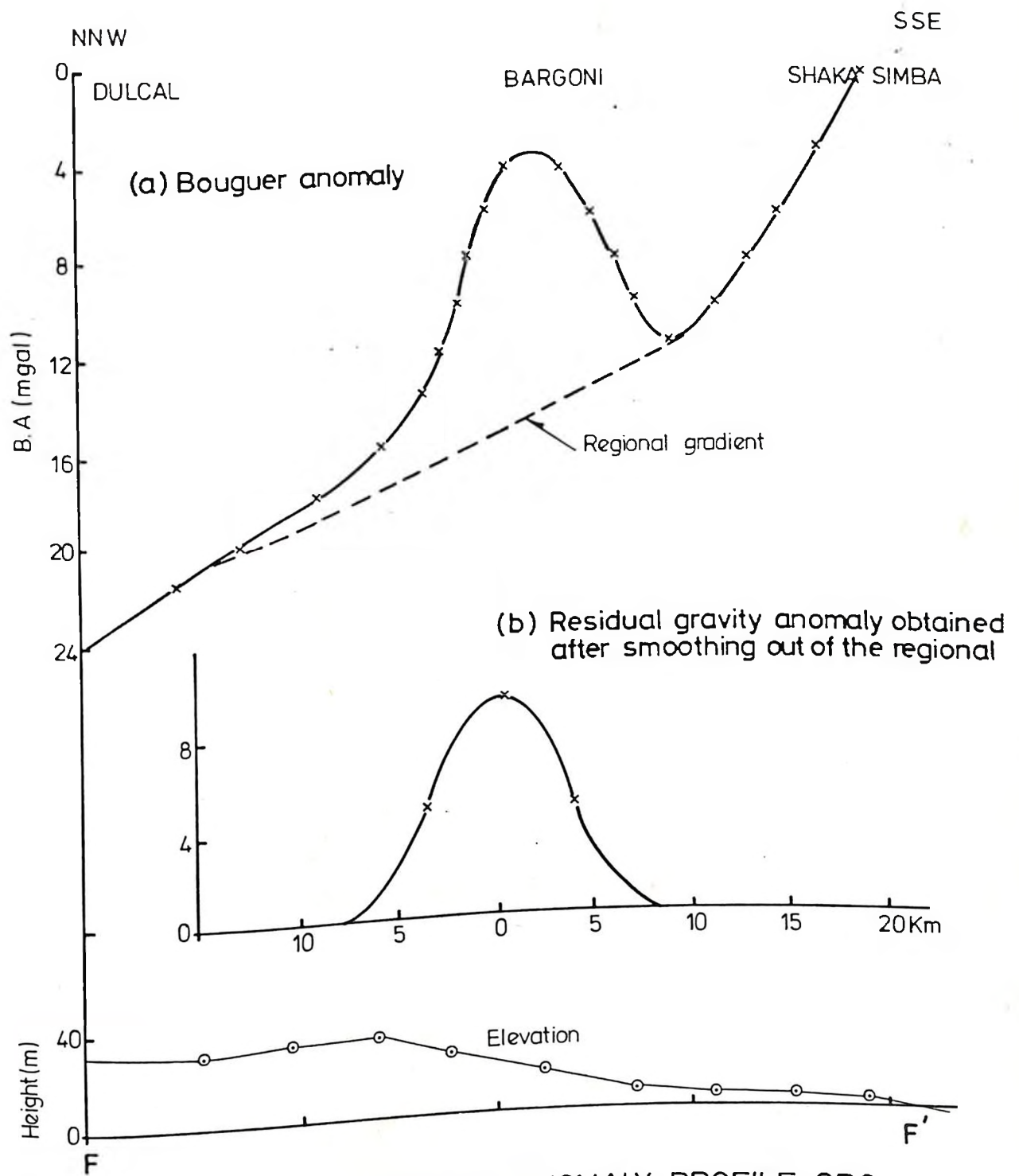


Fig. 2.11

BOUGUER ANOMALY PROFILE GP6
($\rho_2 = 2.67 \text{ gcm}^{-3}$)
Scale = 1: 250,000

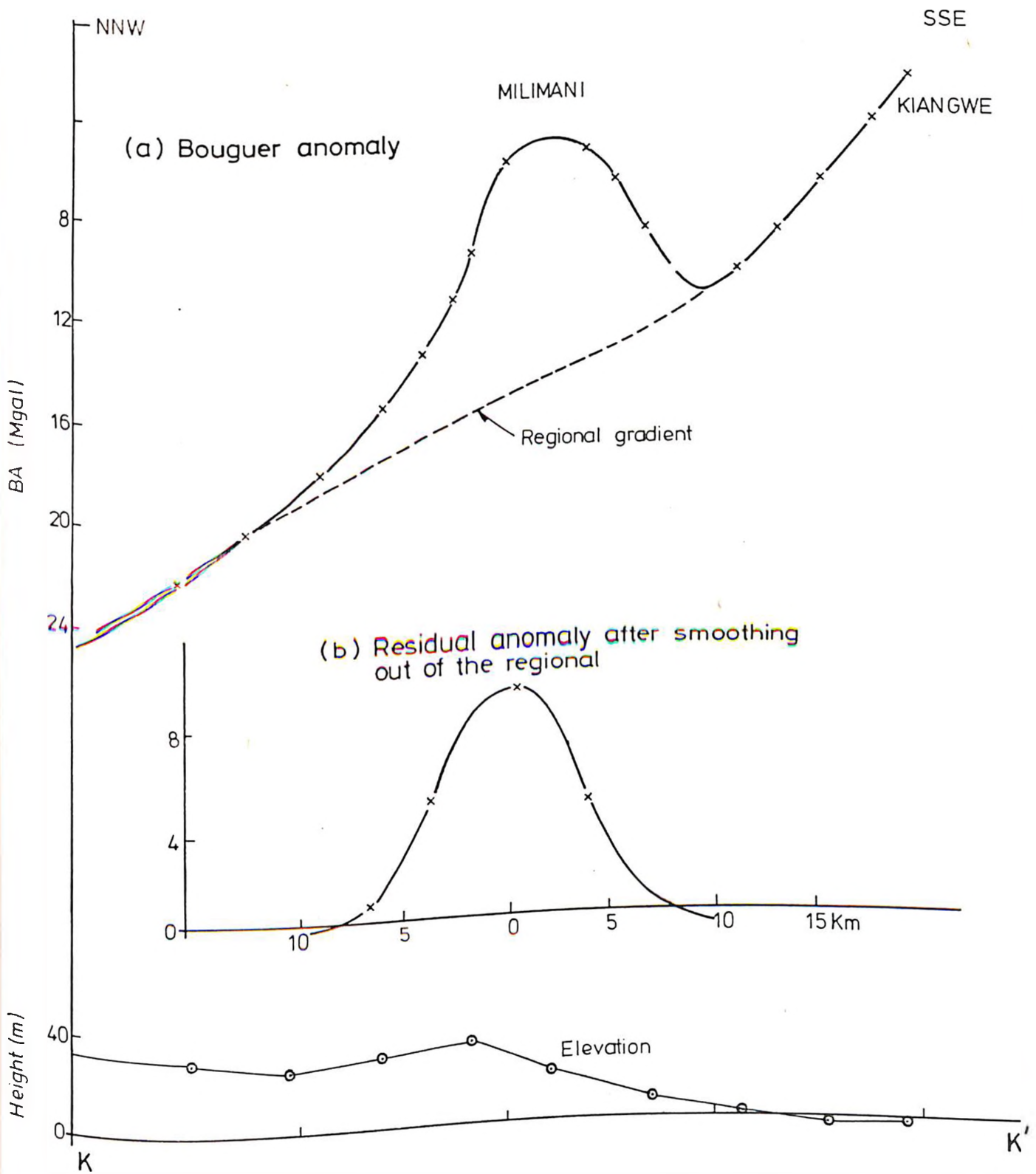


Fig. 212 BOUGUER ANOMALY PROFILE GP 7
($\rho = 2.67 \text{ gcm}^{-3}$)

Scale - 1:250,000

2.5.2 QUANTITATIVE INTERPRETATION

In order to give a quantitative interpretation of the anomalies in the study area, it was necessary to approximate the dimensions of the causative bodies to a geologically realistic geophysical model. The type of model to be chosen (2D or 3D) depends on the shape of the Bouguer anomaly. Bouguer anomalies in Lamu show that the causative bodies have lengths greatly exceeding the width. This calls for the use of two Dimension (2D) models (Dobrin 1976. Grant & West 1965).

The criterion used for determination of whether 2D or 3D models are required is also given by Nettleton (1962). He notes that a body can be approximated to a 2D model, "where conditions perpendicular to the profile are essentially constant for a distance either side of the profile of about 2-3 times the depth of the section calculated". Based on this criterion, the Walu-Pandanguo and Bodhei anomalies can be considered to be due to 2D bodies.

Here we consider an infinitely long cylinder of radius R with a horizontal axis which is buried at a depth Z_c below the datum surface. By division of the cylinder into elementary parts and summation of the total attraction of the parts, it can be shown that the total attraction of the cylinder at a distance r from the axis is:

$$g = \frac{2\pi\delta R^2 G}{r}$$

Along a surface profile perpendicular to the axis of the cylinder (Fig. 2.13), the vertical component of gravity (g_z) is given by:

$$g_z = g \frac{Zc}{r}$$

$$= \frac{2\pi R^2 G \delta Zc}{r^2}$$

where $r = (x^2 + Zc^2)^{0.5}$

Therefore $g_z = \frac{2\pi G \delta R^2}{Zc} \left[1 + \frac{x^2}{Zc^2} \right]^{-1}$

where g_z = vertical component of gravity

G = Gravitational constant

$$= 6.67 \times 10^{-8} \text{ cm}^3 \text{ g}^{-1} \text{ s}^2$$

R = Radius of the cylinder (m)

Zc = depth to the centre of the cylinder (m)

δ = density contrast between the basement and sedimentary material ($\rho_2 - \rho_1$) gcm^{-3}

the value of g_z at $x = 0$ and normally the maximum is given by

$$g_z \text{ (max)} = \frac{2\pi G \delta R^2}{Zc}$$

On the anomaly profile, we call the value X where g is one half its maximum value, the half-width ($X_{1/2}$). At this point the quantity

$\left[1 + \left(\frac{X}{Z} \right)^2 \right]^{-1}$ will be numerically equal to 0.5

(Telford, et. al., 1983, Nettleton, 1962).

Inverting the above relation, we get:

$$1 + \left[\frac{X_{1/2}}{Z_c} \right] = 2$$

$$\frac{X_{1/2}}{Z_c} = 1$$

$$Z_c = X_{1/2}$$

This gives the depth to centre of the cylinder in terms of half width. When Z_c is known, then R , the radius of the cylinder will be determined from the formular.

$$g = \frac{2 \pi G \delta R^2}{Z_c}$$

$$R = 1/ \sqrt{\frac{g_z Z_c}{2 \pi \delta G}}$$

When determining the density contrast which is equal to $\rho_2 - \rho_1$ a density $\rho_2 = 2.67 \text{ gcm}^{-3}$ which is the assumed density of the basement rocks was assigned the cylinder used. The value of $\rho_1 = 2.50 \text{ gcm}^{-3}$ inferred from density measurements was used for sedimentary cover.

2.5.2.1 THE WALU-PANDANGUO ANTICLINE

The Bouguer anomaly outline of the Walu-Pandanguo anticline shows that the structure is not uniform along its entire length. It was necessary to consider all the four profiles across it in order to get a clear picture of the variations in the structure.

When a horizontal cylinder model was applied to them (Figs. 2.14, 2.15, 2.16 and 2.17), the estimates below were obtained.

Profile	Depth (Centre)	Depth (top)	Radius
GP	Z _c	Z (m)	R (m)
1	7000	4000	3000
2	11000	7800	3200
3	9500	6000	3500
4	7500	4300	3200

Comparing depth to the top of the cylinder at Walu (4000) derived from GP 1 and Pandanguo (4300) derived from GP 4, a depth difference of 300 metres is noted. The two profiles are 60 km apart. This gives a gradient of 5m km⁻¹. This value agrees very well with the region's sediment dip determined by using the Walu and Pandanguo wells. It can be concluded from these results that the structure is plunging southeastwards.

Comparing profile GP 1 (Fig. 2.14) with GP 2 (Fig. 2.15) and GP 5, it is noted that the depth to the top of the structure at Walu is 4000 metres and at Alitubo is 7800 metres. This implies that there was a single downthrow of about 3800 metres. The single downthrow is also suggested by the near vertical smooth nature of profile GP 5 between Hara and Alitubo.

The southern part of this structure appears to have had two phases of downthrow. Comparing profile GP 4 (Fig. 2.17) GP 3

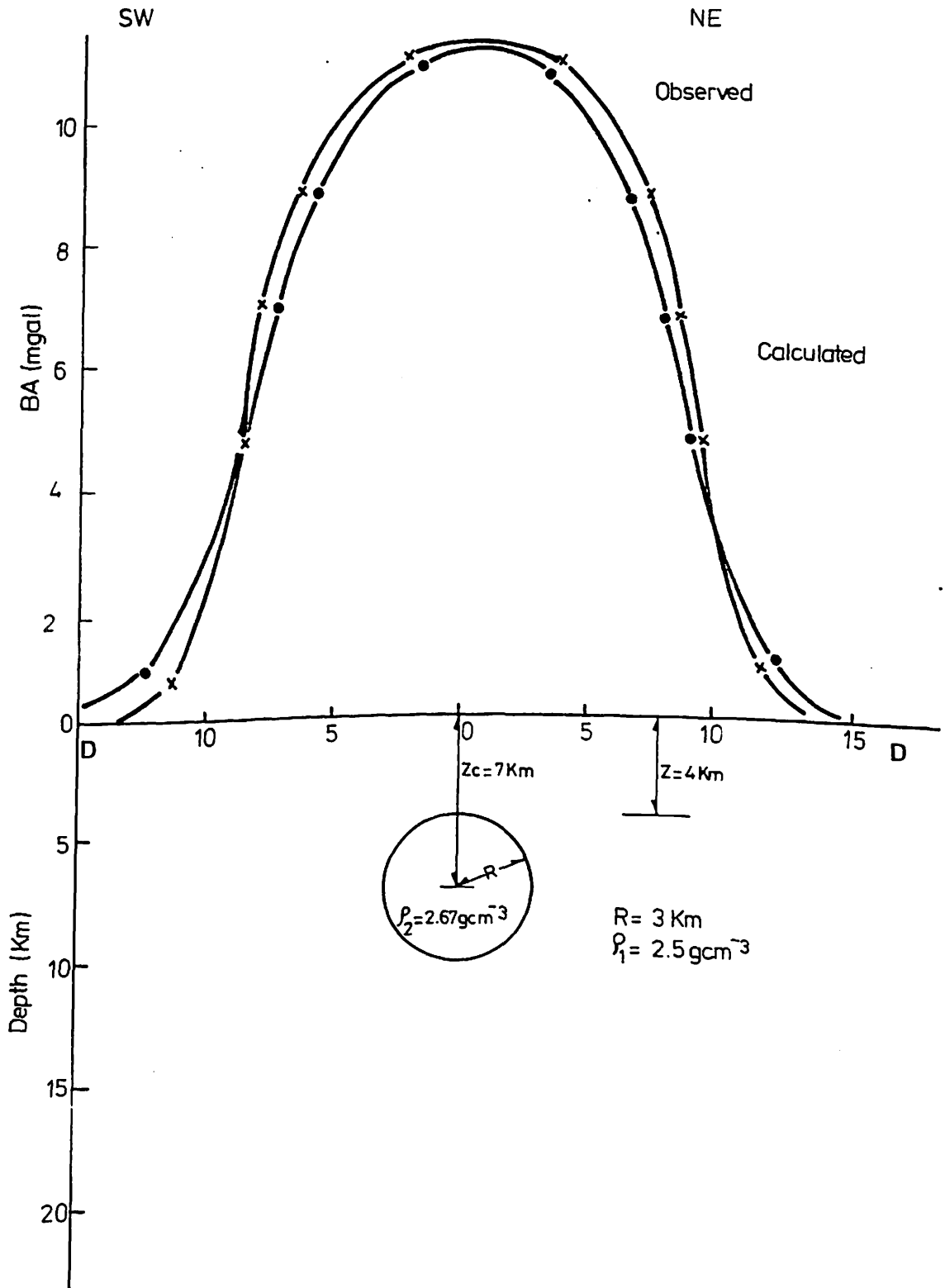


Fig. 2.14

THE FIT OF A CYLINDER MODEL TO BOUGUER ANOMALY PROFILE GP 1

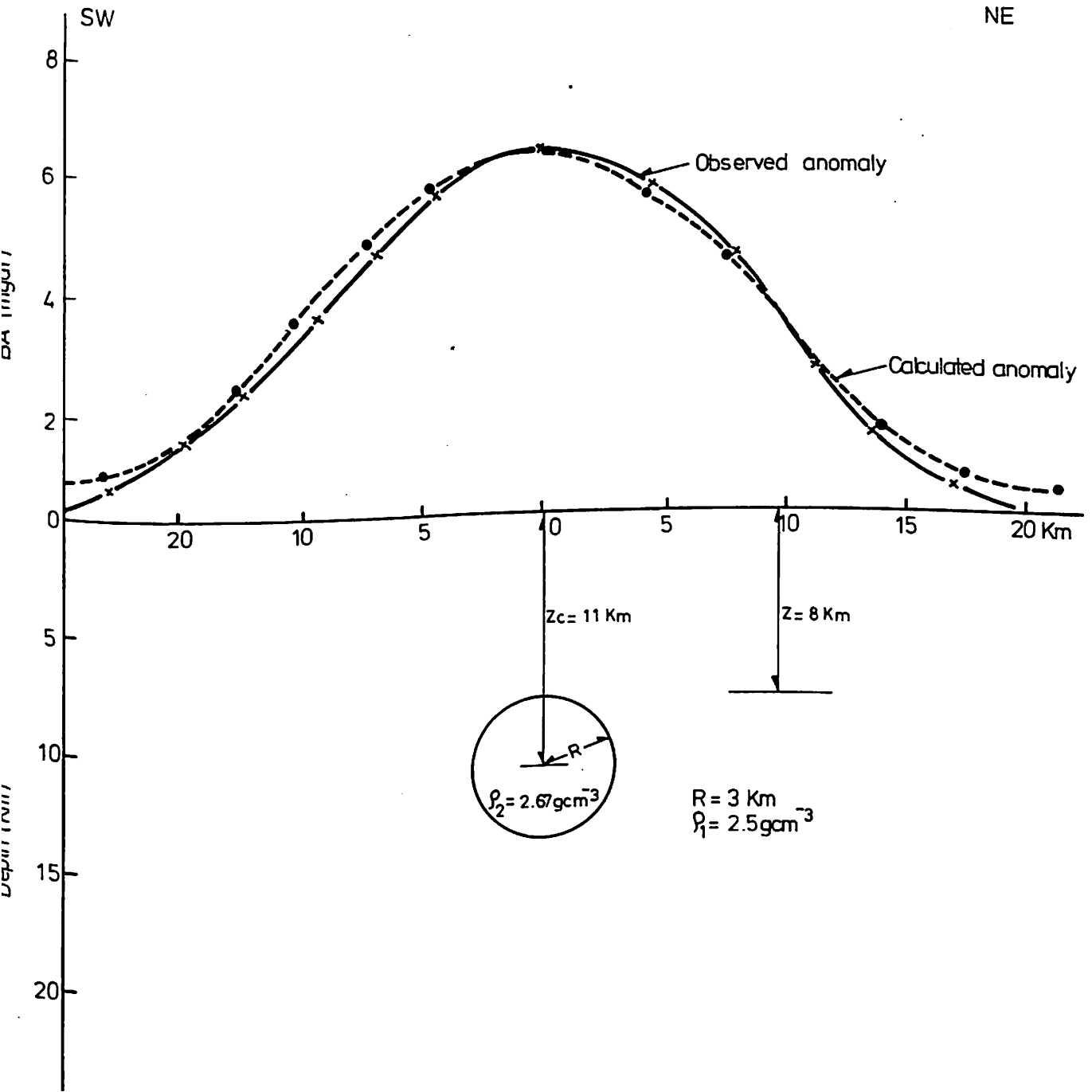


Fig.2.15 THE FIT OF A CYLINDER MODEL TO BOUGUER ANOMALY PROFILE GP2

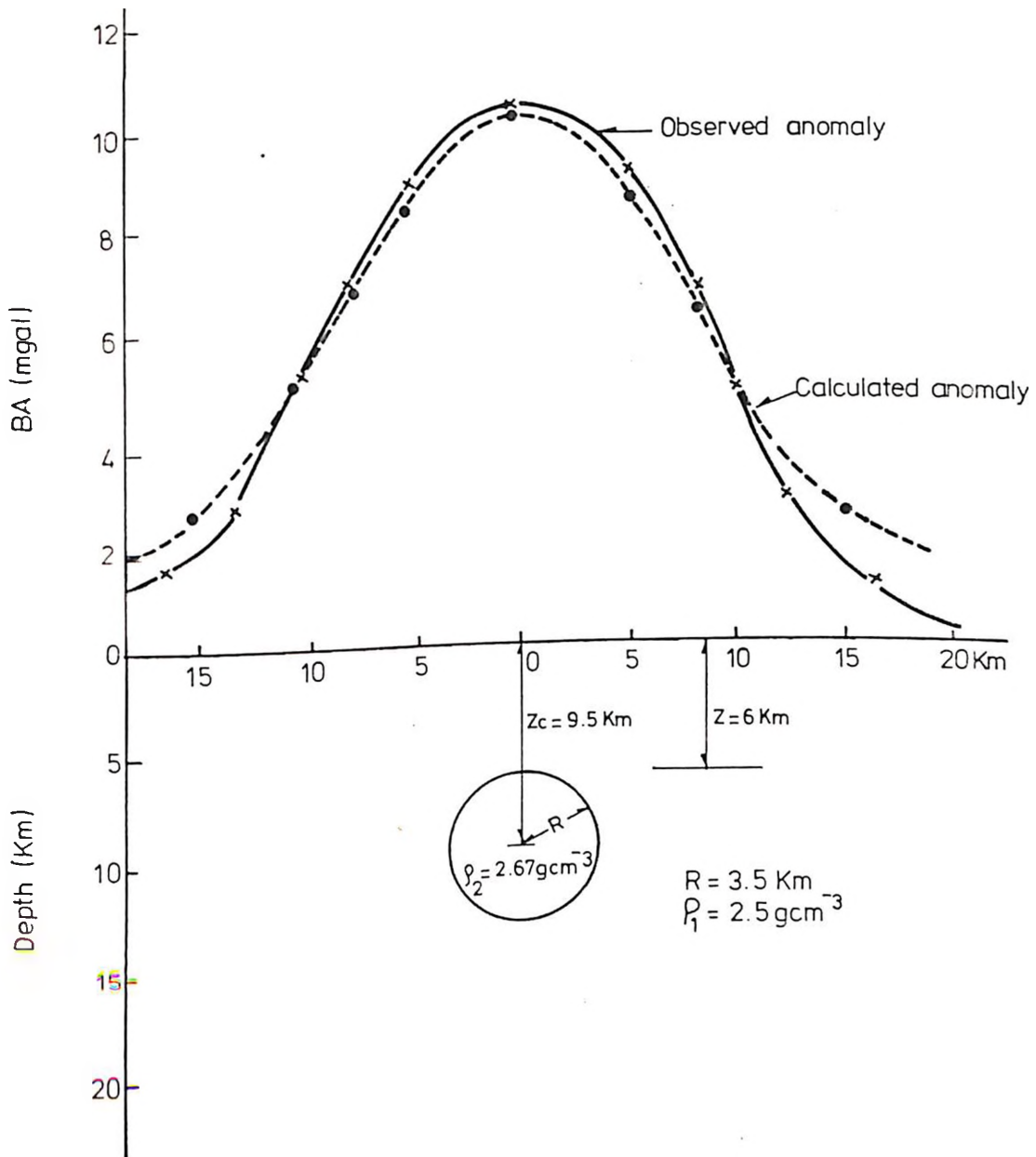


Fig. 2.16 THE FIT OF A CYLINDER MODEL TO BOUGUER ANOMALY PROFILE GP 3

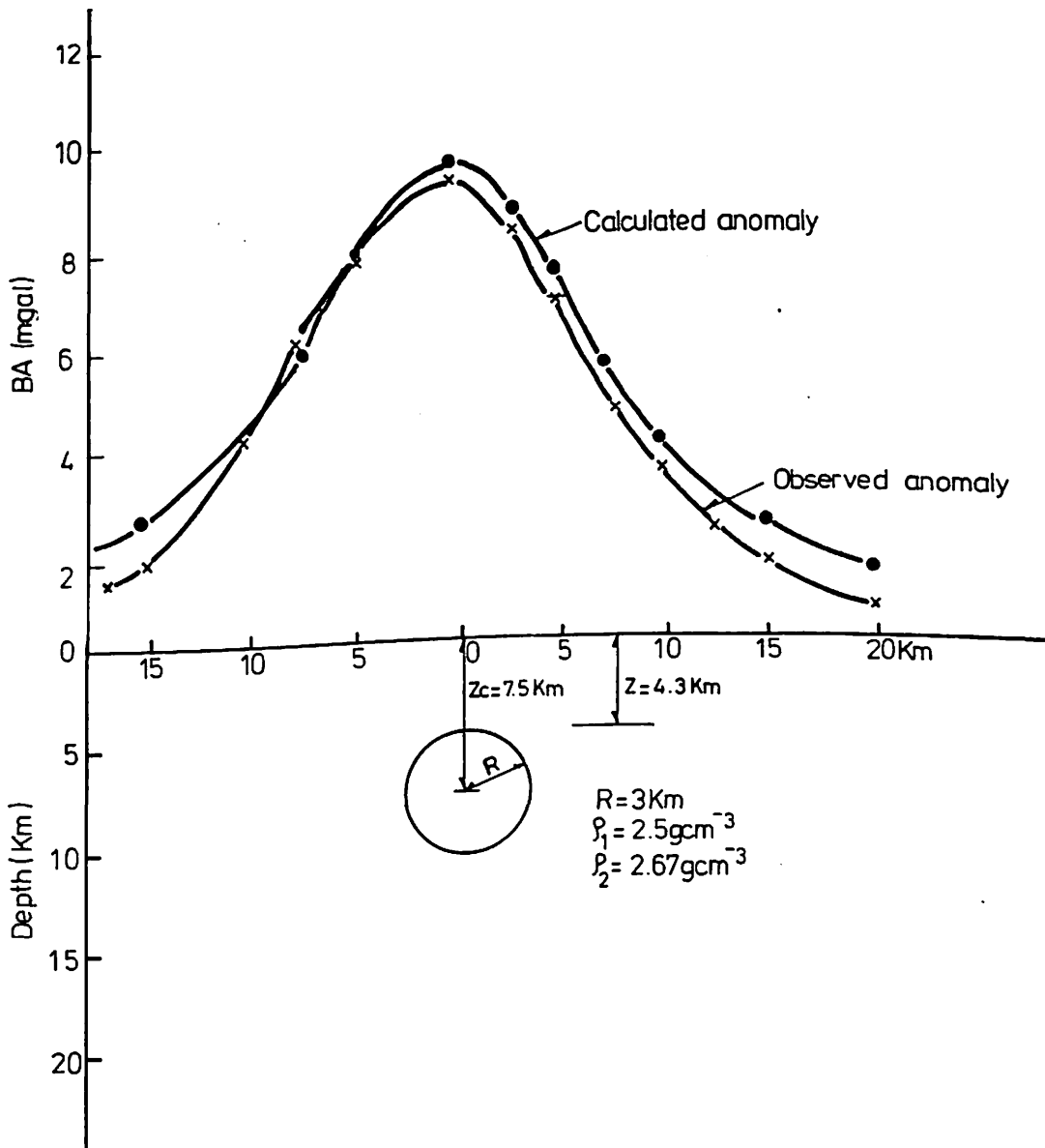


Fig. 2.17 THE FIT OF A CYLINDER MODEL TO BOUGUER ANOMALY PROFILE GP4

(Fig. 2.16) and GP2 (Fig.2.15), it is estimated that a two step downthrow of about 1900 metres each was involved. These values have been used to put forward a model that might depict the probable events that led to the development of this structure. In this model, the Walu Pandanguo structure and the Kitole trough are presented. The Jarakuda trough has been omitted as its inclusion would have made the diagrams very complicated. However, it fits very well in the model.

stage 1. fig. 2.18A

Tensional forces in a NE-SW direction across the anomalous area. Normal faulting in the NW-SE trend takes place from north of Walu to south of Pandanguo.

stage 2. Fig. 2.18B

Vertical movement along faults with the downthrow being away from the central region (Walu-Pandanguo line). A horst structure remains forming the Walu-Pandanguo anticline. The downthrow is estimated to have been about 1900 metres.

stage 3 Fig. 2.18 C

A second phase of tensional forces occur across the area in NW-SE direction. Normal faulting takes place in a NE-SW direction and the faults become more pronounced around Ijara, Jarakuda and Kitole.

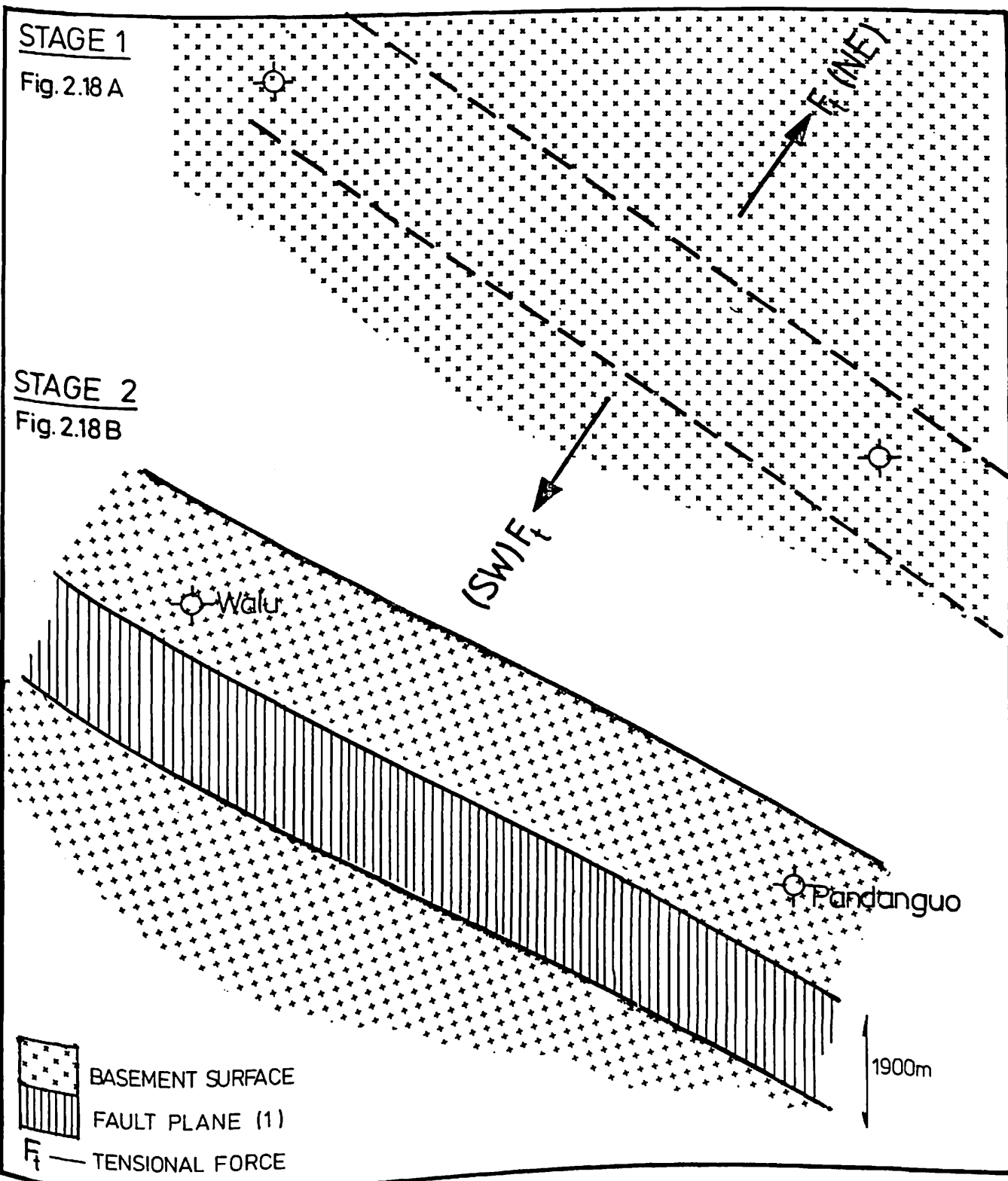


Fig. 2.18 PROPOSED MODEL FOR THE FORMATION OF THE WALU-PANDANGUO STRUCTURE STAGES 1 & 2

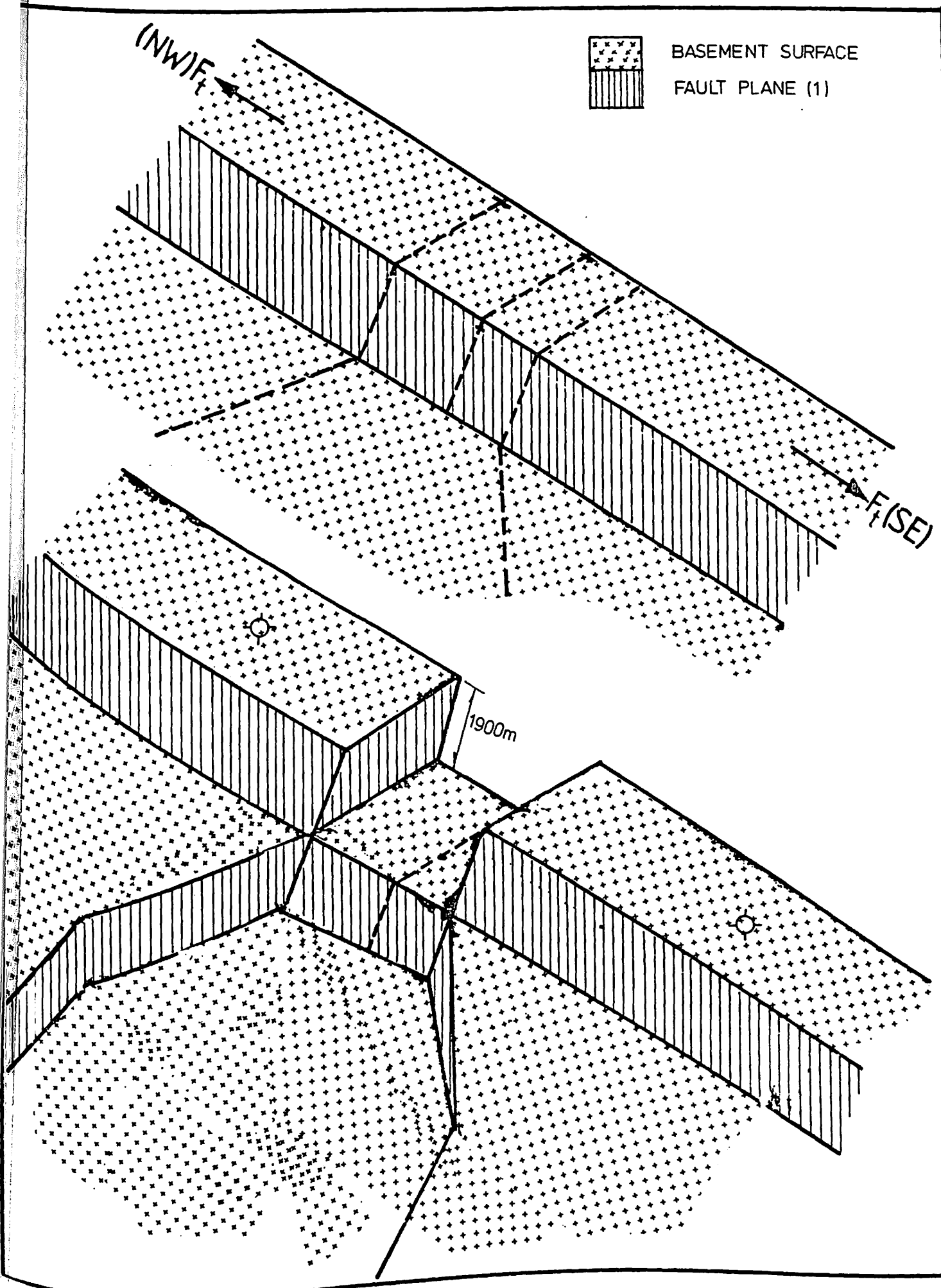


Fig. 2.18C

PROPOSED MODEL FOR THE FORMATION OF
THE WALU-PANDANGUO STRUCTURE STAGE 3

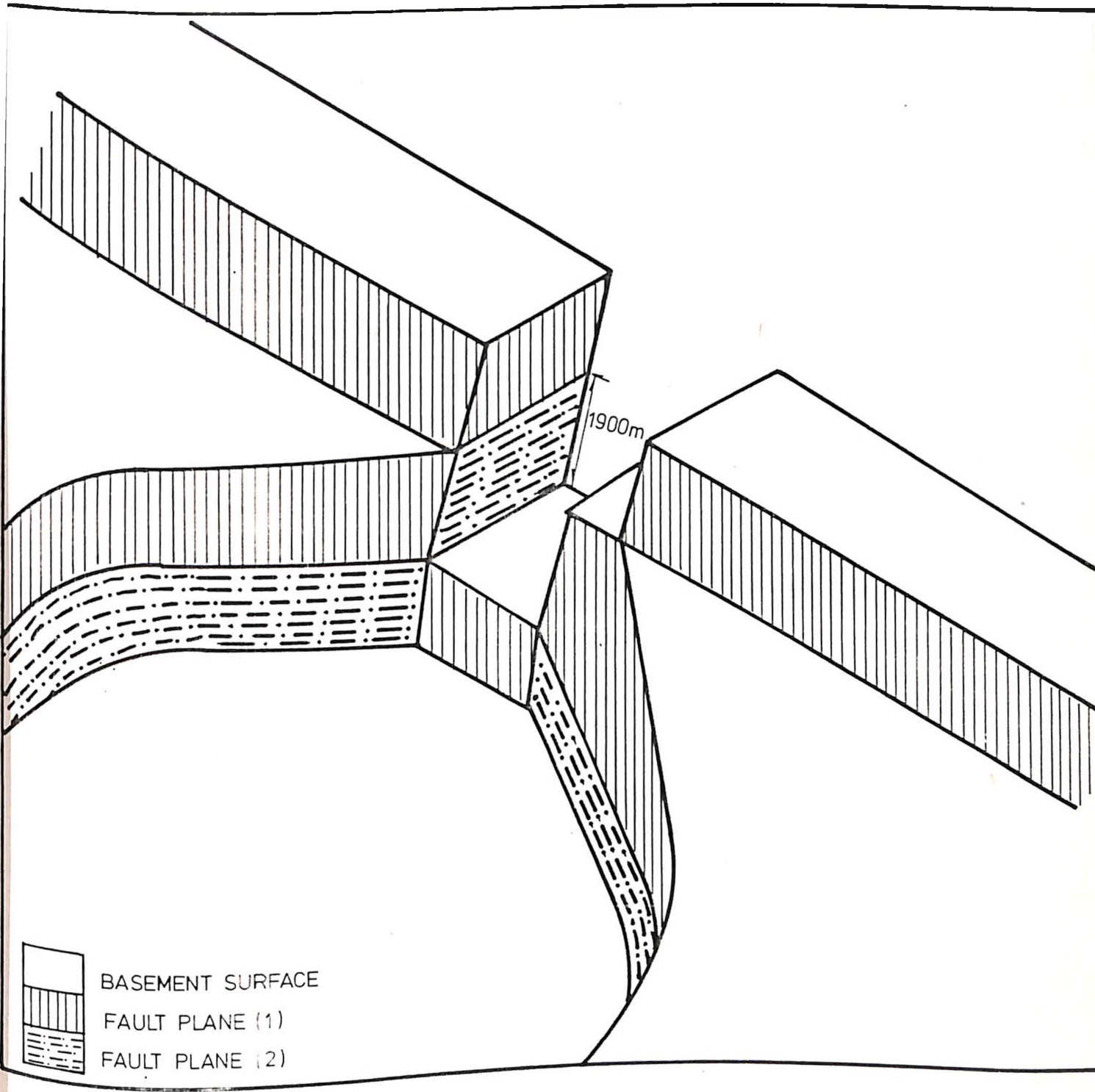


Fig. 2.18D PROPOSED MODEL FOR THE FORMATION OF THE WALU-PANDANGUO STRUCTURE STAGE 4

The Walu-Pandanguo structure resisted the NE-SW faulting thus being affected only at Alitubo.

Stage 4 Fig. 2.18D

Subsidence of the central regions of the fault zone thus forming the Kitole -Jarakuda structure. The amount of throw has been estimated to be about 1900 metres. In order to determine depth estimates to the basement in the two troughs at Kitole and Jarakuda, the writer had to make some assumptions to facilitate the estimation. It was assumed that the amount of downthrow at Alitubo during the second phase of disturbance (NE-SW trend faulting) was the same as that which resulted in the formation of the two troughs (see Fig. 2.19 for validity of assumption). Depth to the two troughs is therefore expected to be the same as depth to the centre Z_c of profile GP 2 (11000 m).

Using the same assumption, the expected average depth to the basement in the western part of the study area can be estimated to be equal to the depth to centre of the cylinder (structure). It is inferred that depth to the basement seawards and to the Tana River region is in excess of 9000 m.

2.5.2.2 THE BODHEI GRAVITY HIGH

Profile GP 6 (Fig. 2.20) was used in the analysis of this structure. When a horizontal cylinder model was applied to the

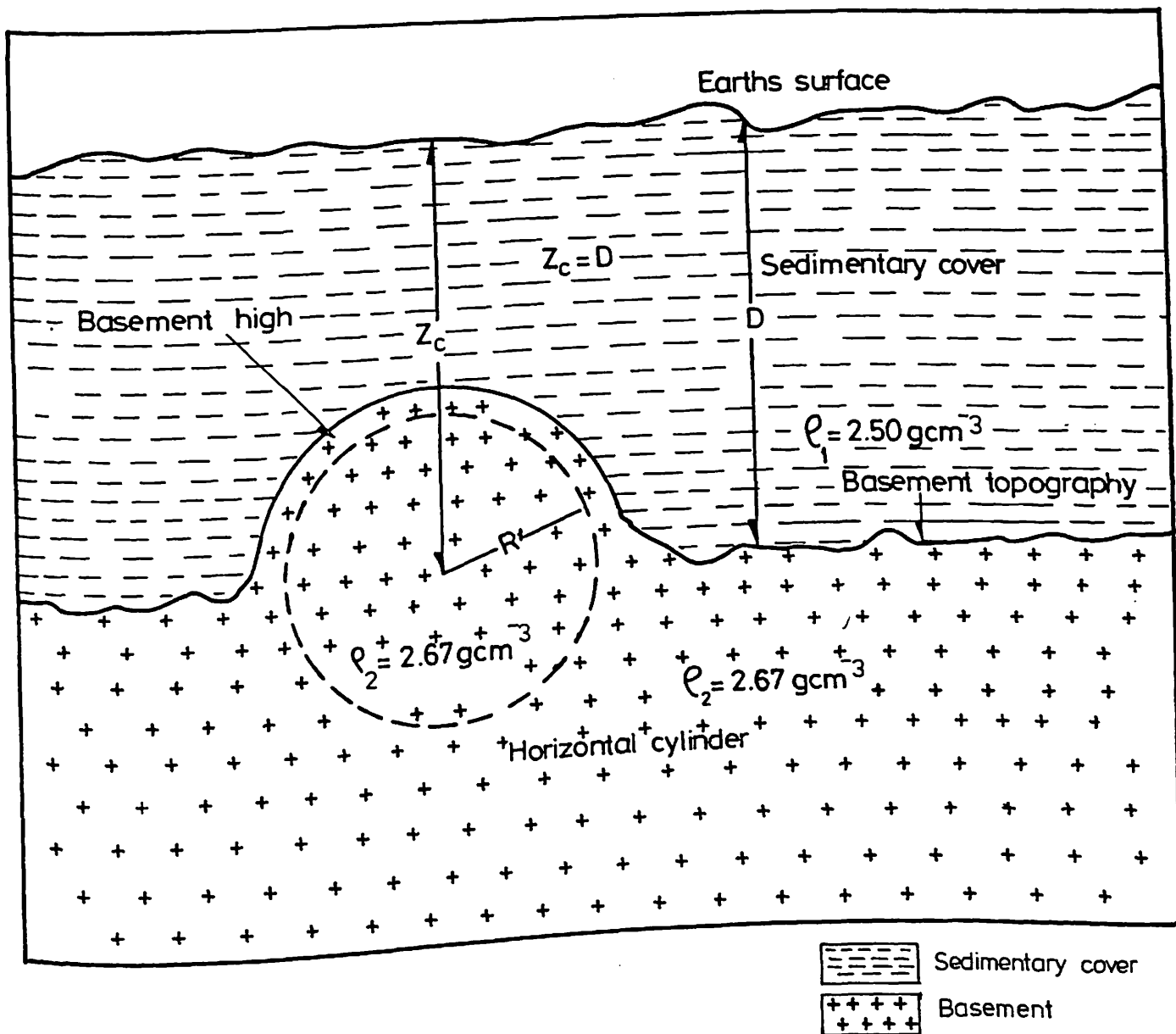


Fig.2.19 VALIDITY OF THE DEPTH ESTIMATION
ASSUMPTION USING A HORIZONTAL
CYLINDER MODEL

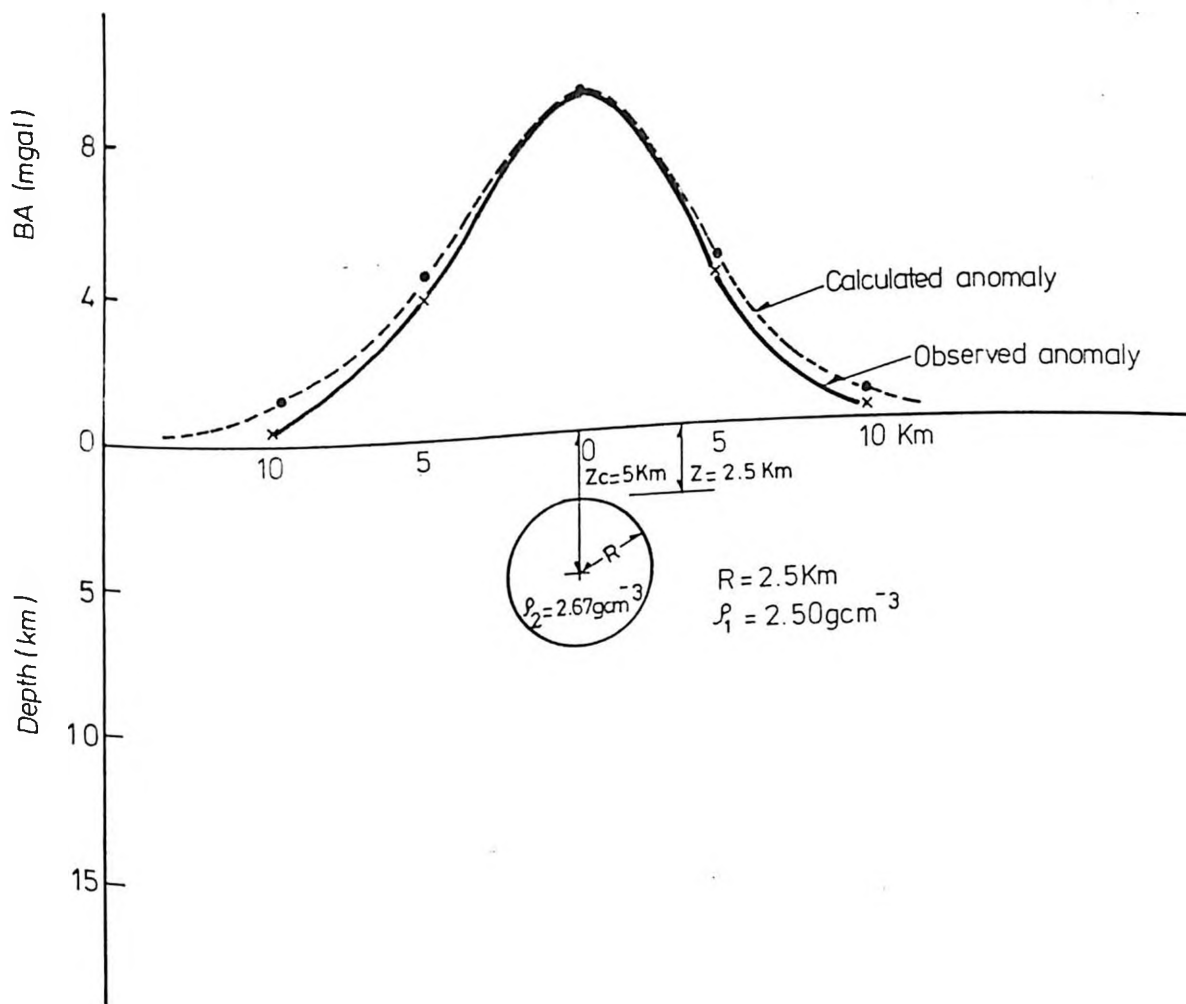


Fig. 2.20 THE FIT OF A CYLINDER MODEL TO BOUGUER ANOMALY PROFILE GP 6.

anomaly profile, a body of radius 2500 m, depth to the centre 5000 m and depth to the top 2500 m was depicted.

The calculated depth to the centre (5000 m) cannot be the same as depth to the basement in this area since this value is too low. This may imply that the anomalous body is a shallow structure of high density material.

2.6 DISCUSSION OF GRAVITY RESULTS

It was shown in sub-section 2.4 that the overall error in the Bouguer anomaly values determined by the writer is about 1.0 mgals. Considering the size of the anomalies in the area, this error is considered to be small. The difference between the oil companies data and the writer's had a maximum value of about 1.1 mgals. Also the data coverage of areas of structural complexity was good. This implies that the data used and therefore the interpreted results are reliable.

Apart from the structures that were noted by BP-Shell oil company, the present gravity study has shown the presence of a NE-SW synclinal structure crossing the Walu-Pandanguo structure at approximately 750 along Kitole-Jarakuda line. A minor localised antiform around Bodhei has also been determined.

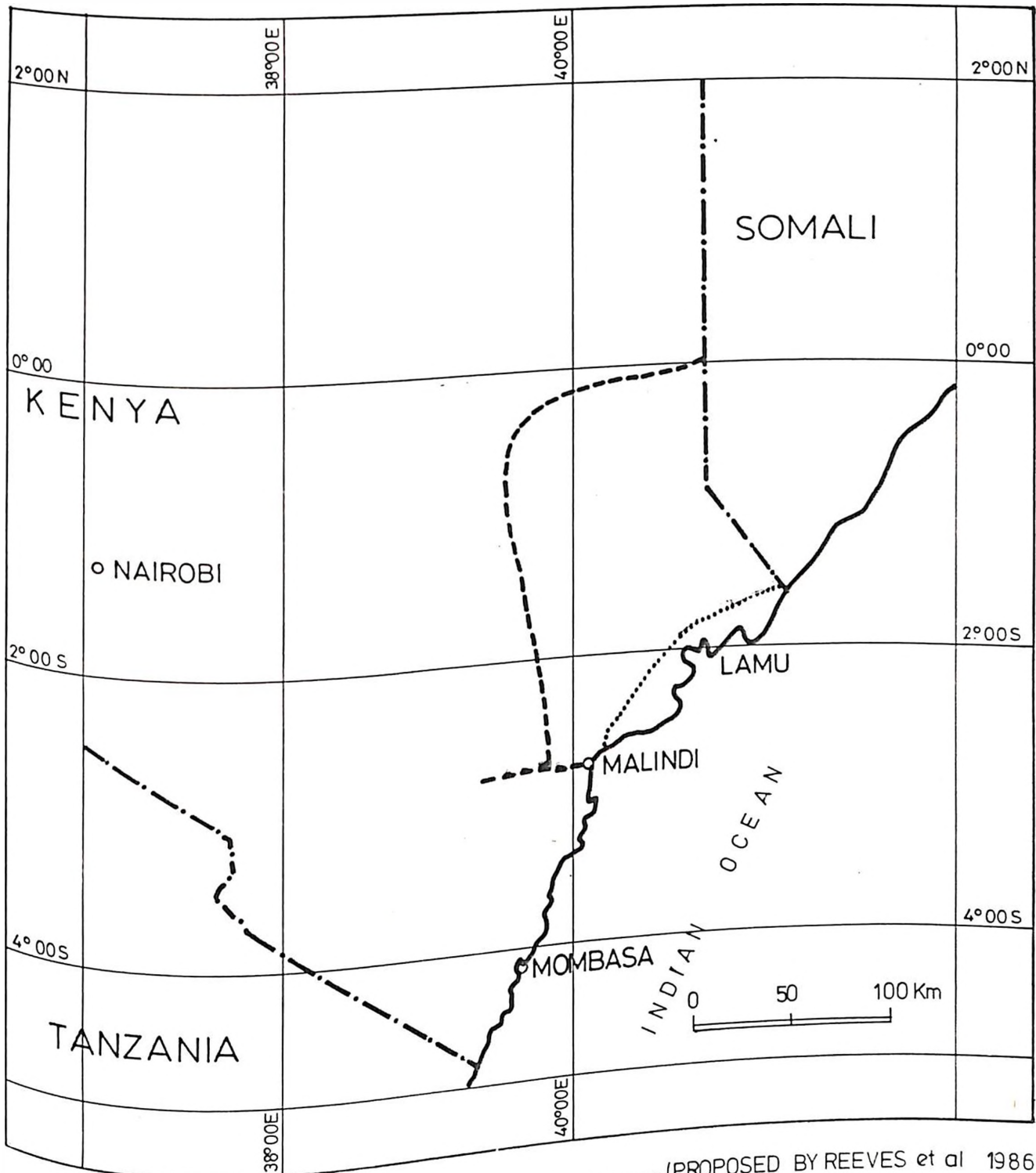
The regional analysis has shown the area to have a gradient in the southeast direction (towards the sea). This occurs in two

parts. On land, the value is 0.4 mgals km⁻¹. Towards the offshore part, the value changes to 1.3 mgals km⁻¹ along a line nearly parallel to the coast. The increase of gravity values in a sedimentary basin implies a decrease in the value of depth to the basement (a decrease in sedimentary cover thickness) (Mesref 1980). Since the study area is thought to be part of a passive margin formed after the break up of Madagascar from the East African Coast, (Tarling and Kent, 1976; Walters and Linton, 1973). It is not geologically plausible to expect thinning of the sedimentary cover towards the Indian Ocean. Infact one expects that with the increasing density deficiencies arising from thickening of sedimentary cover towards the sea will give rise to increasing negative Bouguer anomaly values. Work done in other passive margin basins has shown nearly the same regional trend. Steckler and Watts (1978) who worked on the New York basin have noted a uniform increase in Bouguer anomaly values offshore (but with a single gradient). They attributed the increase to a thinning of the continental crust. In the New York basin, they estimate a gradient 70 metres per every milligal of change.

Whereas the situation is nearly the same in Lamu in terms of the increase in anomaly values towards the offshore, here we have two gradients of increase, the onshore and the offshore one. This implies that in Lamu there might be thinning of the continental crust plus another factor causing the second gradient.

Work done in the Verginia basin(U.S.A) by Mussman (1986) and in the gulf of south California by Harrison and Mathur (1974), has shown that this sort of two step regional anomaly gradient is associated with the thinning of the continental crust then followed by a transition to oceanic crust. This seems to be the situation in Lamu, Coffin, et. al., (1986) who worked in the western Somali basin which is offshore Kenya have also suggested the same.

Assuming that the oceanic crust on which sediments were laid was the cause of the change in gravity gradient, then the present study has led to the delineation of the extent of the oceanic crust below the present onshore sedimentary cover. These results do not agree with those of Reeves, et. al. (1986) who asserts that most of the Lamu embayment, as far north as 0° and west of longitude 40° has a uniform density oceanic basement (Fig. 2.21). If Reeves et al's assertion is true, we should expect the long wavelength regional anomaly fields to be essentially featureless and flat. This is only seen in the south east from offshore to a small strip onshore where the writer has put his demarcation line. Northwards, we have major basement structures that have been discussed and one of them, the Walu-Pandanguo structure disappears just north of the line of demarcation.



----- (PROPOSED BY REEVES et al 1986)
..... (DETERMINED IN THE PRESENT STUDY)

Fig. 2.21 THE EXTENT OF THE OCEANIC CRUST

3. SEISMIC SURVEYS AND INTERPRETATION

3.1 INTRODUCTION

Seismic reflection mapping is principally concerned with the delineation of sedimentary structures and lithologic variations in the uppermost 5 km of the crust. The acquisition and processing of data are designed such that signals are detectable from the deepest target horizons in the highest frequency attainable. This is normally within a range of 12 - 60 Hz. Reflection occurs whenever a wave encounters a discontinuity where there is a change in the physical properties of the transmitting medium. The amount of wave energy reflected and its phase relative to incident wave depends upon contrasts of physical properties of the media on the two sides of contact. This contrast is due to acoustic impedance (pv), where

- P = density of transmitting medium
- v = seismic wave velocity in the medium

The reflection coefficient is given by:

$$R = \frac{P_2V_2 - P_1V_1}{P_2V_2 + P_1V_1} \quad \text{Macquillin, et. al. (1984)}$$

where

P_1V_1 = Acoustic impedance of medium one

P_2V_2 = Acoustic impedance of medium two

A negative reflection coefficient arises when the incident ray is in a medium of higher acoustic impedance. Thus reflectors usually correspond with horizons marking the boundary between

rocks of markedly different lithology. The primary objective of seismic interpretation is usually to prepare contour maps showing the two way travel time to a series of reflectors which have been picked on seismic sections. The interpretation of the Lamu data was done with the aim of achieving this objective. The interpretation was done using the method given by Macquillin et. al. (1984). Overall, the interpretation involved assimilation of a mass of data of varying quality covering 2690km of seismic lines. The techniques used in the acquisition, processing and interpretation of the data are discussed in the following section.

3.2 DATA ACQUISITION AND QUALITY

Most of the seismic data in this area was acquired between 1954 and 1971 using old analog techniques. Between 1954 and 1960 BP-Shell did seismic reflection survey in the western part of the area covering Bura, Garsen, Tana river, Kipini, Witu, Pandanguo and Bodhei (O'Hollarain 1971). During this survey, long spread and long offset method of field recording was used with a recording spread separation of station interval kept at 92 m. Most of the spreads were shot for six-fold subsurface cover with the shot points located centrally and a few lines being shot off-end. Charge size used was 9kg and hole depth kept at 16 m average. Towards the end of this survey in 1960, it was realised that the subsurface structure was complex and highly faulted. A few lines were therefore recorded with a 46 m station interval as

it was found to give better lateral resolution, A spread configuration of 528m - 23m - 0 - 23m - 528m was used.

Overall, the 1954 - 1960 data is noted by O'Hollarain (1971) to be of very poor quality, as it was later found that unless hole depth was in excess of 24m, little seismic penetration beyond 1.0 seconds was obtainable.

Between 1964 and 1969 BP-Shell acquired more seismic data in the east and southeastern part of the area and one line within Kipini and another in the Tana river region (O'Hollarain 1971). During this survey, the decision on spread configuration and charge size was based on complexity of subsurface structure. In areas of less structural complexity a spread configuration of 528m - 23m - 0 - 23m - 528m was used. Where the station interval was kept at 46 m and hole depth at 24m. In areas suspected to be highly faulted and those with lines across strike direction, a station interval of 23m and spread configuration of 264m - 11m - 0 - 11m - 246m was used. This spread was shot for three-fold subsurface cover. Hole depth was maintained at 31 m inspite of drilling difficulties presented by near surface coral limestones in some areas. Charge size was maintained at 18kg in a single hole.

In 1969-1971, a detailed seismic survey was carried out in areas of interest, i.e. areas of structural highs by Geoprosco

(O'Hollarain 1971). This survey covered, Kipini, Pate, Dodori, Mararani and Lamu areas. Since these areas had already been noted as being structurally complex during acquisition of the earlier data the spread configuration, charge size used and hole depth were varied accordingly.

Whereas the earlier BP-Shell data is poor, the 1964-1969 and 1969-1971 data is of good quality in the Tana delta and Tana syncline to the east. The quality becomes poor in Witu Kipini and Bodhei areas due to fractured limestones being encountered near the surface (O'Hollarain 1971). This data is expected to be poor in all structural high areas due to interference from diffracted energy developed from the many faults in the area (Dobrin 1976)

Poor quality of the 1954 - 1960, and partly 1964 - 1969 data can be attributed to :

1. The long spread and long offset methods of field recording which reduced the quality of common depth point stacking results (CDP). This is due to the high intensity of faulting and steep dips towards the sea in the area.
2. The long spreads limited vertical penetration due to low energy.
3. Small charge size limited vertical penetration due to low energy.

4. Shallow shot hole increased the effect of low velocity layer (weathered zone).

Better reflection records are obtained if shots are placed below the low velocity layer. This is due to the reflection of much of the energy at the velocity boundary at the base of the weathered zone when a shot is above it. The low velocity layer is characterised by velocities of 250 to 1000ms⁻¹. The base of a low velocity layer (LVL) corresponds to the aerated zone above the water saturated zone. The effects of the low velocity layer

- (LVL) are:
1. Absorption of seismic energy is high leading to poor vertical resolution.
 2. Low and erratic velocities have disproportionately large effect on travel time.
 3. The marked velocity change at the base of LVL sharply bends seismic waves.
 4. The very high impedance contrast at the base of (LVL) makes an excellent reflector, especially multiple reflection, thus reducing the penetration depth.

The foregoing effects suggest that uncertainties over (LVL) corrections are the largest single source of error in velocity determinations and later depth conversions. The error due to LVL corrections is likely to be higher in the 1954 -1960 data due to shallow shotholes and small charge sizes used.

During processing of this data, different modes were used depending on the field procedure. For data which was recorded with analog magnetic equipment, processing was preceded by analog to digital transcription which allowed these profiles to undergo processing. The results were displayed as variable area seismic sections in which the troughs are deleted and peaks are shaded in solid black. The displays have a vertical resolution of 5cm of two way time (TWT) and a horizontal scale of 1:250,000.

The quality of data in the area can be summarised as:

1954 - 1960	Data - Poor
1964 - 1969	Data - Fair
1969 - 1971	Data - Good

The data available to the writer for interpretation can be summarised in percentage as given below:

1954 - 1960	constituted	60% of total data
1964 - 1969	constituted	24% of total data
1969 - 1971	constituted	16% of total data

These percentages show the majority of data available was poor to fair quality and therefore the overall data used was of low quality. When selecting seismic lines for interpretation, an attempt was made to include as many 1969 - 1971 lines as possible. One setback to this was that the 1969 - 1971 lines were not well spread within the area and constituted only 16% of

the data that was available to the writer. Since the 1954 - 1960 data covered most of the study area, and constituted 60% of the total data available, it forms the bulk of data used followed by the 1964 - 1969 data.

When choosing lines to be interpreted, it was found that most of these had data missing from files. It was therefore anticipated that the overall low quality of data used and incompleteness of this data was going to reduce the quality of interpreted results. The stages followed during the analysis of the data by the writer are discussed in the next sections.

3.3 REFLECTION IDENTIFICATION

Seismic reflection surfaces were identified by inspecting seismic lines through wells. Not only do well logs give a useful subsurface geological picture but they also show where strong reflections might be expected. Thus wells were the most reliable means of seismic reflection identification. It was found sufficient to use compensated sonic logs, density logs and lithology logs. One anticipated a marker at each major seismic, density and lithology change provided that the bed giving rise to it is at least one wavelength (say 100 m) thick (Grant and West, 1965).

The dip lines were always interpreted first. These lines were laid down in a sequence. In this way, it was possible to follow

the major structures in the area. Faults were inferred by:

1. Termination of a reflector giving rise to characteristic quasi-hyperbolic diffraction patterns on a seismic section.
2. Presence of lines showing crushed rock with vertical reflector displacement.
3. Reflection markers terminating sharply at the point of a fault plane and resume again in a displaced position on the other side of an inferred fault. Sometime, markers are prolonged in a small distance beyond the fault plane. In this case, plane positioning was compromised between the two prolonged extensions.

Quite often faulting and other structures made tracing of a reflection marker very difficult. Thus there was a problem of correlation across such structures. This problem was partly solved by using strike lines on sections to carry the interpretation around faults and other structures, using the reflection characteristic and folding a section so as to bring into juxtaposition the undisturbed areas on both sides of the fault.

3.4

MIS-TIES AND THEIR CORRECTIONS

During seismic interpretation, it is expected that reflectors on different lines at their intersection point should coincide.

exactly in terms of the two-way-time. In the present study, it was found that sections from lines shot with the same parameters were mis-tying by a few tens of milliseconds. Lines on the 1969 - 1971 data were noted to have maximum mis-ties of 1 - 35 milliseconds. The greatest mis-ties were on 1954 lines. These gave mis-ties of 80 - 150 milliseconds which were also inconsistent.

The first cause of mis-ties discussed was corrected by giving a bulk shift of one line relative to another. This was facilitated by the fact that the misties on these lines were consistent. Mis-ties of the second type could not be corrected by shifting due to inconsistency and large mis-tie values involved. The error due to these mis-ties was reduced by giving more weight to sections from 1969 - 1971 data. Unfortunately sections from the 1969-1971 data constituted only 16% of the total interpreted. Some sections had higher vertical resolution than others and it became difficult to decide on the basis for adjustment.

Mis-ties were also attributed to:

1. Differences in deconvolution parameters, filter setting and stacking velocity.
2. Difference in gun depths, charge size and survey procedures. This might have led to errors in LVL and elevation corrections resulting in phase distortion of sections.

3. The effect of some lines not being exactly in the dip direction and not having been corrected for during velocity migration in the 1954 - 1960 data. This fact is shown by the greatest mis-ties being towards the sea where beds have dips exceeding 80

3.5 DIGITISATION OF SEISMIC SECTIONS

The first step in making a two-way-time map from the seismic sections is the measurement of the two-way-time to the reflection events along each section. This data is then transferred to a base map in order to produce a two way contour map showing structures.

In areas of much complexity, sections were measured every 1.0 km. In less structurally complex areas, an interval of not more than 3.0 km was used. Position of faults was recorded and horizons time measured on both the up and downthrow sides.

3.6 TWO-WAY-TIME (TWT) MAP CONSTRUCTION

Once seismic sections had been interpreted, the next objective was to produce contour maps of TWT to each horizon of interest. After reading off the TWT from the seismic sections, it was posted onto the shotpoint map. The TWT values posted were tested for reliability by looping, the closing of loops providing an important check. When a loop failed to close within a certain error limit, the case was investigated. The

contouring was first done roughly so as to identify the main structural trends. Insertion of all faults was done and then it was decided on how to join them depending on:

1. Similarity in reflection appearance and amount of throw.
2. Knowledge of dominant geological trends in the area.

Anticlinal axes were identified on the map so as to ensure that contours intersecting them turned along the same axis. This was useful in identifying minor mis-ties which whenever possible were resolved by reference to the section. Isolated values which disturbed the trend were ignored. Final contouring was carried out between faults keeping a minimum spacing of 1 cm for legibility and a maximum spacing of 2.5 cm for detail.

There was a problem of contouring data between lines in the dip and strike direction. The dip and strike direction lines showed mis-ties of about 20 milliseconds on land. This value increased considerably towards the sea to about 100 milliseconds. On land, this problem was solved by shifting one line relative to another. Towards the sea, this problem was minimised by giving more weight to the dip direction ones. Unfortunately, the dip direction lines were widely spaced.

When contouring was completed, it was checked against the original sections, especially in regions of complex structures like in areas of closed highs and in those with faulting disturbances. The final maps of time to different horizons were then prepared with closed highs painted red and closed lows

painted blue (Fig. 3.1). Faults of different throws are shown by different thickness.

3.7 VELOCITY DETERMINATION

In order to convert the TWT maps into depth, we need to know the velocity variations within the area. To determine the lateral and vertical velocity variations, compensated sonic logs from wells and seismic stacking velocities were used.

Since seismic data in the study area was of very low quality it was therefore expected that the quality of stacking velocity was poor. When well velocities were compared with the stacking velocity given by BP-Shell, it was found that the stacking velocity (1758ms⁻¹) was too low as compared to the average compensated sonic log velocity (3344ms⁻¹). Well velocity data were therefore primarily relied on.

The sonic logs were used to deduce the average velocity in each formation. In Lamu, there was noted a rapid variation of velocity in the same formation from one area to another. When density logs were considered, it was found that they have the same trend as sonic logs. This variation is probably due to the deformed nature of the basin. It was found that in a single formation, the top part of it had a lower seismic wave velocity than the base. This was attributed to more compaction at deeper horizons. The compensated sonic logs were used to determine the average velocities for each formation in a particular well. Shown in table 3.1 are velocity values in the Pate well.

TABLE 3.1 VELOCITY VALUES IN PATE WELL

FORMATION	AVERAGE VELOCITY (ms)	DEPTH (m)
Limestone	4554	300-1100
Limestone, sandstone shale	3913	1100-1300
Limestone, mudstone	4247	1300-1400
Limestone, sandstone, shale	2800	1400-1600
Limestone, sandstone	2902	1600-1700
Limestone, sandstone, mudstone	3730	1700-1800
Sandstone, mudstone, siltstone	2913	1800-2400
Sandstone, shale	2700	2400-2600
Limestone	3400	2600-2900
Limestone	3516	2900-3000

The limestones at 300-1100 m depth has an average velocity of 4554 ms⁻¹ and at 2600-2900m depth has an average velocity of 3400ms⁻¹. The low seismic velocity in the deeper limestones is attributed to high porosities which reduced the formational density.

To get accurate velocity values over the whole study area, determination of wave velocities and their variation within the study area is necessary. In Lamu, deep wells are not uniformly distributed and are concentrated on seismic highs. The problem was how to extrapolate the well velocity values into the seismic low regions where there are no wells. This problem was more pronounced where there are lateral facies changes, like in the

case of continental barren Eocene beds in the north which become marine in the south.

An attempt was made at determining an average velocity over the whole area. The value determined was 3344 ms⁻¹. This velocity can be used as a very rough estimate of depths from the TWT.

3.8 DEPTH CONVERSIONS

Maps of TWT to various horizons and average velocities for different formations in a particular area were used in depth determination by multiplying one way time within a particular horizon by velocity. This gave the bed thickness. By making cumulative addition of thickness of formations from the surfaces, depth to a particular horizon was determined as shown in table 3.2.

TABLE 3.2 DEPTH CONVERSION TABLE TIME AND VELOCITY

HORIZON	TIME		V	THICKNESS	DEPTH(TO BASE OF X)
X	(t _{x0})	T1	(MS ⁻¹)	(m)	(m)
1	To	T1	V1	T1xV1	T1xV1
2	T1	T2	V2	(T2-T1)V2	(T2-T1)V2+T1xV1
3	T2	T3	V3	(T3-T2)v3	(T3-T2)V3+(T2-T1)V2+T1V1
N	TN-1	TN	VN	(TN-TN-1)VN	(TN-TN-1)VN+(TN-1-TN-2)VN-1+...+(T2-T1)V2+T1V1

where time t_{x0} is one way time to the top of horizon x and time t_{x1} is one way time to the base of horizon x. The depth to

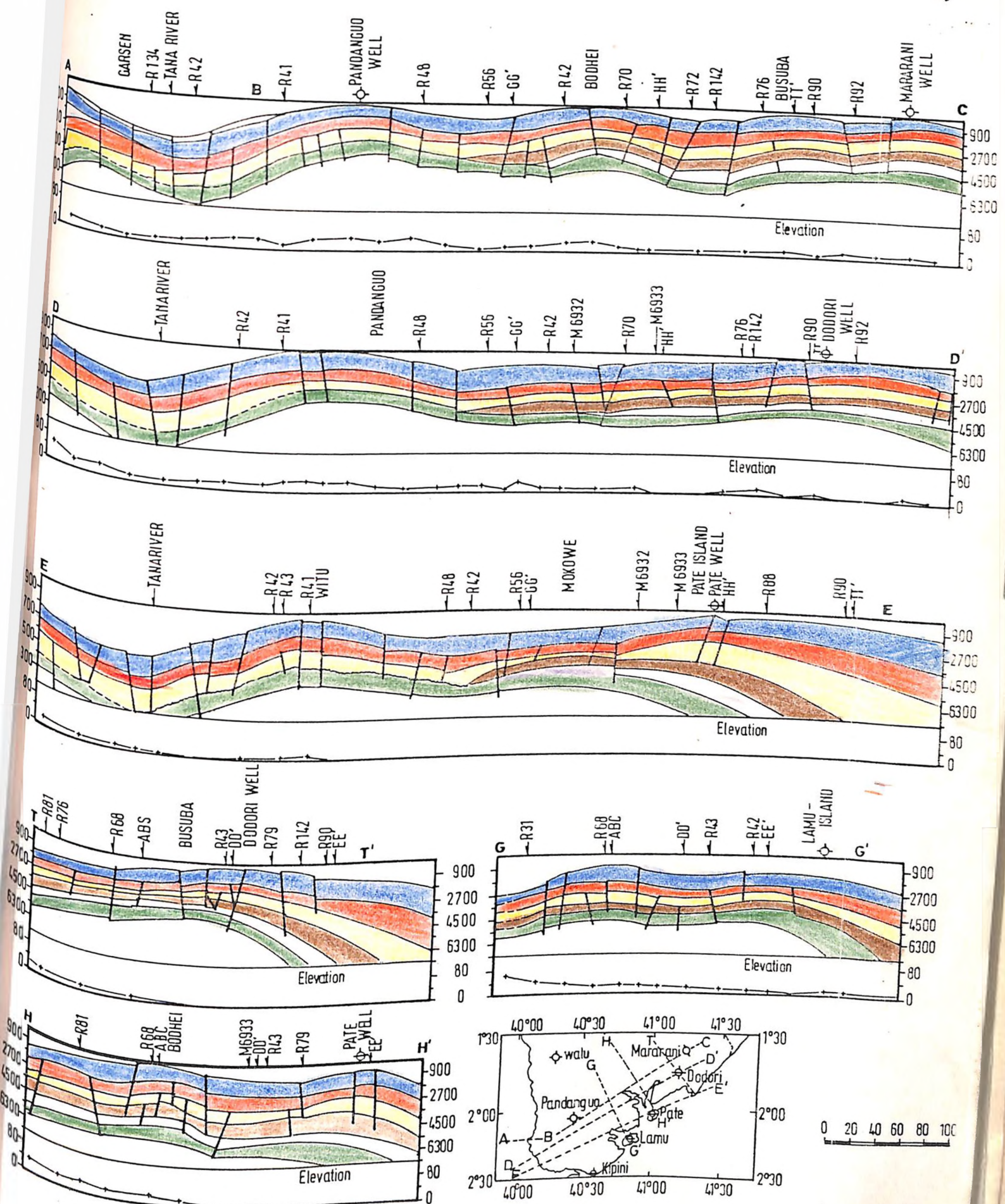
each horizon is build up by a 'layer cake method'. Where the thickness of the second horizon is added to depth to the base of the previous horizon. This gives depth to the base of the second horizon which is also the depth to the top of the third horizon. The resulting depth values were then posted on the seismic sections.

The accuracy of depth conversions depend very largely on how accurate the velocity determinations are. Since velocity determination was based on well logs, it was expected that the accuracy of these depth conversions deteriorates away from wells, especially a round seismic lows. Depth conversion accuracy is also expected to decrease towards the sea due to the high dips of beds and a possibility of diapirism with slumping (Rabinowitz, et. al. 1982). Generally, depth estimates are reliable near wells but becomes less reliable away from the wells.

3.9 CROSS SECTIONS FROM SEISMIC SECTIONS

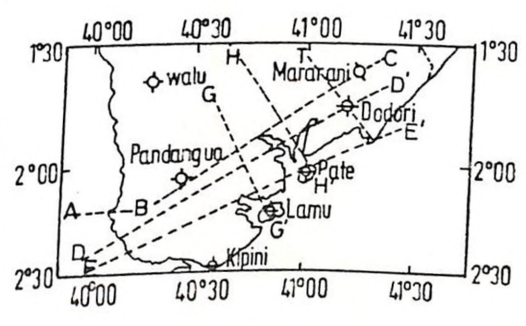
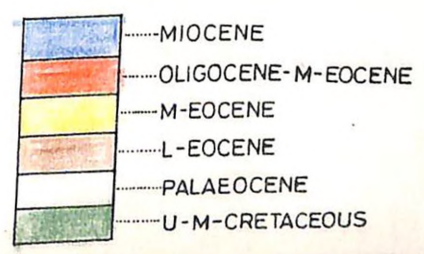
Cross sections were prepared from the TWT maps which had been converted to depth maps. This was done to obtain a rough geological picture of the subsurface. The choice of regions to draw the sections through depended on how interesting an area was in the writer's view in terms of the possibility of delineating subsurface structures. The sections were mostly made across seismic highs (Fig. 3.2). The uneven spread of wells within the area,

Fig.3.2 CROSS SECTIONS OF LAMU AREA (BASED ON SEISMIC TWT MAPS)



Legend :-

- - - - - HORIZON UNCERTAIN
- HORIZON CERTAIN
- ~~~~~ UNCONFORMITY SURFACE
- DRILLED WELL DRY
- ⊙ DRILLED WELL GAS SHOW
- TIE LINE
- EE', GG', HH', TT'..... LINES OF SECTION



dictates that these sections can be relied upon only in few areas where they cross wells. Away from the wells, reliability diminishes..

It should be noted that sections shown in (Fig.3.2) were not necessarily made along seismic lines because they were based on two way time maps that had been prepared by the writer. The cross sections give depth to lithostratigraphic units that form good reflectors. In the area of study, the lithostratigraphic units do not exactly coincide with chronostratigraphic units given in wells. So these seismic cross sections cannot be used as geological sections.

3.10 GEOLOGICAL INTERPRETATION OF SEISMIC DATA

3.10.1 GENERAL STRUCTURE

The seismic two way time maps and cross sections were used to give a picture of the subsurface structures. The study area is highly faulted at depth (Fig. 3.1). The faulting seems to play a role in controlling the structural elements of the area. It is noted that most of the structures in the area have trends similar to fault directions. Faults in the area can be subdivided into two groups based on their orientation (Fig. 3.3).

A major group of faults have a NNW-SSE trend. This trend is pronounced within Witu, Tana river regions and along the Pandanguo Kipini line. In the Tana river region, the faults are

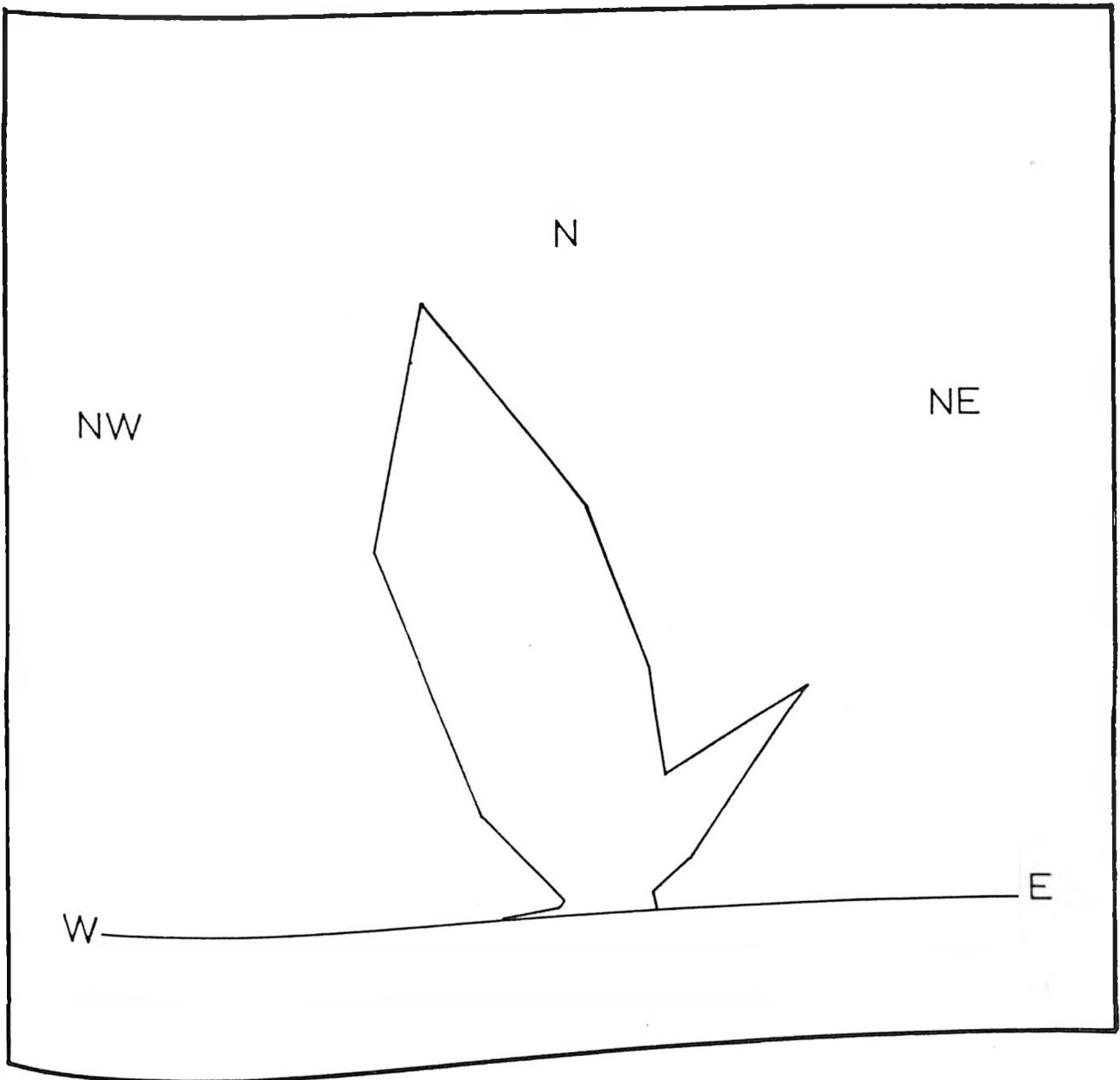


Fig.3.3 ROSE DIAGRAM OF FAULT ORIENTATIONS
IN THE AREA

all parallel and do not have any cross faults intersecting them. They are normal faults with downthrow towards the Tana river which divides their pattern into two. On the western part of this region the faults downthrow to the east. On the east the downthrow is to the west. This fault pattern has resulted into a synclinal structure.

Around Witu, the NNW-SSE faults are connected by cross faults most of which have downthrows to the south. At Bodhei and between Bodhei and Mararani, there are three major faults with a NNW-SSE trend. These are the only faults with this trend in the eastern part of the study area.

Another trend that is not well developed is in the NE-SW direction. This is seen along the coastline, especially along Pate-Kiunga coast where the trend is well developed. The throws are mostly SE (towards the sea). This trend is also seen around Bodhei and the region between Bodhei and Pate.

Most of the central and eastern parts of the study area have a mixture of fault orientations with the NE-SW trend making the majority. Here the NE-SW and NNE-SSW faults constitute about 95% of the total faults. Around Kipini, the NNW-SSE faults trend and the NE-SW faults form a closed fault structure. This makes it a complete closed high.

Within the Tana river region, faults are parallel and continuous

with a systematic pattern of downthrow. Those towards the east are of a short extent and are joined into a fault network without a particular pattern of throw or trend. The difference in fault configuration of the two regions suggests a difference in tectonic events that led to faulting.

3.10.2 SEISMIC STRATIGRAPHY

The sedimentary sequence in the area vary in thickness. Seismic cross sections show that there is a general increase of thickness towards the sea and locally towards the Tana river.

The overall thickness variation towards the sea is seen on TWT sections in Fig. 3.2. The lower Eocene (Horizon G) changes from 2.5s TWT to 4.5 S TWT. The variations are also seen on the cross section TT', GG' and HH'. (Fig 1.4) Sections GG' at point G, the Oligocene (M). Eocene Horizon (C) has an approximate thickness of 540 m, at Mkunumbi - 550 m and 1300m at T1.

When the lower Eocene (horizon G) on section HH' was considered a thickness of 800 m was found at H in the north. At the intersection of seismic line M6933 and R79 (SP 5170), the horizon had a thickness of 950 m. Southwards, the thickness increases to 1500 m at Pate. The thickness of the horizon changes from generally moderate in the north to thick in the south occur along a NE-SW line from Witu to the north of Mkunumbi through shotpoint (SP) 5175 on line R79 and SP 5120 on line R72 to

Dodori, south of this line. To the north the beds have a sub-horizontal dip and the thickness of different horizons is nearly constant with localised thickening and thinning. Thickness is maximum in seismic lows (basins) and minimum on highs. On land, the Tana river region has the greatest sedimentary cover. Here, the basement is estimated to be more than 8 km deep.

3.10.3 MAJOR SEISMIC STRUCTURES

The seismic data has delineated a syncline, an anticline and other seismic highs in the area. The syncline and anticline are identified as Tana and Kipini-Pandanguo respectively. The most prominent seismic high is the Bodhei high.

3.10.3.1 THE TANA SYNCLINE

This lies beneath the Tana river from north of Mnazini to the Tana delta and offshore. It has a NNW-SSE trending axis. The syncline is fault controlled with its geometry conforming to the trend of the near straight and parallel normal faults on the western part of the study area. The faults have an approximate cumulative downthrow of 1600 m based on TWT of 1.0 s and velocity of 3344 ms⁻¹. On the western side, the syncline limb has a more gentle gradient than the eastern side. The syncline is flanked by the Kipini-Pandanguo anticlinal structure on the eastern side which is also step faulted. The Tana syncline is well shown on seismic line R 134 with the deepest part being at SP 7620.

3.10.3.2 KIPINI-PANDANGUO ANTICLINAL TREND

This is a much faulted NNW-SSE trending anticlinal structure (seismic line R 42) that runs North-south from Pandanguo to Kipini. Near Witu, the structure forms a saddle sort of feature and divides into two forming a small anticline. This might have formed as a result of displacement of the Kipini-Pandanguo structure by faulting.

Although the Kipini-Pandanguo structure is continuous (O'Hollarain 1971), it is distorted between Witu and Mkunumbi. This distortion causes culminations of the structure at Pandanguo and Kipini. To the east of the anticline, there is a shallow syncline with two deep horizons at Mkunumbi and east of the Pandanguo well. This syncline's culminations can be seen on the line R 42 at SSP 1715 near Mkunumbi market and SP 1690. The major faults on this side of the anticline are interconnected by minor faults. To the south, at Kipini, the fault configuration results in a closed structure forming an all rounded seismic high with the peak of culmination at Kipini well, line R55.

3.10.3.3 BODHEI SEISMIC HIGH

This structure might be due to faulting with most of the faults being downthrown away from the central region. The nature of faulting makes it a complete closed structure with the faults joining around it. The structure becomes better defined with depth. It could have been formed as a remnant of basement that

resisted basinal subsidence, or as a result of volcanic intrusion with vertical forces from below causing upward movement of the central region relative to the surrounding. On the seismic two-way time maps (Fig 3.1) the top of the structure appears at the base of Miocene in a sort of curved shape. The structural culmination at this level occurs east of Bodhei on seismic line R 70 SP 2096 and R 68 SP 23456. At top Eocene, culmination is on SP 2335 seismic line R 68.

3.10.3.4 OTHER SEISMIC HIGH AREAS

Cross sections show a general shallowing up of depth to seismic horizons towards the north-east and away from the coast line. Closed anticlines occur at Kipini, Lamu, Pate, Dodori and Mararani. The culminations of these anticlines make a northward shift with age (depth). This case can be shown by comparing the culmination positions of TWT maps for Miocene (near base) and Eocene (middle) (Fig.3.2). The Lamu, Pate, and Dodori highs show a northward shift of about 6 km. This northward migration with depth may be attributed to basement subsidence towards the sea after Eocene, leading to younger beds dipping seawards. The Mararani structure does not appear at great depth. This implies that it may be a shallow structure of post Eocene age.

3.10.4 UNCONFORMITIES

The top of horizon E (middle Cretaceous) forms an unconformity surface which is shown on seismic lines R42, R48, R68, R56 and

R41. A trace of the western limit of the unconformity can be followed from Mkunumbi, northwards along the west of Mokowe-Bodhei road to the west of Bodhei road junction around Dulcal.

The onlap of horizon G, lower Eocene onto the upper-middle Cretaceous (horizon E) is seen on seismic line R42 and R48 at their intersection. This is also noted on line R68 SP 1715 and R56 SP 2805. On line R41, the onlap is noted on shotpoint 4554 where this line crosses the Bodhei Ijara road. The onlap of Paleocene (horizon H) on E is similar to G in direction. Its trace limit forms a line that is from Mokowe to slightly east of Bodhei.

3.11 DISCUSSION OF SEISMIC RESULTS

In subsection 3.2, it was shown that the overall quality of data used was fair to poor. It should also be noted that the few better quality lines shot between 1969 and 1971 have their own limitations in terms of vertical penetration due to short spacings used. Normally, this spacing allowed better lateral resolution i.e better definition of structures such as faults.

During the analysis of seismic data, control using well data and gravity data has been ensured and attempts made to reduce the errors inherent in the poor quality. Data interpretation was carried out with knowledge of the limitations of the data, an allowance being made for it. This raises one's confidence level

in the interpreted results.

This study has shown that most of the structures in the area are fault controlled. This is especially shown by the Kipini-Pandanguo anticline which might be a continuation of the Walu Pandanguo structure. Also Bodhei structures and Kipini closed high are fault controlled.

Walters and Linton (1973) have drawn cross sections across the present study area based on well data. Their sections agree with the cross sections of the present study in terms of increase in depth of the sedimentary cover towards the coast. However, one disagreement arises, Walters and Linton (1973) show the Tana syncline which is on the western side of the Walu-Pandanguo-Kipini structure as being shallower than the complimentary syncline on the eastern side. Considering the top of Mesozoic in the Tana area, the Tana Syncline is estimated to be at a depth of 3.5 km and the syncline on the east at 5.0 km.

This implies that at this level, the Tana syncline is shallower by 1.5 km. The present study shows the top of Mesozoic in the Tana syncline to be at a depth of 6.3 km and in the complementary syncline to be at a depth of 4.9 km. The present result is an improvement on the estimates made by Walters and Linton (1973), for the following reasons:-

- a) The sections drawn by Walters and Linton (1973) were highly speculative since the wells used were not uniformly distributed within the area.

- b) All the wells used were on structurally high areas and none in synclines, so the depth estimates in synclines could be highly unreliable.
- c) Since the same wells that they used are also used in the present study, this time with two other methods, the present results are considered to be more reliable.
- d) Gravity data show the Tana syncline as an area with a large negative Bouguer anomaly suggesting thick sedimentary cover, unlike the syncline on the eastern side.

Although gravity data had shown the formation of Walu-Pandanguo structure to be block type, seismic data have shown it to have had greater downthrow of the graben on the western side than the eastern one.

The unconformity (sub-Eocene) that has been noted on seismic sections occurred as a result of uplift of the western part of the embayment or due to eustatic changes in sea level. But since the sea levels were quite high between early Cretaceous and Oligocene times (Mcquillin, et. al., 1984, Gignoux 1955) one's inference would be an uplift of the western part of the study area which include emergence of the Walu-Pandanguo-Kipini anticline.

4. WELL LOG DATA INTERPRETATION

4.1 INTRODUCTION

Between 1954 and 1972, a total of sixteen wells were drilled in the study area results of which are kept at the National Oil Company of Kenya. Six of the sixteen wells were chosen for the present study. The choice of these wells was based on their geographical position and depth. The wells used have a depth of at least 1900 metres. The need to have wells at positions that could ensure uniform distribution within the area was not satisfied. This was due to the fact that drilled wells are concentrated in the western part of the area (Walu, Pandanguo and Kipini) and along the coastal strip (Lamu, Pate, Dodori and Mararani). The area between Walu and Mararani (a distance of 110 km apart) has no wells.

The wells used are Walu, Pandanguo, Kipini, Pate, Dodori and Mararani. The well log data given to the writer by the National Oil company of Kenya (NOCK) for analysis were three types; compensated sonic logs, formational density logs and lithology logs - showing lithostratigraphic and chronostratigraphic units. The compensated sonic logs, density logs and lithology logs were used as controls in the seismic interpretation (c.f. chapter 3). When interpreting well log data, lithology logs were used. For each well, the lithology logs provided by NOCK were accompanied by a description of rock colour, texture, porosity, depth, age,

content and sometimes, salinity of the water in pores.

Many stratigraphers and sedimentologists (Pettijohn 1977, Hallam 1981 and Waller 1960, Hobson and Tiratsoo, 1975) acknowledged the fact that in stratigraphic studies, lithologic analysis and description does not present much problem as it could be done by any average sedimentologist. However, stratigraphic age determination based on palaeontology and lithology is the most difficult task that face a sedimentologist.

Based on the foregoing statement, it is expected that the greatest error in the data given by BP- Shell, could be the chronostratigraphic boundaries. It should also be noted that since all the wells used were drilled by the same oil company, the error in positioning of chronostratigraphic boundaries is expected to be consistent. The aim of using well log data was to correlate data from wells in different parts of the area in order to establish a formal sequence for the whole area, to evaluate contemporaneity of deposits, recognize unconformities, reconstruct palaeotectonic fabrics and delineate depositional patterns.

The stratigraphic correlation of the six wells involved comparison of palaeontology, texture, colour and thickness (given for each well by BP-Shell).

4.2 STRATIGRAPHY

The sedimentary cover in the study area varies considerably in thickness and generally increases from north to south. The deepest horizon reached is the lower Cretaceous which was encountered only in Walu at a depth of 3485 metres. The top of Cretaceous at Walu was encountered at a depth of 1485 metres and 3165 metres at Kipini. This gives a dip of 0.960. This decreases upwards and is nearly horizontal in the younger beds (Fig. 4.1).

Drill hole information indicates that sedimentary lithologies vary considerably throughout the area. The lateral facies changes greatly affect correlation between wells. This suggests different depositional controls within the study area as suggested by lithologies encountered at Kipini and Pate. The same trend has been noted for Mararani and Walu. During Eocene, around Walu and Mararani; continental beds were being deposited while in the south (Kipini, Pate) marine beds were being deposited. The Paleocene and Middle Eocene onlaps upper Cretaceous disconformably (Fig. 4.2). The disconformity cannot be traced northwards due to lack of wells between Walu and Mararani and due to the shallow nature of the Mararani well. The

arse grained, dry matrix

y fine grained - detrital with some unconsolidated sands

interbeds of siltstone

ry fine grained, detrital coralline with small lamellibranchs

interbeds

interbeds

interbeds, fossils and slightly shaley

lignite stringers

calcareous interbedded with foraminiferal limestone

Poorly sorted, fine grained subtidal and shale limestone interbeds
(Numulitic)
(4m)

With occasional siltstone interbeds

non calcareous, carbonaceous pyritic

very fine grained with shale interbeds

very fine grained with thin shale interbeds and fine laminations
and lamellifract (thin shelled)

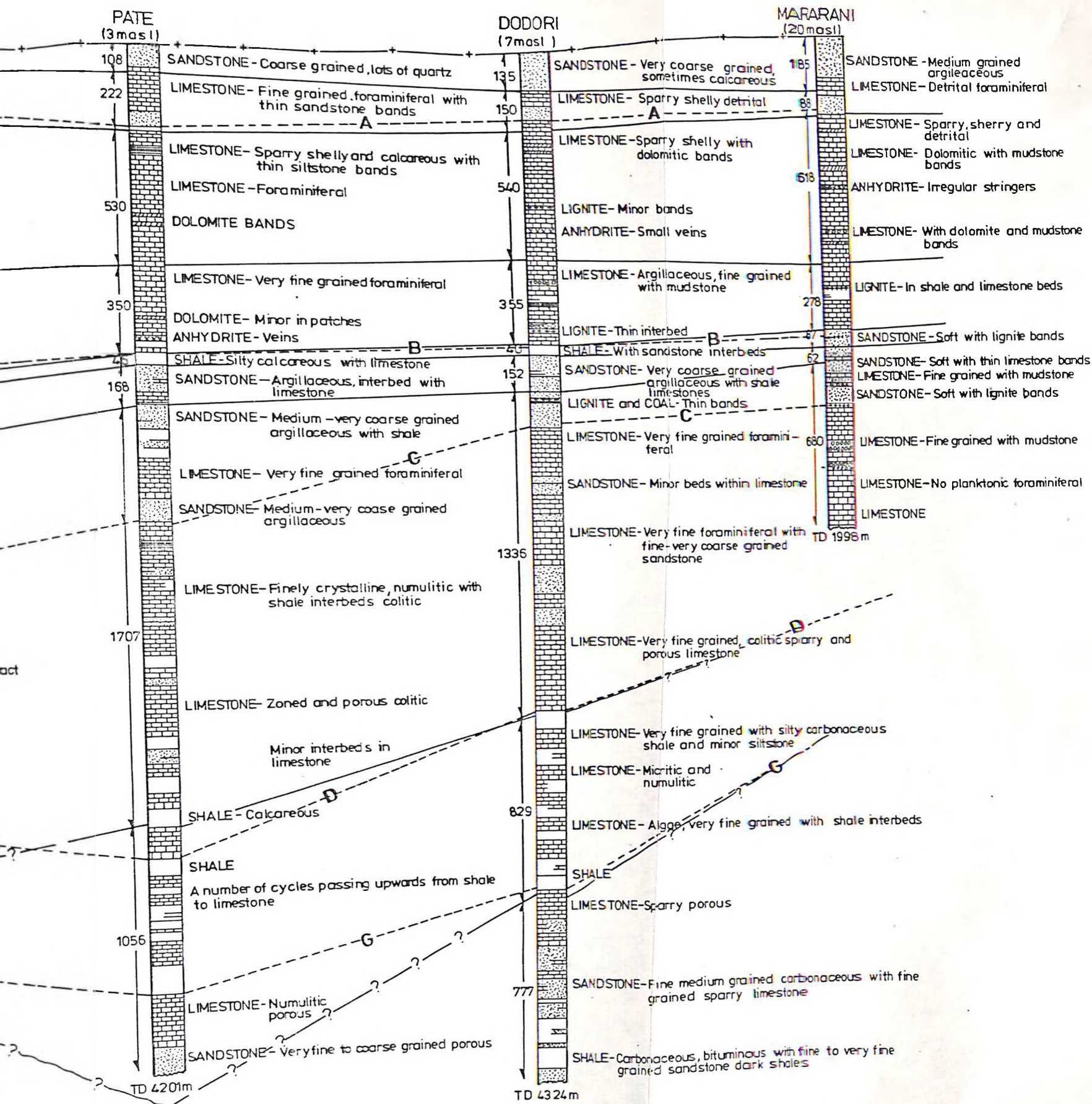
fine to coarse grained, slightly calcareous

calcareous with interbeds of sandstone

poorly sorted with mudstone inclusion

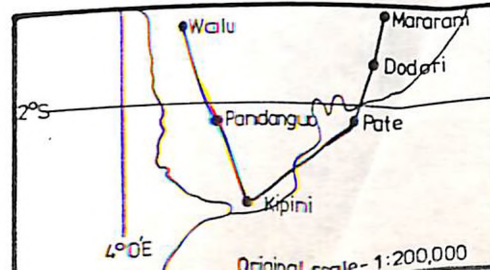
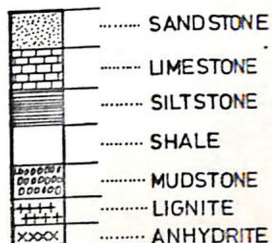
bedded with mudstone, very fine grained and sandstone
(poorly sorted) with carbonaceous

SECTION DIAGRAM FOR KIPINI, PATE, DODORI AND MARARANI WELLS



Legend

- CHRONOLOGICAL BOUNDARY
- UNCONFORMITY
- SEISMIC REFLECTOR



increase of sedimentary thickness towards the south, especially during Tertiary may imply high subsidence rate during this period giving 1485 metres at Walu and 4100 metres at Pate of Tertiary beds.

LOWER CRETACEOUS

This succession which was encountered only in Walu is composed of dark grey calcareous shales with intercalations of hard grey mudstones and fine grained quartzose sandstones. The base is composed of coarse grained sandstones with minor siltstones which change upwards into shales with fine grained calcareous sandstones and minor mudstones. The sandstones become more quartzose and clean towards the top. The brecciation of sandstones is thought to indicate unstable tectonic condition (Dunbar and Rodgers 1957). The clean fine grained quartzose sandstones and dark shales towards the top imply a deepening of the depositional environment and probably the start of marine transgression.

MIDDLE CRETACEOUS

The middle Cretaceous which was encountered only in the Walu well is composed of calcareous mudstones and dark grey, pyritic shales at the base which changes into grey, silty mudstones towards the top.

The presence of dark pyritic shales, in the basal beds indicate

that they are deep water deposits and the silty top beds are shallow water deposits. This implies that the marine transgression that started during the middle of lower Cretaceous continued into the first half of the middle Cretaceous. In the second half of the middle Cretaceous, a regression is most likely to have taken place around Walu.

UPPER CRETACEOUS

The succession in the south is composed mainly of dark grey, slightly calcareous and silty shales. The shales have interbeds of pale brown, fine to medium grained sandstones with subrounded quartz grains and a calcareous matrix. The shales in the lower parts are intercalated with small layers of grey to pale brown, poorly sorted, fine to medium grained sandstones with carbonaceous flecks and mudstone inclusions.

In the north, at Walu, the succession is composed of mudstones and shale interbeds with rare thin sandstone interbeds. Towards the top, mudstones and shales become less argillaceous. The rest of the upper Cretaceous is composed of shales with a few limestone and mudstone interbeds.

The thickness of the Upper Cretaceous deposit increase towards the south i.e from Walu to Kipini. This implies that there was erosion during the Upper Cretaceous which was less at Kipini and more pronounced at Walu. The occurrence of carbonaceous flecks

throughout indicates that the depositional environment was shallow water or close to the shoreline. The Walu area was already a structural high compared to Pandanguo and Kipini at this time as implied by the mudstone deposits at Walu. The lithology implies a shallow marine environment at the beginning of upper Cretaceous which becomes deeper towards the end of this period. Comparing the geographical position of Pate, Dondori and Mararani to Walu, it is expected that the Cretaceous formation in these wells is wholly marine. At Kipini, Walu and pandanguo (presumably) the Upper Cretaceous is followed by the middle Eocene. The Paleocene, lower Eocene and probably the base of middle Eocene is missing. This suggests that the Kipini-Pandanguo-Walu trend was emerging during this period. The Walu area emerging faster than Kipini.

PALEOCENE

This was encountered only in Dodori well and is composed of very fine grained porous sandstones at the top, followed by fine grained sparry nummulitic limestones. The rest of Paleocene to the total depth is composed of interbeds of sandstones and grey, carbonaceous, bituminous and silty shales. It is composed of algal limestone interbeds. The algal limestones at depth indicate very shallow water marine environment. The sediments towards the top indicate a deep water marine environment since the limestones are micritic and contains abundant alveolinids and nummulites. The sandstones at the top are also more marine,

since they are more fine grained, calcareous and with less argillaceous matrix than the basal ones. This suggests that there was a transgression that started during the middle Paleocene and continued to the end of it.

LOWER EOCENE

The Lower Eocene was encountered in the wells at Pate and Dodori. Otherwise, it is missing in the wells at Kipini and Walu. It was not penetrated in the Mararani and Pandanguo wells. From the geographical position of Walu and Kipini, it can be concluded that the lower Eocene is missing in Pandanguo. In Mararani, this formation should be existing at depth. In Pate, the succession is mainly fine grained detrital limestones with plentiful foraminifera intergrading with conquinoid limestones of corals and lamellibranchs.

There is a series of cyclic limestones and shales. At the bottom of each unit, there is dark pyritic shale with limestone stringers which grades upwards into pale brown, clean, fine grained limestones at the top. The shales become less dark coloured towards the top implying shallowing of depositional environment. At the end of each unit, there is an abrupt change to the previous unit. The whole succession becomes more coarse grained, poor in nummulites, poorly sorted and non-calcareous towards the top implying a change from quite clear waters to shallow marine.

In Dodori the lower Eocene is composed of a series of porous sparry micro-oolitic limestones with some slight interbeds of dense micritic limestones and thin shales. The limestone-shale cycles are less developed. The lower Eocene in Pate has more clastic contents than its equivalent at Dodori where most of the lower Eocene is limestone. It is probable that in the lower Eocene, a deltaic axis was developed to the south and southwest of Pate in addition to the northerly one which persisted through the lower Eocene. However, the lower Eocene succession at Pate was more influenced by a delta to the southwest.

The cycles are probably edge deltaics (Tucker, 1973). The fauna is comparatively deep water, but the persistent carbonaceous flecks indicate that the shales were deposited close to land. The limestones at the top of each cycle represent periods when the influx of sediments was not great (Dunbar and Rodgers, 1957). The sandstones and siltstones towards the base show increase in size thus indicating decreasing deltaic conditions upwards.

MIDDLE EOCENE

In the south of Lamu embayment (Pate area), the succession shows more marine influence than in other wells. This is shown by the transition from the lignitic, coally and glauconitic coastal sediments in the north to the dark shales, pyritic and foraminiferal sparry limestones in the south. Generally, there is a decrease in grain size and proportions of clastics from NE

to SW. This suggests that Pate was on the southern flank of the middle Eocene-Oligocene delta into which the continental sediments were carried and so received less coarse clastics than wells further NE. In Pate, the succession consists of interbedded shales and sandstones, generally finer grained with more frequent limestone intercalations than their counterparts in Dodori. Below 2347m depth, the middle Eocene in Pate consists of massive foraminiferal limestones, which in Dodori are interbedded with clastics. The sandstones and siltstones towards the base show increase in size thus indicating decreasing deltaic conditions upwards.

At Kipini, the succession may be put into the following subdivisions from the oldest upwards:

Limestone-Clastics-Shales-Clastics.
These sub-divisions might imply that there were different cycles of environmental conditions prevailing at Kipini.

The subdivision of Kipini succession does not fit the pattern of decreasing grain size and clastics content to the west and SW over the embayment. They appear to be related to a delta originating from the western edge of the Lamu embayment activated periodically by movement of boundary faults (Mussman, 1986, Tucker 1973). The sediments of unit 3 (2394-323) were probably deposited during a period of quiescence, along the western edge of the embayment and were influenced by a larger delta to the

north-east. Unit 1 may be equivalent (2657-3017) to part of the thick clean limestones below 2347 at Pate and below 2200 at Dodori. However, the Kipini limestones are not clean and are some sedimentation from the NW and W. The linderina limestones which occurs in Mararani, Dodori and Pate does not occur at Kipini. This implies that Kipini was in a different depositional environment. At this stage, Pate appears to have been situated mid-way between two deltas, thus not receiving any coarse sediments from either of the deltas. The current bedding and coarse grained size of sands at Dodori suggest that they are foreset beds of the delta (Krumbein and Sloss 1963). They could be equivalent to the variegated mudstones and sandstone beds in Pandanguo which represent the top-set beds of the delta. The delta could probably have been a large ancestral Tana river draining from the west.

At Walu, the middle Eocene succession is composed of poorly sorted, fine to very coarse grained pebbly, argillaceous sandstones. It is non fossiliferous with red mudstone beds. This implies a continental environment of deposition. The middle Eocene in Kipini and Walu sits on the Cretaceous disconformably.

UPPER EOCENE

The upper Eocene in Pate show more marine influence than elsewhere in the Lamu embayment. The Pate well contains more

limestones (nummulitic) than Dodori and Mararani which have only thin sandy limestone bands.

The Mararani, Dodori and Pate wells show that during the upper Eocene, a large delta whose main axis might have laid to the north of Pate covered most of the upper part of the embayment. Consequently, a consistent decrease in coarse clastics content in Eocene strata is observed from NE to SW. The upper part of the upper Eocene at Kipini is consistent with this pattern in that sediments are less coarse grained than their equivalent in Pate and Dodori. Near the base, the Kipini succession contains more coarse clastics, coal and less limestones than its equivalent in Pate. This implies that the source of clastic sediments in Kipini may well have been to the west of Lamu embayment, from a river system flowing over the western side.

At this level, Kipini cannot be lithologically correlated with Pate, Dodori and Mararani. This is probably due to deposition being influenced by stratigraphic events. In the northwest, the depositional environment appears to have been consistently continental. At Walu, the succession consists of very coarse non-fossiliferous sandstones with red clays and clay matrix.

At Pandangio, the depositional environment was also non-marine with mudstones implying some shallow continental water deposition. Overall, the depositional environment during upper Eocene was shallow water.

OLIGOCENE

The Oligocene limestones¹ deposits are similar in wells Kipini, Pate and Dodori. This indicates that the Oligocene limestones¹ deposition was widespread along the present coastal area. Further inland, at Mararani and Pandanguo, clastics dominate. However, the intermittent limestones deposition at the top of the succession indicates that the large delta which might have caused the deposition of continental sandstone beds in Walu and Pandanguo area was waning during the Oligocene.

The wells at Kipini, Pate, Dodori and Mararani have sufficient marine fauna. The succession in Pate is more marine than the rest. This marine environment decreases towards Mararani where we have lignite stringers, implying close proximity to the Oligocene shoreline. Walu and Pandanguo wells have deltaic deposits which suggest that this region formed part of the upper region of the ancestral Tana river delta and was thus more flooded by continental beds.

Sorting and fine grained size sediments increases towards Pate. This indicates that Pate was the deepest part of the study area during Oligocene time. The limestone deposition at the top suggests the start of marine transgression during this period.

LOWER MIOCENE

This succession is chiefly composed of limestones in most of the

wells except in Walu and Pandanguo where we have mudstones. This implies that the Oligocene transgression continued into lower Miocene.

At Pandanguo, the hard dense mudstones have thin limestone interbeds which correspond with the thin conglomerate interbeds within the Walu mudstone beds. This suggests some local marine incursions into continental environments (Gignoux, 1955). The red beds at Walu strongly point to continental deposition. The Pandanguo area was the shoreline of the sea. At Mararani the limestones are hard, dense and pale grey with detrital fossils and bands of dolomite, lignite and anhydrite.

In Dodori, the limestones are vuggy reefal with porosities of about 15%. They also have traces of anhydrite and lignite towards the base. The succession becomes micritic towards the top part suggesting quiet water environment of deposition. In Pate, the lower Miocene is composed of limestones throughout. The limestones are more compact, fine grained and foraminiferal than in the rest of the wells. Grain size decrease is generally upwards.

At Kipini, limestones are detrital, very fine grain with well consolidated sparry matrix at the top. Towards the base, limestones become fawn, detrital and interbedded with pale grey soft marls and calcareous shales which changes into sandstones

with dolomites and lignite stringers.

The well data suggests that the depositional environment becomes more continental towards the north. The Oligocene transgression continued into lower Miocene. This resulted in the formation of shallow shelf marine limestones at the base with occasional lignite and argillaceous horizons. The dolomites could be secondary, formed by percolation of sea water through limestones (Selley, 1985). The succession of lignite and carbonaceous beds by extensive marine deposits indicate widespread marine transgressions in the embayment (Reineck and Singh, 1975). The facies in Kipini falls midway between that of Pandanguo and Pate. The succession is mainly marine in Pate where we have reef limestones. In Walu and Pandanguo, the succession is composed of mudstones with limestone interbeds.

MIDDLE MIOCENE

At Dodori, Pate and Kipini, the succession is mainly marine. It has sparry and shelly limestones with dolomite bands and minor lignite at Dodori. The succession becomes fine grained, foraminiferal and coralline with lamellibranchs at Pate. The Kipini formation is mainly detrital, sparry, calcareous and argillaceous with minor dolomitisation and thin lignite interbeds. The whole succession is foraminiferal with porosities of 25%.

In Mararani area, limestones are dolomitic with rare mudstone bands. Trace anhydride occurs near the base. Some parts are purely limestones which are chiefly fawn, micritic and buffy containing foraminifera. The whole succession has no planktonic foraminifera. This suggests marginal deposition of limestones and possible lack of open sea connections with some short semi-arid conditions.

At Pandanguo, the limestones are argillaceous, marly, silty and less pure than in all other Lamu wells. The succession becomes micritic and partly argillaceous at Walu with an abrupt change to loose unfossiliferous sands at the base. The micritic nature of the limestones suggest probable deposition in shallow quite waters, maybe enclosed lake with occasional marine influx. The abrupt change from loose clastic sands to limestones at Walu suggest a northward marine transgression that might have started during middle Miocene.

In the other wells, the depositional environment is mainly shallow water, composed of limestones with minor mudstone intercalations. The occurrence of mudstone interbeds within limestones seem to increase towards the west. Dodori having less mudstones than Pate and in turn Pate having less than Kipini and Pandanguo. This could be related to the position of Tana river and suggests that the mudstone deposition was influenced by the Tana river.

In Kipini and Pandanguo, the succession through middle Miocene contain mudstones. The environment of deposition at Kipini was probably further from the shoreline (more marine) as compared with Pandanguo which has more mudstones and lignite suggesting a minor regression. The lignite occurrence in Lamu seem to increase away from Pate and Dodori area which probably remained as a deep marine environment during middle Miocene. The Kipini-Pandanguo limestones are more argillaceous, more silty and less foraminiferal than Pate and Dodori.

This implies that the predominantly reef and lagoonal environment in Pate and Dodori and partly Mararani does not extend to Kipini. This is probably due to proximity to the supply of sediments from the ancestral Tana river and interference by the Walu-Pandanguo-Kipini anticlinal trend.

UPPER MIOCENE

At Mararani, the limestones are sparry, shelly and detrital at the top and becomes grey fossiliferous and argillaceous in the upper parts grading into mudstones. The rest are pure limestones which are fossiliferous with amicritic matrix. At Dodori, they are sparry fossiliferous, vuggy and reef type with some sandstones. Limestones at Pate are poorly consolidated, porous with conquinoid bands, lamellibranchs, gastropods and small solitary corals. They are fine grained forminiferal. The sandstones occur as poorly consolidated coarse to very coarse

interbeds with clean well rounded quartz in abundant clay matrix at 200-258m.

The Kipini formation is composed of limestones which are detrital, shelly coralline and foraminiferal and becomes silty and finely sandy below 202m. At 232-263m the limestones are mixed with unconsolidated coarse sands and hard calcareous medium sandstones with lignite stringers. At the base, the limestones are coralline with gastropods and lamellibranchs. Towards the north west, at Pandanguo, limestones are detrital and sandy with marl successions suggesting a more shallow water environment of deposition.

At this time, the depositional environment at Walu appears to have been deeper than at Pandanguo. The limestones at Walu are micritic, sparry, partly argillaceous with Bryozoan implying quiet marine environment of deposition. It is important to note from the above discussion that Pate does not have any regional significance. The limestone-marl succession of Pandanguo could be considered to be the onshore less calcareous equivalent of detrital limestones penetrated at Kipini.

The Pate limestones are more sandy than Dodori which are in turn more than Mararani. Thus the predominant facies varies from reef limestones in the east to deltaics in the west as shown in the Kipini, Pandanguo and Walu wells. This implies that the delta to

the NE had ceased by the upper Miocene time.

At Mararani, the sparry limestones encountered at the top implies deep water deposition. The dolomitisation at the base suggests that there was a marine transgression during this period. The foraminiferal and fossiliferous nature of the entire upper Miocene show that the sea extended beyond the present Mararani and Walu regions although it was shallower at Mararani as shown by the presence of calcareous mudstones. At Walu, the clear deep water and sea connection is shown by the presence of sparry Bryozoan limestones. Kipini was shallower than Walu and was covered by the sea (marine).

PLIOCENE-QUATERNARY

The Pliocene-Quaternary succession is chiefly composed of sands, sandstones and detrital limestones.

At Mararani, the sandstones are soft, argillaceous with sandy clays and are poorly sorted. This grades into detrital fossiliferous limestones with calcareous mudstone bands at the base. At Dodori, the limestones are fossiliferous, sparry and shelly.

The succession at Kipini has medium to coarse grained coral limestones forming the top 37 metres. The remaining part of the 177 metres succession is composed of limestones interbedded with

unconsolidated sands. The sands are subrounded, iron stained, medium to coarse grained. The limestones at the top are detrital and are exposed sporadically at the surface between Tana river and Lamu island. This was seen at Witu, Hindi and Mpeketoni. Anywhere else, the thick coral limestones do not occur at outcrop level.

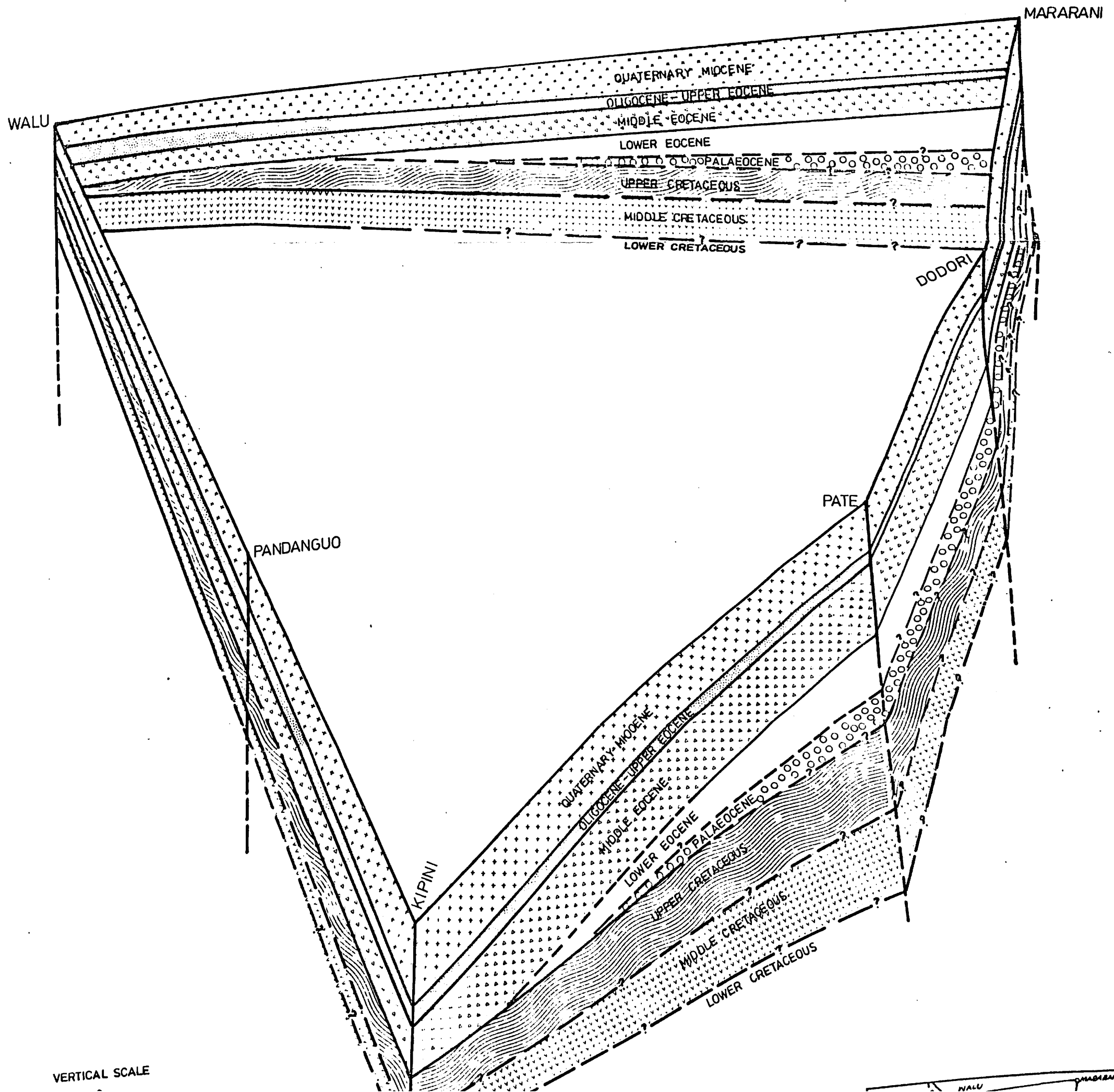
The sandstones at Pate and Dodori are similar to that at Kipini and becomes more argillaceous towards Mararani but less feldspathic. This implies that the sediments consists of material eroded and transported from the basement areas further west into shallow water marine environment. This is shown by the decrease in the presence of feldspars.

The fact that most of the surviving grains are quartzose and rounded, implies long distance of transport from source area. The thin limestone bands at Pate and Mararani might have been formed during lulls or cycles of no deposition from outside, implying that Pate and Mararani had the same geographical control on sedimentation.

4.3 DISCUSSION OF WELL LOG RESULTS

The well log data show that the Lamu basin is composed of a thick sequence of sediments varying from continental to marine. The thickness of beds increase towards the sea, thus forming wedge shaped sedimentary beds (Fig. 4.3). This has been noted by

Fig.4.3 FENCE DIAGRAM FOR THE CORRELATION OF WELLS KIPINI ,PATE,
DODORI, MARARANI AND WALU



Steckler and Watts (1978) and , Norton and Scalter(1976) to be characteristic of passive margins.

Sedimentary beds in the area become more marine towards the sea although on the mainland, the beds exhibit both shallow water (lagoonal deltaics) and deep water sediments. This suggests that the area was experiencing marine transgression and regressions from time to time. This implies that throughout the period of deposition, the area was under periodical uplifts and downwarps.

During the Cretaceous to lower Eocene, shallow water sediments were deposited along the western edge of the embayment. This consists of quartzose sandstones and shales indicating a continental to deltaic environment of deposition during lower Cretaceous. These sediments were followed by mudstones in the Walu regions and limestone intercalations in Kipini which indicate a major change in the environment of deposition and may suggest a minor transgression with Walu being on the shoreline for calcareous mudstones to be deposited.

In the upper Cretaceous times, conditions became shallow and much of the Lamu embayment especially the western part was lifted above sea-level and eroded. At this time, the major phase of faulting along the Walu-Pandanguo-Kipini structural trend might have occurred. Greater thicknesses were eroded off the axis than the south. This is shown by the pitching nature of the

structure.

Sedimentation at the beginning of lower Eocene was less intercepted to the east of the Walu Kipini trend and presumably reworked Cretaceous-lower Eocene material from the trends was washed into the centre of the basin giving rise to the lower Eocene deltaics in Pate. The sediments during the lower Eocene probably had a widely dispersed origin as it is likely that Precambrian Permo-Triassic and Mesozoic rocks were exposed during lower Eocene. The shale limestone cycles reflect periodic rejuvenation and erosion inland. Whereas erosion of exposed Cretaceous was taking place onshore, offshore shallow water limestones and shales were being deposited.

At the beginning of the middle Eocene time, the source areas in the west were uplifted and a general subsidence occurred to the east with the Tana river sediments being deposited in the basin. The uplift and subsidence was followed by a non tectonic period. It is during this period that the covering of the entire onshore part with massive continental sandstones and mudstones of granitic origin occurred. At this time, Walu was onshore, Pandanguo was on the shoreline and Kipini, Pate, Dodori and Mararani were offshore.

A minor marine transgression occurred during the start of middle Eocene with the deposition of more marine sediments in the south.

This was followed by a minor regression during the mid-middle Eocene. During the lower part of middle Eocene, widespread shelf marine limestones were deposited along the coast of Kenya. At Pate and to the north east (Mararani) the environment of deposition became shallow from mid-middle Eocene upwards with sporadic dolomitisation towards the top. In the upper part of middle Eocene upwards, extensive rejuvenation of the source area might have occurred. The sediments are related to a delta whose main axis might have been to the north of Pate. The decline in the importance of the river system to the Southwest during the middle Eocene was probably partly due to the rejuvenation of Walu-Pandanguo anticlinal trend at the time.

A major marine transgression began during the Oligocene, resulting in shallow water marginal limestones being deposited on continental beds in the west and northeast (Pandanguo, Walu area). Basin subsidence continued during lower Miocene leading to a major marine transgression and deposition of marginal shelf limestones and mudstones as far north as Walu.

The mudstones, also noted at Kipini, were probably related to clastic sedimentation along the western margin of the Lamu embayment and were swept across the area periodically. Miocene shelf limestones with variable dolomites and anhydrites were deposited in Pate, Dodori and Mararani, implying that they have similar deposition environment.

Towards the end of upper Miocene, the limestones are interbedded with coarse, poorly consolidated sands, implying a short distance of transport and close proximity to land. This suggests a general regression within the basin and increased influence from the Tana river.

During the Pliocene, coarse clastics were deposited, presumably related to an ancestral Tana river and drifted along the shore from it. The clastics are interbedded with reef coral limestones which becomes rare towards the top implying a shallowing of the depositional environment.

The Quaternary is composed of clastics which are partly continental and partly marine. The very well sorted, fine grained sands at the surface are probably dune sands.

5. GEOLOGICAL SYNTHESIS OF GEOPHYSICAL AND WELL LOG DATA

5.1 STRUCTURE

Gravity, seismic and well data was used to prepare a structural map of the area (Fig. 5.1). The structural map shows that the events leading to the occurrence of Lamu basin are complex and that there is a close relationship between faulting and folding. The western part of the study area appears to be the most disturbed and has major structures.

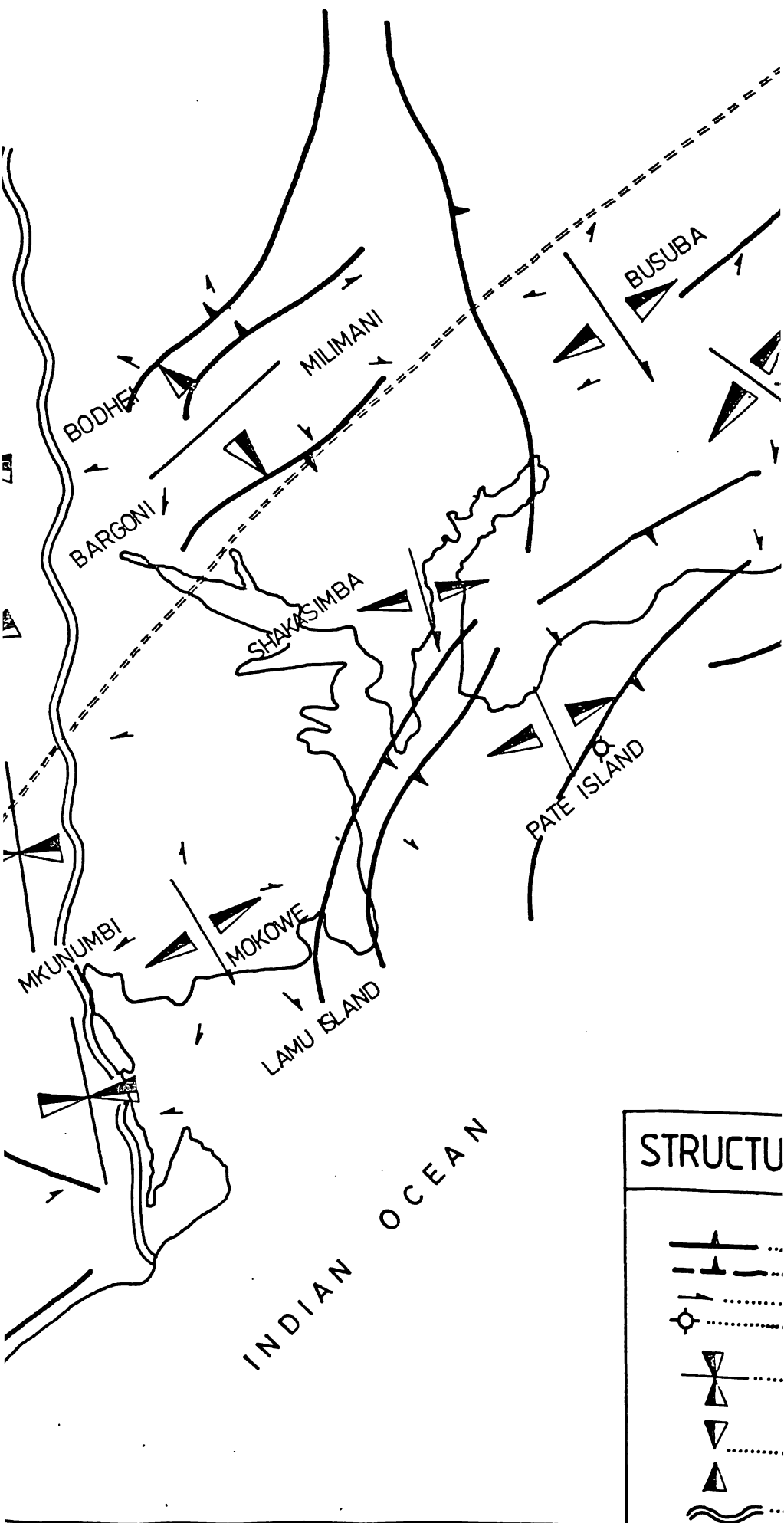
Most of the faults are of normal type and increase in number with depth (as discussed in subsection 3.10). This might have occurred as a result of movement on the old faults (Alastair 1984). The fact that most faults downthrow sea-wards might suggest that they are formational faults although a clear picture can only be acquired if deep seismic study was done.

The well developed major faults (with a uniform trend) in the western parts suggest that these faults may be due to regional effects associated with the formation of the entire embayment. They could be deep seated and related to listric faults that were formed during rifting and subsidence (Shelton, 1968).

The NE-SW faults along the coast (with a seaward throw) are more likely compensation faults formed as a result of slumping or coastal subsidence due to thick sediment load adjustment along the buried basement slope (Shephard, 1973). The faulting in the

40°45

41°00



STRUCTU

-
-
-
-
-
-

40°45

41°00

area has led to block-faulting associated with subsidence during the basin's evolution. Major faults discussed and localised ones form a network of closed structural highs and lows in the area.

Seismic and well log data show an unconformity which runs across the area NNE from Mkunumbi and Bodhei. Bradley (1984) noted that the boundary between post-rift, and underlying synrift and pre-rift sequences in the basin of the any passive margin is characterised by a major unconformity.

A model for the onlap of the post-rift beds onto the unconformity for passive margins has been described by Watts (1982). He proposed a disconformable onlap of the post-rift beds onto the unconformable surface. This proposal agrees very well with the situation in Lamu.

The sub-Eocene unconformity in Lamu basin appear to be a divide between the pre-unconformity beds of higher dips to post-unconformity beds with dips decreasing upwards towards sub-horizontal inclination. This suggests that the older gentle dipping beds were produced by rifting and tilting and the sub-horizontal younger beds by rifting and subsidence (Jackson and Mackenzie 1983). For the tilting and subsidence to occur, there must have been a hingeline along which the subsidence and tilting were taking place.

The writer expects the Tana synclinal axis to have been the hingeline. Hutchinson et al (1986) who did some work on the long Plateform (New York) have noted that the hinge zone is usually characterised by an uplifted block near the hingeline within the basin and gradual subsidence seawards. In the study area, the Walu-Pandanguo-Kipini anticline fits into that model very well.

The role of normal faults in the post-rift stage of basin development is an important consequence of subsidence in the syn rift phase. The faulting and subsidence leads to complex fault scarps associated with major tilted fault blocks and are responsible for the present-day fault block basement topography. These imply that the basement highs in Lamu embayment were formed during the second phase of basin evolution.

Thickening of beds seawards could also be attributed to salt diapirism, but deep reflections are too poor and too discontinuous to allow a thorough interpretation.

5.2 BASIN GEOLOGICAL HISTORY

The Lamu embayment is a sedimentary basin superimposed on the eastern margin of the African platform. The gravity data suggest a very thick sequence of deposits. This fact together with well data direct to the suggestion that the basin might have come into being at the same time with Karroo sediments at the beginning of the upper Carboniferous times (Walters and Linton, 1973).

The area of sedimentation formed as a result of downwarping of the eastern margin of the African platform. It is very likely that the downwarping continued from Carboniferous to the end of Triassic (Miller, 1952). The general palaeogeographic aspect of the sedimentary basin is proposed by Miller (1952), Caswell, (1953 and 1956) Thompson, (1956) and Williams, (1962). From upper Carboniferous to upper Triassic, the sedimentation was controlled by generally continuous negative epeirogenic movement. This also included the present Mombasa-Malindi basin.

The Karroo sediments accumulated in a NNE-SSW trough which developed along what is now the eastern margin of the African continent. Only the western part of this margin is present in Kenya, while sediments of the eastern side of the trough are now to be found in Madagascar. The Karroo sequence thickens from coastal Kenya to southern Tanzania (Haughton, 1963).

The Lamu-Mombasa basin was initiated as a continental rift which

was tectonically controlled by the main deformation trend of the Precambrian rocks and developed from late Carboniferous to Jurassic.

A number of models have been suggested to explain the mechanism of continental rifting (Watts, 1982; Hutchinson, et. al. 1986; Brunet, 1984 and Mackenzie, 1978). All models proposed can be combined into one that is a simplified version of all of them. It is suggested in the combined model that the process of continental rifting follows the following stages.

- i) Convective doming of the continental crust.
- ii) Erosion of the updomed part of the crust leading to thinning.
- iii) Cooling as the crust returns to thermal equilibrium due to loss of heat. This leads to more thinning.
- iv) Differential loading and regional extension leading to listric faulting in the brittle upper crust and necking in the ductile lower crust and mantle.

This model has been used to divide the evolution of the Lamu embayment into three stages:

- i) Pre-rift stage
- ii) Rift stage
- iii) Post rift stage

1. Pre-rift stage

Doming might have started and continued during the Carboniferous times. At these time, erosion of the domed region continued. At the end of the Carboniferous and possibly early Permian, erosion following doming led to thinning of the upper crust. With the return to equilibrium, the thinned crust formed a topographic low in which glacial sediments were deposited leading to differential loading. The loading, coupled with tensional forces associated with the break-up of Gondwanaland led to listric faulting.

2. Syn-Rift Stage

The listric faulting from mid Permian to Triassic resulted in a number of horsts and grabens into which the Permo-Triassic sediments were deposited. Caswell (1956) has noted that subsidence in the Permian times along what is now the Margin of the East African continent was controlled by the NW-SE directed tension forces. This resulted into a NNE-SSW trending trough into which the drainage systems were directed by rivers. The resultant sediments form the Duruma sandstone series.

During the upper part of Permian, more rapid subsidence occurred. This is shown by the sequence of beds becoming coarse grained upwards. Gentle subsidence continued during the Triassic with sediments becoming more marine. With the break-up of Gondwanaland and the beginning of the drift of Madagascar, the

Lamu embayment developed into a passive margin basin. In the offshore, Jurassic beds were deposited directly on newly formed oceanic crust (Rabinowitz, et. al. 1982).

3. Post rift stage (passive margin stage)

The predominantly continental Karroo age of Duruma sedimentation in the Lamu-Mombasa basin came to an end after a major pre-middle Jurassic faulting phase (associated with the Madagascar drift), which triggered faulting and tilting that resulted in marine incursion into the basin. This led to deposition of post rift marine limestones and shales over Duruma group. The faulting is likely to have occurred by movement along the old existing faults. During the middle Jurassic, the transgression in Lamu was more limited in extent than in the horn of Africa, but the fauna (from the Garissa well) indicates that marine depths were considerably greater in the Lamu area than in the horn area (Arkell, 1956). This suggests a narrow zone of crustal tilting and faulting in the Lamu area.

Towards the upper Jurassic, there is likely to have been an uplift thus stopping the marine transgression by closing connections with the sea. This led to enclosed water masses without sea connections. It is in this sort of environment that deposition of salts noted by Rabinowitz, et. al. (1982) occurred.

The post rift (passive margin) sedimentation appears to have been controlled by continental uplift movements in central Kenya. These were sporadic and separated by long periods of crustal stability and erosion.

In the upper Cretaceous, an uplift of more than 400 m was initiated in central Kenya. This uplift had a gentle gradient decreasing eastwards until beyond longitude 39.5 degrees East (Baker, et. al. 1972). At this time, the Kipini-Walu anticlinal structure is thought to have formed and there was subsidence in the east. This led to much erosion of the western part of the study area. The erosion process must have continued into the lower Eocene because the middle Eocene beds disconformably overly the Cretaceous beds along the Kipini-Walu line.

While erosion of the exposed Cretaceous and possibly lower Eocene was taking place onshore, offshore shallow water limestones and shales were being deposited. The upper Cretaceous uplift and subsidence were followed by a non tectonic period during which there was deposition of the sandstones and mudstones of granitic origin in the western part of the study area (Walu and Pandanguo area). This condition seem to have prevailed also during the Oligocene.

During the Oligocene a major marine transgression began resulting in shallow water marginal marine limestones being deposited on

continental beds in the Walu-Pandanguo area. At the beginning of Miocene time, there was an uplift around mount Kenya (Searle, 1952 McCall, 1958 and King, 1965). This was followed by a further uplift of about 300 m in central Kenya decreasing in magnitude to 150 m in the east to 100 m in the south. The coastal region was a zone of flexing and subsidence (Pulfrey, 1960). The coastal subsidence led to the continuation of the Oligocene transgression leading to deposition of marginal shelf limestones and mudstone as far north as Walu.

Towards the top of the upper Miocene succession, limestone are interbedded with coarse, poorly consolidated sands. This suggests a general regression within the study area. The marine regression is likely to be related to a major uplift of the Kenyan dome which occurred close to the end of Miocene. An uplift of the order of 1,500 m in central Kenya was suggested by Pulfrey, (1960).

The end-Miocene doming is likely to have continued into the Pliocene leading to a regression of the coastline to where it is at present. Saggerson and Baker (1965) have noted that arching and flexing within the Kenyan dome have continued on small scale at intervals throughout the Quaternary. This is indicated by the 300m uplift of the Plio-Pleistocene sediments of the Upper Tana river basin.

6. PETROLEUM POTENTIAL OF THE BASIN

The Lamu basin is an epicratonic type of basin or epicratonic embayment. Selley (1985) has noted that embayments are the most productive sedimentary basins for petroleum, much more than the intra-cratonic basins. Not only do they contain marine sediments and better petroleum source potential but they occur where the continental crust is thinning and less stable. Thus heat flow is high which favours hydrocarbon generation. Crustal instability also favours structural entrapment (North, 1984).

Examples of proven petroliferous embayments include the Tertiary Gulf coast basin of the United States and the Niger delta. These are predominantly terrigenous filled basins. The Sirte embayment of Libya is carbonate filled. The Lamu embayment lies between the two, namely it is terrigenous as well as carbonate filled.

By relating the geological evolution of Lamu embayment to similar basins in other parts of the world, one is inclined to suggest that this embayment meets the conditions ideal for petroleum occurrence.

6.1 STRATIGRAPHIC EVIDENCE

For oil accumulations to occur in large quantities in a trap, there is need to have a rich source rock (not necessarily in the vicinity of the trap), a reservoir rock and a caprock.

From the lithology logs, the Cretaceous has sandstone units encountered in Walu and Kipini with a porosity of 15% which is good enough for a reservoir. As for caprock, the shales are well developed above and within the Cretaceous to provide a potential reservoir bed. Source potential of the intervening shales could be good since gas has been noted in both Walu and Kipini wells (O'hollarain 1971). The sparry porous limestones and fine grained sandstones have porosities 5-9%. This porosity is too low to be a good reservoir. Here the source potential of the bituminous, dark shales could be good.

The lower Eocene is composed of transgressive, porous, sparry and micro-oolitic limestones offering a very good reservoir possibility with porosities of 25%. The sandstones have porosities of about 20%. In this succession, the interbedded dense micritic limestones and shales form good caprocks. Development of source rock is moderate and gas was noted within the limestones and shales of Kipini and Pate.

Sandstones during the middle Eocene have porosities of 26-29%, in some areas, the values are low due to argillaceous matrix. The middle Eocene sandstones constitute a potential reservoir. The shales and fine grained foraminiferal limestone interbeds form good caprocks. The petroleum source potential in shales throughout is probably low, as they have a low organic content and limited thickness. The limestones are organic and probably

have source rock potential, though no significant hydrocarbon indications occurred in them.

Between the upper Eocene and Oligocene, sandstones occur with porosities of 24-26%. The Oligocene and upper Eocene beds have no well developed caprock. Thus, they cannot form good reservoirs. The source rock is not well developed.

During Miocene, vuggy, reef limestones constitute good potential reservoirs with porosities of 16% at Dodori and Mararani. At Pate, the Porosity increases to 25%. The caprock may be formed by anhydride stringers although they might not be well developed or continuous enough to form seals. Thin fine grained argillaceous limestones and dolomite bands may form good caprocks if not fractured. At Kipini, the limestones are interspersed with mudstone bands which should provide good caprocks. Rich organic contents of the limestones indicate source rock potential.

Coarse unconsolidated sands have some high porosities (more than 28%) between Pliocene and Quaternary. There is no caprock, so they are not considered to be potential reservoirs.

The stratigraphic analysis show that the potential of sediments as oil progenators in Lamu increases with depth and towards the sea where the sedimentary thickness is high. This might imply that there is a possibility of getting a richer source rock

towards the sea at greater depth than where the present wells have reached.

6.2 STRUCTURAL EVIDENCE

The structural map of Lamu show that the area has a number of highs that could form good traps. Here trapping is expected to be in anticlines of block faulting type related to tension and compensation faulting.

The quality of some anticlinal structures as traps is reduced by the high intensity of faulting in the area. It is therefore necessary to determine the fault closure as related to the structural culmination. Considering all the structural high culminations in the area, Walu, Pandanguo, Witu, Kipini, Lamu, Dodori, Pate, Mararani and Bodhei, their trap quality based on fault configuration, can be classified as follows:-

1. Good - Kipini, Walu (?), Bodhei.
2. Fair - Pandanguo, Witu, Lamu, Pate, Dodori and Mararani.

The Kipini, Bodhei and Walu structures have a fault configuration that surrounds the point of culmination, thus forming a closed fault nature. Bodhei structure has the best network with all faults down throwing away from the central region, they are inter-connected but without an outlet. The faulting at Bodhei provide the most favourable conditions for oil migration to the

anticline and accumulation (ideal for a test well). Although seismic work has not been done around Walu, the inferred faults from gravity suggest that it is an all round closed structure that is in a good position to trap hydrocarbons from the deep Tana syncline to the west, Kitole-Jarakuda syncline across it and the shallow syncline on the east of Walu-Pandanguo structure. On the seismic section, it was shown that the highs along the coast have a northward shift with depth (age) increase. The existing wells drilled by BP-Shell were located on the basis of base Miocene culminations (O'Hollarain 1971). At lower horizons (Cretaceous) the culminations have moved northwards a distance of about six kilometres. Therefore negative results of these wells cannot be relied upon.

The coastal wells Kipini, Lamu, Pate and Dodori are in a very good position to receive oil from the offshore parts as a result of updip migration from the deep offshore sediments.

In the study area, the sub-Eocene unconformity can also form a very good trap. Since the rock above the unconformity is chiefly composed of shales, it can be combined with the lower Eocene shales that overly sandstones such that the unconformity forms a good stratigraphic trap.

7. CONCLUSIONS AND RECOMMENDATIONS

The combined gravity and seismic results show a number of highs (basement and sedimentary) that could form good traps. Most of them are fault controlled forming blocks of anticlines. The deep seated structures of interest are Walu, Bodhei(?) and Pandanguo. Other structures that have been located based on seismic alone are Kipini, Lamu, Dodori and Pate (along the coastline). The fact that they have not been detected on gravity implies that they may not be associated with the basement. They have also been noted to have a northward shift of culminations with depth (age) increase. Gravity results show that part of the coastal Jurassic sediments were laid on an oceanic crust.

Seismic and well log data results show an increase of sediments thickness and marine conditions towards the offshore. The well data results show that the area has source rocks, reservoirs and caprocks, especially the early and mid-Tertiary along the coastline. This make the traps in the coastal regions (Kipini, Lamu, Pate and Dodori) favourable for oil trapment from the offshore due to updip migration.

The stratigraphy and structures make Lamu area a potential region for detailed petroleum exploration. Future work should be concentrated on proper definition of the culminations of structural highs. The failure of wells drilled by BP-Shell might be attributed to siting of wells on the downdip sides of

culminations and basing the siting on shallow structures. This was evident in the wells at Lamu, Pate, Dodori and Mararani.

Walu well was located based on gravity results alone. The present study recommends a deep seismic data acquisition of the area in order to define the structure fully. At Bodhei, poor quality data had been used and no test well drilled. Bodhei and Walu areas offer a good opportunity for testing the deep sediments in the area. For proper definition of the Bodhei structure, new data is required and maybe reprocessing of the old data using modern techniques might be necessary.

The syn-rift sequences of Karoo age are likely not to be oil prone due to the fact that during rifting, heat flows are normally high. So that if there was any hydrocarbon generating sediments, then over-maturation is expected to have occurred.

The only hope is the possibility that this oil could have migrated though the Karroo beds into shallow traps to reduce thermal destruction. If this migration took place, then the most favourable areas to test for it is in the Walu-Pandanguo area (for the possibility of migration from the deep Tana syncline) and Bodhei structures. Because of this, the writer recommends wells not to reach the deep Karroo sediments.

Possibility of the Jurassic sediments having good oil reserves is reduced for the offshore part, but could be good onshore. This

is due to the fact that these sediments have been deposited directly onto an oceanic crust. This implies that they are likely to be overmature seawards but mature shorewards. The possibility of migration to younger beds before overmaturation exists.

Overall, the oil prospects of the study area are good. With the Tertiary offering the best prospects. The quantity of Petroleum in the area will be controlled by the source rocks which have limited thicknesses.

REFERENCES

- Alastair, B., 1984. Structural evolution of the witch ground graben. J. Geol Soc-London Vol 141 pp 621 -628.
- Arkell, W.j., 1956. Jurassic Geology for the World. Edinburgh, Oliver and Boyd. 806 p.
- Baker, B.H., Mohr, P.A. and Williams, L.A.J., 1972. Geology of the eastern rift system of Africa. Geol. Soc. Am. Bull. Sec. pub. No. 136. pp 67
- Bradley, M.E., Egerberg T. and Mipen, O., 1984. Development of rift basins. J. Struct. Geol. Vol. 5 pp 361-3672.
- Brunet, M.F., 1984. Subsidence history of the Aquitaine basin determined from subsidence curves. Geol. Mag. Vol. 121 No. 5 pp 523-546.
- Busk, H.G. and De Verteuil, J.P. 1933. Notes on the geology and oil prospect of Kenya colony (unpub-rept.) 10pp.
- Caswell, P.V., 1953. The geology of the Mombasa Kwale area. Geol. Surv. Kenya Rept. No. 24. pp 42.
- Caswell, P.V., 1956. Geology of the Kilifi-Mazeras area. Geol. Surv. Kenya Rept. No. 34 pp 38.
- Chapman, R.E., 1973. Petroleum Geology - A Concise Study. Elsevier Scientific Pub. Company. pp 15-48.

- Clack, D., 1944. Plane and Geodetic Surveying 2, 3rd Ed. Constable London. pp 283.
- Clendinning, J. and Oliver, J.G., 1969. Principles and use of Surveying instruments. 3rd Ed. Blackie, London. pp 24-46
- Coffin, M.F., Rabinowitz, P.D. and Hautz, R.E., 1986. Crustal structure in the Western Somali basin. Geophy. J. Roy Astr. Soc. Vol. 86.No. 2. pp 346-371.
- Dindi, E.W., 1982. A gravity survey of the Jombo hill area south coast, Kenya. M.Sc. thesis, University of Nairobi. pp 93.
- Dobrin, M.B., 1976. Introduction to Geophysical prospecting. 3rd Ed. New York, McGraw Hill. pp 58-475.
- Dunbar, C.O., and Rodgers, J., 1957. Principles of stratigraphy. John Wiley and Sons. Inc. New York. pp 6- 44, 53-59.
- Gedge, E., 1892. A recent exploration under captain F.G. Dundas up the Tana river to Mount Kenya. Pro. Malacol. Soc. Vol. 3 pp 513-533.
- Geoprosco, 1955. Report on the Kenya gravimetric survey 1955. (Unpubl rept.) pp.52.

Gignoux, M. 1955. Stratigraphic Geology. Freeman and Company. San Francisco. pp 23-35, 39-41, 51-54.

Grant, F.S. and West G.F., 1965. Interpretation Theory in Applied Geophysics. MacCrew Hill. New York. pp 190-304.

Hallam, S. and Weller, J.M., 1981. Facies Interpretation and Stratigraphic Record. Freeman and Company. San Francisco. pp 45-96

Harrison, J.C. and Mathur, S.P., 1974. Gravity anomalies in gulf of California. Am. Assoc. Pet. Geol. Mem 3. pp 76-89.

Haughton, S.H., 1963. Stratigraphic History of Africa South of the Sahara. Oliver and Boyd. Edinburgh. pp 76- 89.

Hobley, C.W., 1894. People places and prospects in British East Africa. Geog. J. vol. IV pp 97-123.

Hobson, G.D. and Tiratsoo, E.N., 1975. Petroleum Geology. Scientific press Ltd. Beaconsfield, England. pp 44-56.

Hutchinson, R.W. and Engles, G.G., 1986. Tectonic evolution of the long island plateform. Geol. Soc., AM. Bull. New York. vol. 97. pp 315 - 326.

- Jackson, J. and Mackenzie, D., 1983. The geometrical evolution of normal fault system. J. Struct. Geol. Vol. 5 pp 471-482.
- King, B.C., 1965. Petrogenesis of the alkaline igneous rocks suits of the volcanic and intrusive centres of Eastern Uganda. J. Petrology. v. 6 pp 67-100.
- Krumbein, W.C. and Sloss, L.L., 1963. Stratigraphy and Sedimentation. Freeman. San Francisco. pp 4-104
- Mackenzie, D. 1978. Some remarks on the development of sedimentary basins. Earth Planet Sci. lett Vol. 40 pp 25- 32.
- Matherson, F.G., 1963. Geological reconnaissance of the Galole-Lamu area. Geol. Surv. Kenya. (unpub. Rept). pp 42
- McCall, G.J.H., 1958. Geology of the Gwasi area. Geol. Surv. Kenya. Rept. No. 45. pp 54.
- Macquillin, R., Bacon, M. and Barclay, W. 1984. An introduction to seismic interpretation. Graham and Trontman. pp 1-146, 174-188.
- Mesref, W.M., 1980. Structural geophysical interpretation of basement rocks of Northwest desert of Egypt. Annals of Geol. Surv. of Egypt. Vol X. pp 923- 937.

Miller, J.M., 1952. The Geology of the Mariakani- Mackinnon road area. Geol. Surv. Kenya. Rept. No. pp 49

Mussman, W.J., 1986. Sedimentary and development of a passive to convergent margin unconformity, Virginia Apalachians. Geol. Soc. Am. Bull. Vol. 97 pp 282-295.

Nettleton, L.L., 1962. Geophysical Prospecting for oil. McGraw Hill, New York, London. pp 1-58.

North, F.K., 1984. Petroleum Geology. Allen and Unwin. London and Sydney. pp 96-120, 240-290.

Norton, I.D. and Scalter, J.G., 1976. A model for the evolution of the Indian Ocean and break up of the Gondwanaland. J. Geophys. research. v. 84 pp 803-830.

O'Hollarain, M., 1971. Report on seismic interpretation of kipini area For BP-Shell petroleum company (Unpub. rept.) pp. 72

Pettijohn, F.J., 1977. Sedimentary Rocks. Harper, New York. pp 718.

Pulfrey, W.P., 1960. The Geology of Maragoli area. Geol. Surv. Kenya. Rept. No. 9. pp 51.

- Rabinowitz, P.O., Coffin, N.F. and Falcey, D. 1982. Salt diapirs bordering the continental margin of northern Kenya and Southern Somali. Scie. Vol. 215. No. 4533. pp. 835
- Reineck, H.E. and Singh, I.B., 1975., Depositional sedimentary environment. Springer - Verlag - Berlin. pp 45- 111, 125-366.
- Reeves, C.V., Karanja, F.M. and Macleod, I.N., 1986. Geophysical Evidence for a Jurassic triple junction in Kenya. (Unpub.rept.) pp 12.
- Saggerson, E.P. and Baker, B.H., 1965. Post Jurassic erosion surfaces in eastern Kenya and their deformation in relation to rift structure. Geol. Soc. London. Quart. J. V. 121. pp 51-72.
- Sanders, L.D., 1959. Geology of the Mid-Galana area. Geol. Surv. Kenya. Rept. No. 46. pp 50.
- Searle, D.L., 1952. Geology of the area northwest of Kitale township. Geol. Surv. Kenya. Rept. No. 19. pp 58.
- Selley, R.C., 1985. Elements of Petroleum Geology. Freeman and Company, New York. pp. 6-8, 15-65, 70-83
- Shelton, P., 1968. Role of contemporaneous faulting during basinal subsidence. Am. Assoc. Petr. Geol. Bull. 52 pp 399-413.

Shephard, F.P., 1973. Submarine Geology. 3rd Ed. Harper and Reid. New York, San Fransisca, London. pp 481.

Steckler, M.S. and Watts, A.B., 1978. Subsidence of the atlantic type continental margin of New york. Earth. Plan. Scie. Lett. No. 41 pp 1-13.

Stockley, G.M., 1928. Report on the geology of the Zanzibar Protectorate. Government of Zamnzibar. vol 4 pp 34-65.

Swain, C.J. and Khan, M.A., 1977. Kenya: A catalogue of gravity measurements in kenya. Geol. Dept. Leceister University pp 40.

Tarling, D.H. and Kent, P.E., 1976. The madagasgar controversty still lives. Nature vol. 225 pp 139-144.

Telford, W.M., Geldart, L.P., Sheriff, R.E and Keys, D.A., 1983. Applied Geophysics. Cambridge University Press. pp 1-103, 218-434, 771-813.

Thompson, A.O., 1956. Geology of the Malindi area. Geol. Surv. Kenya. Rept. No. 36. pp 63.

Tucker. M.E., 1973. Sedimentary environment of tropical African estuaries, Free town Penensuala, Sierra Leone, J. ROY. Geol. Min. Soc. Netherlands. No. 4. vol. 52.

Walters, R. and Linton, R.E., 1973. The sedimentary basin of coastal Kenya. In Sedimentary basins of Africa. pp 133- 158.

Watts, A.B., 1982. Tectonic subsidence, flexure and global changes at sea level. Nature vol. 267 pp 469-474.

Weller, J.M. 1960. Stratigraphic Principles and Practice. Harper and Brothers, New York. pp 235-290.

Williams, L.A.J., 1962. Geology of the Hadu-Fundi Isa area, north of Malindi. Geol. Surv. Kenya. Rept. No. 52. pp 62.

A P P E N D I X

STATION

GRAVITY

DATA.

ST. NO.	CR. REF. E (KM)	CR. REF N (KM)	LONGITUDE	LATITUDE	HEIGHT (M)	GO mgals	ANOMALY SBA (P=2.5) mgals/2
SM 01	651.4	975.0	40.3607	-2.2652	20.4	978028.6	-17.6
SM 02	657.3	975.4	40.4167	-2.2275	23.3	978030.7	-16.2
SM 03	661.8	975.7	40.4583	-2.1942	26.4	978033.6	-14.0
SM 04	664.0	975.9	40.4753	-2.1833	27.5	978037.8	-10.1
SM 05	665.8	976.0	40.4942	-2.1722	28.9	978041.2	-07.0
SM 06	670.5	976.3	40.5332	-2.1417	28.5	978040.9	-07.0
SM 07	678.1	976.9	40.5988	-2.0917	24.3	978036.2	-10.0
SM 08	676.1	976.3	40.5833	-2.1458	23.1	978042.2	- 4.0
SM 09	677.6	976.2	40.5957	-2.1583	21.4	978045.8	0
SM 10	678.4	976.0	40.6035	-2.2833	19.8	978051.2	5.0
SM 11	680.0	975.8	40.6201	-2.1917	17.64	978033.9	9.0
SM 12	671.6	975.7	40.5443	-2.1917	22.9	978046.5	0
SM 13	660.1	974.6	40.4416	-2.3071	20.11	978039.45	-7.0
SM 14	659.5	974.1	40.4367	-2.3399	17.6	978041.4	- 4.5
SM 15	661.4	973.4	40.4533	-2.4567	8.7	978053.0	9.0
SM 16	663.4	972.9	40.4699	-2.4583	9.0	978054.1	10.0
SM 17	666.2	972.6	40.4967	-2.4799	6.4	978056.4	12.9
SM 18	669.1	972.5	40.5225	-2.4918	13.0	978060.65	15.0
SM 19	669.9	972.3	40.5268	-2.4986	10.3	978062.9	18.0
SM 20	685.6	974.0	40.6688	-2.3524	19.1	978071.5	25.0
SM 21	688.5	973.7	40.6950	-2.3903	13.0	978072.4	27.5
SM 22	628.0	973.3	40.1593	-1.7125	68.4	978051.1	-6.6
SM 24	636.9	973.0	40.2274	-1.7154	72.8	978051.0	-7.7

ST. NO.	CR. REF. E (KM)	CR. REF N (KM)	LONGITUDE	LATITUDE	HEIGHT (M)	GO mgals	ANOMALY SBA (P=2.5) mgals/2
SM 25	647.0	972.7	40.3171	-1.6878	78.5	978048.8	-11.8
SM 25.	649.9	975.6	40.4256	-1.6084	68.8	978036.4	-20.8
SM 26	647.2	975.9	40.3250	-1.1750	22.0	978023.1	-23.0
SM 27	645.8	976.2	40.3126	-2.1583	23.4	978022.4	-24.0
SM 28	650.0	976.5	40.3529	-2.1302	40.0	978029.1	-22.3
SM 29	654.2	976.9	40.3878	-2.0894	48.6	978026.6	-20.3
SM 30	659.9	977.1	40.4100	-2.0583	51.2	978037.3	-17.1
SM 31	660.0	977.5	40.4391	-2.0410	55.0	978038.5	-16.9
SM 32	629.2	972.2	40.1643	-2.5167	10.2	977998.7	-46.3
SM 33	632.2	972.7	40.1892	-2.4667	15.4	978005.7	-40.5
SM 34	710.0	974.7	40.8720	-2.2980	55	977996.4	35.0
SM 35	728.0	980.3	41.0387	-2.7816	31.2	978049.7	-4.0
SM 36	739.6	980.6	41.1542	-2.7541	21.6	978058.8	8.3
SM 37	746.8	980.8	41.2133	-2.7587	17.0	978063.7	14.6
SM 38	757.1	981.1	41.3083	-2.7013	13.5	978073.9	24.4
SM 39	768.1	980.9	41.4166	-2.7192	18.4	978081.7	32.5
SM 40	695.0	977.1	40.7510	-2.0770	15.2	978049.2	5.9
SM 41	690.6	977.1	40.7102	-2.0768	18.3	978043.9	-4.0
SM 42	707.4	976.0	40.8724	-2.1707	9.2	978067.1	25.0
SM 43	712.3	976.3	40.9103	-2.1499	7.8	978063.2	21.7
SM 44	693.1	978.3	40.7399	-1.9582	6.9	978030.0	-10.0
SM 45	690.4	978.5	40.7102	-1.9430	7.1	978027.0	-13.0

ST. NO.	CR. REF. E (KM)	CR. REF. N (KM)	LONGITUDE	LATITUDE	HEIGHT (M)	GO mgals	ANOMALY SBA(P=2.5) mgals/2
SM 46	685.8	978.8	40.6720	-1.9204	26.2	978028.9	-16.9
SM 47	683.8	979.1	40.6504	-1.9100	18.1	978026.3	-16.9
SM 48	680.0	979.2	40.6178	-1.8834	43.4	978030.9	-20.0
SM 49	676.6	979.4	40.5867	-1.8104	40.1	978026.5	-22.9
SM 50	673.3	979.7	40.5554	-1.8401	36.4	978024.4	-24.0
SM 51	669.7	979.5	40.5250	-1.8570	32.6	978019.5	-28.1
SM 52	664.4	979.2	40.4832	-1.8834	61.7	978032.1	-24.4
SM 53	662.2	979.5	40.4583	-1.8583	61.2	978030.0	-26.3
SM 54	660.0	979.7	40.4418	-1.8334	61.5	978033.5	-23.2
SM 55	657.2	980.1	40.4167	-1.8012	64.9	978040.9	-16.1
SM 56	655.0	980.2	40.3917	-1.7831	68.8	978043.8	-14.4
SM 57	652.5	980.6	40.3710	-1.7583	76.6	978047.9	-12.5
SM 58	649.3	980.7	40.3420	-1.7420	76.4	978050.9	-9.4
SM 59	645.0	980.9	40.3002	-1.7250	76.5	978053.2	-7.0
SM 60	645.7	980.5	40.3130	-1.7666	84.1	978055.3	-7.5
SM 61	647.7	980.1	40.3209	-1.8002	73.4	978051.4	-8.5
SM 62	645.5	979.9	40.3112	-1.8199	76.5	978051.7	-9.0
SM 63	643.6	979.7	40.2906	-1.8614	68.8	978048.6	-10.0
SM 64	641.5	979.4	40.2704	-1.8657	53.5	978041.4	-12.5
SM 65	640.0	979.2	40.2583	-1.8832	61.2	978042.0	-14.4
SM 66	638.8	979.1	40.2475	-1.9000	53.5	978038.1	-16.0
SM 67	637.4	978.9	40.2333	-1.9085	48.9	978029.7	-23.0
SM 68	636.0	978.7	40.2249	-1.9583	45.9	978026.1	-26.0

ST. NO.	CR. REF. E (KM)	CR. REF. N (KM)	LONGITUDE	LATITUDE	HEIGHT (M)	GO mgals	ANOMALY SBA (P=2.5) mgals/2
SM 69	633.4	978.4	40.2000	-1.9584	34.3	978022.4	-26.1
SM 70	645.4	978.9	40.3068	-1.8885	61.2	978039.2	-17.2
SM 71	647.0	978.6	40.3220	-1.9166	57.3	978031.3	-18.0
SM 72	648.8	978.3	40.3370	-1.9352	53.5	978031.3	-23.0
SM 73	651.0	977.9	40.3585	-1.9652	49.7	978029.4	-23.9
SM 74	703.5	977.2	40.8311	-2.0643	10.0	978050.6	9.0
SM 75	708.3	977.5	40.8761	-2.0332	12.2	978046.4	8.0
SM 76	711.6	980.5	40.9061	-1.7590	28.9	978033.1	-12.6
SM 77	711.8	980.2	40.9092	-1.7831	27.2	978039.3	-6.0
SM 78	711.9	979.9	40.9110	-1.7810	26.0	978031.9	-13.0
SM 79	712.1	979.6	40.9120	-1.7842	23.6	978034.0	-10.2
SM 80	712.5	979.4	40.9132	-1.8702	20.4	978035.0	-8.7
SM 81	717.2	979.3	40.9550	-1.8667	20.5	978037.7	-6.0
SM 82	721.0	979.7	40.9846	-1.8590	19.1	978037.3	-5.9
SM 83	646.0	973.7	40.8080	-1.3833	18.3	978028.6	-11.9
SM 84	705.0	981.3	40.8370	-1.6888	33.5	978026.6	-20.1
SM 85	702.1	981.8	40.8167	-1.6411	36.4	978025.5	-21.9
SM 86	702.8	982.2	40.8253	-1.6167	49.1	978025.6	-22.5
SM 87	642.9	974.7	40.2849	-2.2931	10.6	978022.4	-21.0
SM 88	648.0	974.3	40.3339	-2.3336	14.4	978028.9	-16.0
SM 89	651.0	974.0	40.3569	-2.3569	11.6	978046.9	-12.4
SM 91	662.3	973.2	40.4610	-2.4574	8.9	978053.7	9.6

ST. NO.	CR. REF. E (KM)	CR. REF. N (KM)	LONGITUDE	LATITUDE	HEIGHT (M)	GO mgals	ANOMALY SBA (P=2.5 mgals/2
SM 92	616.0	980.0	40.0428	-2.8138	43.9	978033.1	-24.8
SM 93	619.5	979.1	40.9524	-2.8958	35.2	978029.3	-26.6
SM 94	618.4	976.3	40.6465	-2.1375	31.4	978012.5	-36.2
SM 95	624.5	972.2	40.1197	-2.5208	17.5	977998.9	-48.5
SM 96	683.2	980.5	40.6497	-1.7708	38.4	978007.5	-21.0
SM 97	692.8	979.0	40.7341	-1.8792	23.4	978017.6	-14.6
SM 98	689.5	979.5	40.7049	-1.8792	20.1	978016.0	-16.4
SM 99	691.7	979.6	40.7240	-1.8549	24.1	978015.4	-16.3
SM 46B	688.0	978.7	40.6911	-1.9317	16.5	978027.9	-14.9
SM 84B	703.5	981.6	40.2685	-1.6495	35.1	978026.0	-21.0
SM 83B	705.3	981.0	40.8430	-1.7305	29.8	978020.1	-18.0
SM 82B	724.9	979.9	40.1165	-2.3203	25.1	978043.5	-4.5
SM 1B	654.6	975.2	40.3870	-2.2460	21.0	978029.8	-16.8
SM 2B	659.5	975.4	40.4372	-2.2110	24.8	978032.3	-15.0
SM 5B	667.5	976.2	40.5135	-2.1565	28.5	978046.9	-7.0
SM 6B	672.5	976.5	40.5540	-2.1075	26.4	978039.0	-9.8
SM 12B	665.5	975.5	40.4940	-2.2494	24.4	978036.2	-1.0
SM 20B	687.0	973.8	40.6820	-2.3714	16.0	978071.76	26.4
SM 21B	686.2	973.5	40.4265	-2.5516	40.2	978061.4	-20.2
SM 27B	647.2	976.5	40.3327	-2.1443	27.0	978025.4	-23.6
SM 30B	659.5	977.4	40.4241	-2.0496	53.0	978037.8	-16.6
SM 32B	630.6	972.5	40.1766	-2.4916	12.6	978002.2	-45.0

ST. NO.	CR. REF. E (KM)	CR. REF. N (KM)	LONGITUDE	LATITUDE	HEIGHT (M)	GO mgals	ANOMALY SBA (P=2.5) mgals/2
KF 49	636.3	988.8	40.2252	-1.0111	96.6	977994.9	-19.5
KF 52	630.0	988.5	40.6685	-1.0417	103.9	977994.0	-19.0
KF 55	630.3	988.2	40.1712	-1.0539	100.2	977993.5	-20.3
KF 60	631.3	987.9	40.1802	-1.0944	95.5	977993.4	-21.5
KJ 5	693.9	979.8	40.7432	-1.8389	28.7	978014.7	-16.8
KJ 10	697.6	980.1	40.7766	-1.8306	27.4	978014.7	-16.9
KJ 15	700.1	980.1	40.7991	-1.8111	24.2	978015.4	-16.7
KJ 20	703.1	980.4	40.8257	-1.7972	25.7	978015.7	-16.1
KJ 25	705.7	980.7	40.8491	-1.7722	26.2	978015.5	-16.1
KJ 30	709.2	980.7	40.8806	-1.7556	33.5	978014.1	-16.0
KJ 35	712.8	980.8	40.9131	-1.75	32.9	978015.5	-14.7
KJ 40	716.0	980.9	40.9414	-1.7361	32.3	978017.1	-13.1
KJ 45	719.6	980.9	40.9739	-1.7250	30.6	978019.1	-11.3
KZ 1	623.1	978.0	40.1072	-1.9861	29.5	978004.1	-28.1
KZ 5	625.7	978.1	40.1306	-1.4806	26.4	978008.0	-24.8
A 295	612.0	981.3	40.0072	-1.7139	55.3	978001.2	-24.4
A 298	613.5	980.7	40.0203	-1.7556	50.7	978002.2	-24.6
A 301	614.7	980.3	40.0315	-1.7944	46.5	978002.3	-25.4
A 304	617.2	979.8	40.0541	-1.8333	41.5	978002.4	-24.5
A 307	619.0	979.4	40.0703	-1.8750	37.1	978004.2	-25.8
A 310	620.1	978.8	40.0802	-1.9167	34.1	978003.5	-27.3
A 313	621.2	978.4	40.0901	-1.9583	30.1	978003.7	-28.2

ST. NO.	CR. REF. E (KM)	CR. REF. N (KM)	LONGITUDE	LATITUDE	HEIGHT (M)	GO mgals	ANOMALY SBA (P=2.5) mgals/2
A 292	610.4	981.5	39.9923	-1.6722	60.5	977999.7	-24.6
M 15	610.1	975.4	39.9901	-2.2194	51.9	977994.4	-34.9
M 20	608.4	975.8	39.9748	-2.1944	54.8	977994.1	-34.4
M 25	605.1	976.0	39.9450	-2.1833	60.2	977993.7	-33.7
KA 225	677.4	981.1	40.5946	-1.7056	36.8	9780006.1	-24.1
KA 260	680.2	980.9	40.6203	-1.7278	40.2	978005.4	-23.2
KA 265	682.4	980.6	40.6396	-1.7556	38.3	978006.8	-22.3
KA 270	684.6	980.3	40.6599	-1.7861	38.6	978008.4	-20.8
KA 275	605.9	980.1	40.6712	-1.8167	35.3	978010.9	-19.1
KA 280	687.9	979.7	40.6892	-1.8472	19.3	978016.5	-16.9
KA 285	691.4	979.3	40.7207	-1.8667	29.3	978015.7	-15.9
KA 290	694.4	978.8	40.7477	-1.8917	17.7	978019.3	-14.1
KA 295	695.6	978.5	40.7581	-1.9278	1.7	978026.3	-11.0
KA 300	697.4	978.4	40.7748	-1.9500	3.9	978028.1	-8.9
KA 305	699.2	978.1	40.7905	-1.9694	15.3	978028.0	-6.8
KA 310	698.4	977.9	40.7838	-2.000	14.5	978031.5	-3.8
KD 245	641.8	981.2	40.2748	-1.7058	79.6	978013.9	-6.8
KD 250	638.2	981.1	40.2423	-1.7139	70.6	978015.2	-7.4
KD 255	634.8	981.1	40.2117	-1.7167	73.4	978014.4	-7.5
KD 260	630.7	981.1	40.1748	-1.7139	69.2	978017.7	-5.1
KD 265	626.8	981.2	40.1396	-1.7111	66.8	978014.9	-8.3
KD 270	623.8	981.2	40.1126	-1.7000	43.2	978018.8	-9.1

ST. NO.	CR. REF. E (KM)	CR. REF. N (KM)	LONGITUDE	LATITUDE	HEIGHT (ft)	TO mgals	ANOMALY SBA (P=2.5) mgals/2
A 316	622.9	977.9	40.1050	-2.0000	29.0	978003.0	-29.4
KJ 50	723.3	980.9	41.0068	-1.7306	28.8	978022.2	-8.6
KJ 55	725.4	980.6	41.0351	-1.7417	32.6	978024.2	-5.9
KJ 60	728.8	980.3	41.0563	-1.7694	28.4	978028.5	-2.7
KJ 65	730.7	980.3	41.0734	-1.7806	21.6	978033.0	5.0
KJ 75	737.5	980.6	41.1351	-1.7556	22.5	978039.0	6.8
KJ 80	741.1	980.6	41.1676	-1.7556	20.2	978042.5	9.8
KJ 85	744.3	980.8	41.1959	-1.7472	17.6	978046.2	13.0
KJ 90	748.3	980.9	41.2297	-1.7361	16.7	978049.9	16.7
KJ 95	751.0	980.9	41.2559	-1.7250	14.9	978052.2	18.6
KJ100	754.3	981.1	41.2860	-1.7111	15.4	978053.4	20.0
KJ105	758.1	981.0	41.3198	-1.7000	11.9	978055.8	21.8
KJ110	759.9	981.0	41.3359	-1.7194	16.2	978059.3	26.1
KJ115	763.4	981.1	41.3671	-1.7085	21.4	978060.5	28.5
KJ120	766.9	980.9	41.3986	-1.7159	19.5	978064.3	31.7
KJ125	770.4	980.9	41.4302	-1.7250	17.9	978066.5	33.6
KJ130	773.9	980.7	41.4617	-1.7353	13.4	978069.0	35.2
KJ135	779	980.7	41.4932	-1.7417	4.5	978072.3	36.7
A 316	622.9	977.9	40.1050	-2.0000	29.0	977999.0	-33.2
A 319	620.4	977.5	40.0824	-2.0333	30.8	977997.1	-35.0
A 322	618	977.1	40.0658	-2.0722	32.7	977996.4	36.1
A 325	618.1	976.5	40.0617	-2.1167	32.2		

ST. NO.	CR. REF.		LONGITUDE	LATITUDE	HEIGHT (M)	GD mgals	ANOMALY
	E (KM)	N (KM)					SBA (P=2.5) mgals/2
L 35	644.9	974.7	40.5032	-2.2944	9.7	978020.3	-17.8
L 40	647.0	974.5	40.3221	-2.3222	16.0	978020.0	-17.2
L 45	649.0	974.2	40.3455	-2.3444	13.4	978023.0	-14.8
L 50	652.3	973.9	40.3694	-2.3694	9.6	978028.4	10.5
L 55	655.8	973.7	40.4009	-2.3833	11.0	978034.0	-4.5
L 60	659.3	973.6	40.4324	-2.3861	15.1	978041.6	3.9
L 65	662.8	973.7	40.4640	-2.3806	13.6	978047.4	9.4
L 70	666.5	973.7	40.4977	-2.3861	18.0	978051.9	17.7
L 75	670.3	973.7	40.5315	-2.3806	18.6	978054.7	17.7
L 80	673.2	973.9	40.5572	-2.3611	14.9	978056.7	19.1
L 85	676.8	974.1	40.5901	-2.3472	12.9	978059.5	21.6
L 90	680.6	974.2	40.6239	-2.3361	18.9	978060.4	23.6
L 95	683.9	974.3	40.6541	-2.3275	15.0	978062.1	24.8
L100	687.6	974.5	40.6369	-2.3139	7.2	978065.0	26.2
L105	687.8	974.7	40.6892	-2.2972	3.8	978064.1	24.7
L110	688.1	974.9	40.6914	-2.2611	6.0	978061.0	22.4
L115	688.9	975.6	40.6982	-2.2278	6.9	978058.3	20.1
L120	690.5	975.6	40.7140	-2.2083	7.8	978056.7	18.8
L125	693.4	975.6	40.7387	-2.2056	8.3	978057.6	19.8
L130	697.1	975.8	40.7725	-2.0000	11.4	978059.0	21.9
L135	700.5	975.9	40.8036	-2.1833	11.6	978059.8	24.1
L140	703.9	975.7	40.8333	-2.2028	11.4	978064.0	26.8
L 145	705.2	975.4	40.84.55	-2.2333	4.5	978070.4	31.7

ST. NO.	CR. REF. E (KM)	CR. REF. N (KM)	LONGITUDE	LATITUDE	HEIGHT (M)	GO mgals	ANOMALY SBA (P=2.5) mgals/2
A 328	618.7	976.0	40.0676	-2.1583	30.5	977996.6	-36.5
A 331	619.0	975.6	40.0703	-2.2028	27.2	977996.9	-37.1
A 334	619.0	975.3	40.0803	-2.2444	26.3	977996.7	-37.8
A 337	621.0	974.9	40.0878	-2.2806	21.1	977996.3	-39.5
A 340	622.3	974.7	40.1000	-2.2944	17.9	977996.1	-40.4
A 345	624.0	974.4	40.1149	-2.3167	16.5	977996.2	-40.8
A 350	624.7	974.2	40.1212	-2.3470	17.5	977994.5	-42.5
A 355	624.4	973.7	40.1189	-2.3833	19.1	977992.6	-44.4
A 360	624.5	973.3	40.1194	-2.4194	21.0	977991.7	-45.2
A 365	624.4	972.9	40.1185	-2.4528	18.7	977991.7	-45.8
A 370	624.4	972.5	40.1185	-2.4861	22.3	977989.8	-47.3
A 380	624.8	971.8	40.1228	-2.5556	12.2	9779990.1	-40.6
A 390	626.2	971.4	40.1348	-2.6194	13.5	977989.7	-50.2
A 400	626.7	970.9	40.1397	-2.6889	6.0	977993.7	-48.3
A 410	626.9	974.9	40.1419	-2.7583	3.4	977997.0	-46.1
L 1	622.3	974.9	40.1014	-2.2778	18.3	977996.7	-39.6
L 5	624.7	975.0	40.1216	-2.2722	14.5	977997.7	-39.3
L10	628.2	975.1	40.1532	-2.2611	14.6	977995.5	-37.5
L15	631.0	974.9	40.1779	-2.2722	11.9	978002.0	-35.5
L20	634.9	974.9	40.2131	-2.2594	11.7	978005.5	-32.1
L25	638.2	974.8	40.2432	-2.2806	10.8	978009.3	-28.5
L30	640.9	974.7	40.2667	-2.2917	11.5	978013.4	-24.3

ST. NO.	CR. REF. E (KM)	CR. REF. N (KM)	LONGITUDE	LATITUDE	HEIGHT (M)	GO mgals	ANOMALY SBA (P=2.5) mgals/2
L149	707.4	975.2	40.8649	-2.2500	2.7	.978073.3	34.1
M 5	615.8	975.1	40.0414	-2.2566	34.9	977996.0	-36.9
M10	612.6	975.3	40.0122	-2.2389	45.9	977994.7	-35.9
KA310	698.4	977.9	40.7838	-2.000	14.5	978031.5	-3.8
KA315	699.7	977.7	40.7950	-2.0306	13.5	978035.6	0.0
KA320	699.3	977.3	40.7919	-2.0611	12.9	978040.6	4.6
KA325	697.9	977.0	40.7793	-2.0917	11.7	978045.5	9.1
KA330	699.2	976.6	40.7910	-2.1222	11.3	978050.5	13.9
KA335	700.4	976.4	40.8018	-2.1528	10.6	978055.2	18.2
KA340	702.1	975.9	40.8171	-2.1861	10.6	978060.5	23.3
KA135	613.0	987.1	40.0158	-1.1639	88.3	977991.7	-24.9
KA140	615.3	986.8	40.0360	-1.1889	88.8	977995.0	-21.5
KA215	654.2	983.4	40.4248	-1.5000	65.3	977098.3	-24.2
KA220	659.7	983.1	40.4356	-1.5333	64.7	977999.3	-23.5
KA225	662.9	982.5	40.4577	-1.5583	63.8	977999.5	-23.5
KD185	679.3	983.5	40.6117	-1.4917	61.5	977994.5	-28.7
KD190	675.9	983.3	40.5811	-1.5111	60.2	977995.7	-27.8
KD200	668.5	983.0	40.5149	-1.5389	59.1	977998.3	-25.6
KD205	668.2	982.8	40.5117	-1.5667	56.6	977998.2	-26.3
KD215	659.9	982.2	40.4369	-1.5472	65.5	978001.4	-21.5
KD220	657.3	982.1	40.4144	-1.6194	69.6	978001.9	-20.4
KD225	654.0	981.9	40.3842	-1.6361	71.6	978005.2	-16.7

ST. NO	CR. REF. E (KM)	CR. REF. N (KM)	LONGITUDE	LATITUDE	HEIGHT (M)	GO mgals	ANOMALY SBA (P=2.5) mgals/2
KD230	651.3	981.5	40.3604	-1.6611	74.3	978007.2	-14.4
KD235	648.2	981.4	40.3324	-1.6833	75.5	978008.4	-13.0
KD240	649.8	981.3	40.3018	-1.6917	82.7	978010.1	-10.0
A280	611.7	983.2	40.0045	-1.5139	66.2	978007.6	-15.4
A274	600.5	983.6	39.9676	-1.4361	74.7	978000.5	-19.6
A283	609.4	982.9	39.9833	-1.5528	64.2	978002.5	-20.4
A286	607.9	982.4	39.9698	-1.5889	67.2	977998.0	-24.5
A289	608.8	982.0	39.9779	-1.6306	62.9	977999.0	-24.6